FACULDADE DE ENGENHARIA DA UNIVERSIDADE DO PORTO

Getting a Cell to Walk from the Inside: Modelling How Subcellular Components Responsible for Mechanosensing Affect Cell Migration

Maria Inês Gonçalves

MESTRADO INTEGRADO EM BIOENGENHARIA

Supervisor: Diego Vargas, PhD

Co-Supervisor: Cristina Barrias, PhD

September 16, 2019

Getting a Cell to Walk from the Inside: Modelling How Subcellular Components Responsible for Mechanosensing Affect Cell Migration

Maria Inês Gonçalves

September 16, 2019

Resumo

A migração celular é um fenómeno essencial para a sobrevivência de um organismo. Desde processos simples como a migração em direção a um alimento, ou na direção oposta, caso se trate de uma substância tóxica, até mecanismos complexos, associados ao desenvolvimento, à diferenciação de tecidos e à resposta imunitária, todos eles têm por base a migração. No entanto, este fenómeno também pode ser prejudicial, sendo o caso mais significativo a metástase, a migração de células tumorais de uma região do corpo para outras regiões, que resulta numa diminuição da taxa de sobrevivência.

Deste modo, estudar e compreender melhor a migração celular revela-se essencial para compreender a doença do cancro e para desenvolver novas soluções, tanto de terapia como de prevenção desta doença. Da mesma forma, devido à importância que a migração tem na diferenciação de tecidos, um maior conhecimento na área pode levar a avanços em áreas emergentes como a medicina regenerativa e a reparação de tecidos.

Atualmente, os mecanismos de migração celular estão relativamente bem definidos a um nível conceptual. Para além disso, os avanços tecnológicos em técnicas experimentais, como técnicas de imagiologia e de medição de forças, permitiu a consolidação destes conhecimentos teóricos, assim como introduziu novas questões. No entanto, a tecnologia existente tem limitações, como os custos a ela associados e o tempo que consome.

A modelação e simulação aparecem, então, como estratégias que podem ser adotadas para ultrapassar alguns destes obstáculos, permitindo a recriação de cenários experimentais, ou o planeamento de novos estudos, numa menor escala temporal e com custos reduzidos. Também o poder computacional que tem vindo a estar cada vez mais disponível é uma vantagem para estes métodos, já que permite a criação e desenvolvimento de métodos mais robustos e complexos, associados a melhores resultados.

Esta dissertação consiste num estudo *in silico*, realizado através de um novo modelo computacional 3D que recria a migração celular, usando o Método dos Elementos Discretos e que inclui descrições discretas de componentes sub-celulares, mais especificamente adesões focais e filamentos de actina. Ainda, o modelo considera o efeito de forças no processo de migração e pretende explorar como mecanismos de mecanosensibilidade afetam o deslocamento das células e as forças exercidas pelas mesmas.

Através deste estudo, foi possível comprovar como os modelos computacionais podem ser usados para recriar cenários experimentais que seriam difíceis de replicar, e que necessitariam de métodos bastante sofisticados para a medição de forças a um nível sub-celular. Para além disso, o modelo permitiu descrever comportamentos encontrados na literatura e descritos por outros modelos, mas também revelou novas associações entre os mecanismos de mecanosensibildade em estudo e diferentes tipos de migração.

Abstract

Cell motility is essential to an organism's survival. From something as basic as a single cell being able to move towards food and moving away from hazardous conditions, to more complex processes, such as tissue differentiation, development and the immune response, all these phenomena share something in common: they rely on migration. However, it can also introduce problems in an organism's health, the most significant example being metastasis, the migration of tumour cells from a specific region to other parts of the body, resulting in a decrease in survival's rate.

Accordingly, studying and understanding migration reveals to be essential to comprehend cancer and to develop new solutions that can serve as therapy or prevention for this disease. Likewise, it is also a highly important key to understand tissue differentiation, hence contributing to advances in emerging fields like regenerative medicine and tissue regeneration.

Currently, migration mechanisms are relatively well-defined conceptually. Furthermore, new technological advances in cell imaging and force-measuring techniques have enabled scientists to strengthen the theoretical knowledge available and introduced new questions. Nevertheless, the existing technology has limitations, such as their costs and the time they consume.

Modelling and simulation strategies appear as a solution to overcome these limitations, as they enable the recreation of experiments, or the planning of new ones, within a reduced time scale and with lower costs. Moreover, with the increasingly available computational power, more robust and complex computational models have been developed, which provide better results.

This dissertation presents an *in silico* study performed through a novel 3D computational model of cell migration built using the Discrete Element Method, which describes the cell cortex as a Deformable Cell Model and includes discrete descriptions of subcellular components, notably focal adhesions and stress fibres. Besides, the model accounts for the effect of forces on migration and aims to explore how mechanosensing strategies associated with focal adhesions and stress fibres affect a cell's displacement and the forces exerted by the cell.

Through this study, it has been shown how computational approaches can be used to recreate experimental settings that would be difficult to achieve, and that would require sophisticated techniques to measure traction forces at a subcellular level. Moreover, the model has been able to capture behaviours described in the literature and by other models, but as also revealed associations between mechanosensing strategies under study and different migration phenotypes.

Para a Professora Edviges.

Agradecimentos

Aos meus pais, por terem confiado em mim e me terem apoiado desde o início desta jornada de ir embora para longe, para acabar num sítio mais longíquo ainda. Obrigada pelo rigor e pela sede pela excelência a que me habituaram, mas também por todo o apoio e carinho que nunca faltou. Também à minha avó, por tudo, mas em especial pelo "mau feitio" que não me deixa ficar indiferente e que me permitiu desbravar o caminho destes 5 anos.

To the Mechanobiology and Tissue Engineering group at KU Leuven, for letting me be part of such an interesting project and such an unique environment. To Hans, for the opportunity and his insights; to Tommy, for being always right; to Marie-Mo, for taking care of the members of the group; and, of course, to Diego, for all the support and all the lessons.

À professora Cristina Barrias, agradeço a forma como tão bem me acolheu no seu grupo e por todo o apoio dado, independentemente das dificuldades que a distância trouxe.

A quem me acompanhou neste percurso. Aos meus amigos, sejam eles Mitocôndrias ou (Bio)Tecos, obrigado por terem tornado estes 5 anos memoráveis. Ao meu curso, e aos Reis da Selva em particular, uma palavra de apreço. Ao NEB, ANEEB, CSB e Adapttech, obrigado por me terem dado a oportunidade de me superar e crescer... E pela Tuna Feminina de Engenharia não vai nada, nada, nada? Tudo!

À DéjàVu, por todas as horas. Todas as horas que passámos juntas a beber cafézinhos inofensivamente, e todos os maravilhosos hits que delas resultaram. Todos os momentos insólitos, mas muito funny. Todas as pequenas e grandes coisas em que, para além de uma amiga e de um refúgio, é para mim um exemplo de pura dedicação.

À Caricatura, à Next e à Play. Digam o que disserem, o que vivemos neste 5 anos foi hilariante e foi virtuoso. Foi saber rir de tudo e foi refilar sobre tudo. Foi tenso e foi triste. Foi uma razão de orgulho. Mas, acima de tudo, foi, e é, a verdadeira Amizade na Faculdade de Engenharia.

À LOK, por me ter ensinado e acompanhado desde o início, no bandolim e no curso (passando em ambas a subtil arte da aldrabice), e... bem, na vida académica, no geral. Por ainda ter paciência para escutar todos os meus dramas, mas, acima de tudo, pelo exemplo que é e por me fazer querer ser melhor e marcar os que me rodeiam da mesma forma como me marcou.

À Bela. Não sei como é que tu, no meio das tuas 50 crises de ansiedade diárias, me foste convencer a mim, no meio das minhas múltiplas crises existenciais, que ia ser capaz de ultrapassar estes 5 anos. Mas afinal tinhas razão, aconteceu. Ou se calhar aconteceu porque tu não me deixaste desistir. Mas pronto, é como o Tico e o Teco, nunca sei.

Por fim, (mas não menos importante). Desde o início do curso que nunca tive muitas certezas, mas havia duas a que eu gostava de me agarrar: Iria fazer Erasmus no 4º ano, e nunca, mas nunca, faria a tese fora. Obrigada, Universo, por me trocares as voltas quanto a ambas.

A todos, obrigada.

Inês Gonçalves

"E o resto que venha se vier, ou tiver que vir, ou não venha."

Álvaro de Campos, Tabacaria

Contents

1 Introduction **1**
- 1.1 Context . . . 1
- 1.2 Motivation . . . 2
- 1.3 Objectives . . . 3
- 1.4 Document Structure . . . 3

2 Background **5**
- 2.1 Cell Environment Sensing . . . 5
  - 2.1.1 The Extracellular Matrix . . . 5
  - 2.1.2 Cell-Substrate Adhesions . . . 6
  - 2.1.3 The Cytoskeleton . . . 7
  - 2.1.4 Signaling Pathways . . . 8
- 2.2 Mechanobiology . . . 9

3 Cell Migration **13**
- 3.1 Migration Modes . . . 13
- 3.2 The Migration Cycle . . . 14
  - 3.2.1 Protrusion . . . 15
  - 3.2.2 Adhesion . . . 16
  - 3.2.3 Contraction . . . 16
- 3.3 Characterizing Cell Migration . . . 16
  - 3.3.1 Imaging Techniques . . . 16
  - 3.3.2 Force Measurement . . . 17

4 Computational Models of Cell Migration **19**
- 4.1 Computational Modelling in Cell Biology . . . 19
  - 4.1.1 Continuum vs Discrete Modelling . . . 20
  - 4.1.2 Agent-Based Models . . . 20
- 4.2 Modelling Cell Migration . . . 21
  - 4.2.1 Cell Adhesions . . . 23
  - 4.2.2 Actomyosin Contraction . . . 24
  - 4.2.3 Protrusion and Other Dynamics . . . 24
  - 4.2.4 Whole-Cell Models . . . 25

5 Methodology **27**
- 5.1 Computational Model . . . 27
  - 5.1.1 Deformable Cell Model . . . 27
  - 5.1.2 Substrate . . . 29

5.1.3 Cell Anatomy . . . 29
5.1.4 Cell Adhesions . . . 30
5.1.5 Stress Fibers . . . 32
5.1.6 Fiber Contraction and Cell Detachment . . . 34
5.1.7 Equation of Motion . . . 35
5.2 Post-Processing . . . 35
5.3 Study Design . . . 36

6 Results and Discussion **39**
6.1 A First Look into the Simulated Cells . . . 39
6.2 Force-Independent Adhesions . . . 41
6.2.1 When Fibers Cannot Mature, Excessive Adhesion Hinders Migration . . . 41
6.2.2 The Strengthening of Stress Fibers Enables Collective Retraction, but Requires Long-Lived Adhesions and High Stiffnesses . . . 44
6.2.3 Summary . . . 46
6.3 Introducing Force-Dependent Lifetimes . . . 47
6.3.1 Maturation of FAs without Strengthening of SFs Further Inhibits the Cells' Migration Ability, Specially on High Stiffness Substrates . . . 47
6.3.2 Combining Both Mechanosensing Strategies Enables Collective Retraction in Physiological Conditions . . . 48
6.3.3 Summary . . . 50

7 Conclusions and Future Work **53**

A Parameters Used in the Simulations **55**

B Model Optimization **61**
B.1 Stress Fibers' Strengthening Optimization . . . 61
B.2 Fiber Relaxation and Cell Detachment . . . 62

References **65**

List of Figures

2.1 Environment Sensing Cell Components 6
2.2 Actin Filament Assembly Mechanism 8
2.3 Focal Adhesion Kinase Signalling Pathway 9
2.4 Focal Adhesions Maturation Process 11

3.1 Migration Phenotypes 14
3.2 The Migration Cycle 15
3.3 Traction Force Microscopy Imaging 17

4.1 Deformable Cell Models 22
4.2 Molecular Clutch Model 23

5.1 Diagram of the Proposed Model 28
5.2 Spring Model of the Focal Adhesions 31
5.3 Description of the Focal Adhesions Maturation Mechanism 32
5.4 Description of the Stress Fibers Strengthening Mechanism 33

6.1 Migration Patterns of the Simulated Cells 40
6.2 Final Displacement of the Simulated Cells 42
6.3 Results for $FA_{mat}OFF/SF_{str}OFF$ 43
6.4 Results for $FA_{mat}OFF/SF_{str}ON$ 45
6.5 Comparison Between the Simulations with no Focal Adhesion Maturation 47
6.6 Results for $FA_{mat}ON/SF_{str}OFF$ 49
6.7 Results for $FA_{mat}ON/SF_{str}ON$ 50
6.8 Comparison Between the Simulations with Focal Adhesion Maturation 51

B.1 Preliminary Results for the Stress Fibers Optimization Studies 62
B.2 Preliminary Results for the Stress Fibers Relaxation Mechanism 63

List of Tables

5.1 Values for Substrate Stiffness and FAs Disassembly Rate Used in the Study 37

A.1 List of Parameters Used in the First Period of the Simulation (Spreading) 56
A.2 List of Parameters Used in the Second Period of the Simulation (Migration) . . . 59

Abbreviations

AF Actin Filament

CSK Cytoskeleton

DEM Discrete Element Method

DCM Deformable Cell Model

ECM Extracellular Matrix

FA Focal Adhesion

FAK Focal Adhesion Kinase

IF Intermediate Filaments

Lm Lamella

Lp Lamellipodia

MT Microtubules

SF Stress Fiber

TCM Traction Force Microscopy

Chapter 1

Introduction

1.1 Context

Multicellular organisms are composed of cells found in a scaffold known as the extracellular matrix (ECM), which provides both biochemical and biomechanical cues for cellular movement. These cues, alongside the ability that cells possess to sense and transduce them into movement, lead to cellular migration, a phenomenon essential for a variety of biological processes, (Lauffenburger and Horwitz, 1996). For instance, during development, there are a series of morphogenetic events, which result in the formation of tissues and organs, that require cells to migrate in a coordinated manner, (Scarpa and Mayor, 2016). Likewise, in an adult organism, many phenomena depend on migration as well. Among others, these include angiogenesis, (Lamalice et al., 2007), tissue regeneration, (de Lucas et al., 2018), and the inflammatory response, (Luster et al., 2005). Being such an important process, when the migration mechanism fails to occur, several problems may arise, such as birth defects as well as autoimmune diseases and defective wound repair. Similarly, inappropriate migration can be hazardous, for instance, when it enables tumour dissemination, also known as metastasis, (Fletcher and Theriot, 2004).

Tumour cells can invade the lymphatic and blood system and circulate in them until reaching a new organ or tissue, where they proliferate. This is a critical step, that accounts for 90% of cancer mortality, (Mehlen and Puisieux, 2006), and that depends on the growth of the vascular network, through angiogenesis, to reach the tumours, easing the invasion process, and to supply them with the necessary nutrients and oxygen, as tumours could become apoptotic without these substances, (Nishida et al., 2006). Therefore, since both tumour cell spreading and vascularization of the tumour require migration and are a partial cause of cancer's mortality, new treatments could be developed hindering migration, (Folkman, 1995). This would have an important social and economic impact, as cancer is currently the second leading cause of death globally, according to the World Health Organization [1], and it has a high associated financial burden, including direct

[1] https://www.who.int/news-room/fact-sheets/detail/cancer

(treatment and rehabilitation) and indirect (productivity losses) costs, (Viegas et al., 2017). For example, in 2015 the direct costs related to cancer were $80.2 billion in the US alone [2].

A variety of other pathologies can also benefit from the study of migration and the development of new therapies based on this knowledge. Furthermore, tissue engineering and regenerative medicine are emerging areas that appear as a promise in medicine, with high social and economical impact, (Lysaght et al., 2008), to assist in the regeneration of wounds that are too deep to completely heal by themselves and in the development of substitutes for damaged organs, (Tabata, 2003). Both these areas, in order to produce scaffolds and biomaterials that promote the desired behaviour, rely on the understanding of morphogenetic events, and, subsequently, the understanding of the migration process and how the physical properties of the environment affect it.

1.2 Motivation

Migration has been fascinating scientists for over one hundred years, (Caton), but it was not always an easy task to study this phenomenon, mainly because of the lack of experimental techniques necessary to understand its chemical and mechanical components, as well as the feedback interactions they are involved in, (Danuser et al., 2013). In recent years, however, technological advances have enabled the development of molecular biology, imaging and force measuring techniques which provided a lot of new experimental data, shedding a new light on the migration process, (Prahl and Odde, 2018). Nonetheless, the quantity and complexity of this data require powerful tools to integrate the knowledge they may provide, (Mogilner et al., 2006). Thus, modelling appears as a solution to this issue, by enabling the creation of new frameworks, which could integrate experimental data, and be used to better understand migration.

For instance, modelling has provided scientists with the ability to recreate experiments that would otherwise be too expensive or too difficult to perform and has aided in experimental design as well as in predicting outcomes, (Liu et al., 2014), proving to be a good complement to experimental studies. Furthermore, with technological advances and the increasingly available computational power, modelling started reaching its full potential, allowing for faster solutions and the study of more complex problems.

Particularly in the study of cell migration, many models have been built, both to describe migration as a whole, and to characterize some of its components. However, there is still a need for whole-cell models that actively account for how tractions are exerted by a migrating cell, and how forces affect migration at a subcellular level, a field of study that has been of interest for the Mechanobiology and Tissue Engineering group [3], at KU Leuven. Accordingly, combining the experimental knowledge that has been developed in the group, (Izquierdo-Álvarez et al., 2019; Jorge-Penas et al., 2015), with computational tools also developed at KU Leuven, (Odenthal et al., 2013), there has been an effort to build cell migration models that meet these requirements, (Heck et al., 2019), and that can serve as frameworks for custom studies.

[2] https://www.cancer.org/cancer/cancer-basics/economic-impact-of-cancer.html
[3] https://www.mech.kuleuven.be/mechbio

1.3 Objectives

This dissertation aims to perform an *in silico* study to better understand the effects of force sensing mechanisms on cell migration. To do so, the study was conducted using a computational model that simulates a single cell migrating over a substrate, built using the Discrete Element Method (DEM) to create a triangulated mesh describing the cell surface, that was later further developed to simulate cell migration, with the inclusion of subcellular discrete structures, namely focal adhesions (FAs) and stress fibers (SFs).

Accordingly, the study presented in this document intends to characterize how migration occurs in the proposed model for different substrate stiffnesses and different turnover rates of the FAs, both when mechanosensing mechanisms are active, or not. Specifically, two mechanisms are considered: the maturation of FAs, that became stabilized in response to force; and the strengthening of SFs, which enables them to exert more force when their contraction ceases to occur.

1.4 Document Structure

Chapter 2 presents some prior knowledge to understand cell migration, and, particularly, how mechanical interactions affect migration. Accordingly, it is presented how cells interact with the environment they live in, as well as the main components that participate in and regulate this interaction, with the inclusion of some more specific insights on the effect of mechanical stimuli, particularly the mechanosensing mechanisms under study.

Chapter 3 integrates the ideas presented in Chapter 2 in the context of cell migration, providing an overview of the migration patterns cells may adopt, as a response to external cues. Additionally, some of the current experimental methods, namely imaging and force-measuring techniques, used to characterize migration are also presented.

Chapter 4 describes how computational modelling techniques may be applied to replicate biological systems, giving emphasis to the importance of discrete modelling to build models that account for the behaviour of specific subcellular components. Furthermore, this chapter characterizes the state-of-the-art of cell migration modelling, presenting models that specialize in one or two migration aspects, but also whole-cell models that provide a more comprehensive view of migration.

Chapter 5 exposes the implementation of the proposed computational model and how the obtained results were processed. Moreover, it presents how the study to explore the effects of mechanosensing was designed and implemented.

Chapter 6 presents and discusses the gathered results, with Section 6.1 showing the general migration patterns found in the simulated cells and Sections 6.2 and 6.3 focusing on the effect of the studied mechanosensing mechanisms. Section 6.2 reveals the effect of the strengthening of the SFs and Section 6.3, on the other hand, showcases the effect of the maturation of the FAs.

Chapter 7 summarizes the main conclusions drawn from this study, and presents some ideas that could be implemented to provide better results, as well as possible future work.

Chapter 2

Background

"A cell is not an island, entire of itself"

— Paul A. Weiss, Biologist

Migration is a cell's response to external cues. Henceforth, to fully understand this process, it is first crucial to have a basic notion of the cellular components and mechanisms that allow cells to sense the environment, and to respond accordingly. Also, in this study, a specific emphasis is given to the idea of mechanosensing, i.e. how mechanical stimuli influence the cell's behaviour. Thus, it is also required to acknowledge the effect forces can have on cells. With this in mind, the present chapter aims to provide a brief introduction to these concepts.

2.1 Cell Environment Sensing

Three main structures are responsible for environmental sensing: the ECM, which provides the chemical and mechanical stimuli sensed by the cell; the adhesion points between the cell and the ECM, where the major components responsible for signalling are located; and the cytoskeleton (CSK), which is connected to the adhesion points and reacts upon the signals they transfer. Fig 2.1 presents a visual description of these elements and how they are connected. Furthermore, the regulation of the communication between the cell environment sensing components relies on signalling pathways.

2.1.1 The Extracellular Matrix

The ECM is the non-cellular component present in all tissues, which not only serves as a physical scaffold but also interacts with cells, (Frantz et al., 2010). It can be divided into the basement membrane, a 2D substrate onto which polarized cells adhere, and connective tissue, a 3D fibrous scaffold, (Jansen et al., 2015). Although it is composed mostly of water, proteins and polysaccharides, the composition of the ECM largely varies from tissue to tissue, and can even vary inside the same tissue. It is this difference that generates the mechanical properties of each organ. Moreover, conditions such as age and the presence of a wound or a tumour can affect the ECM's structure

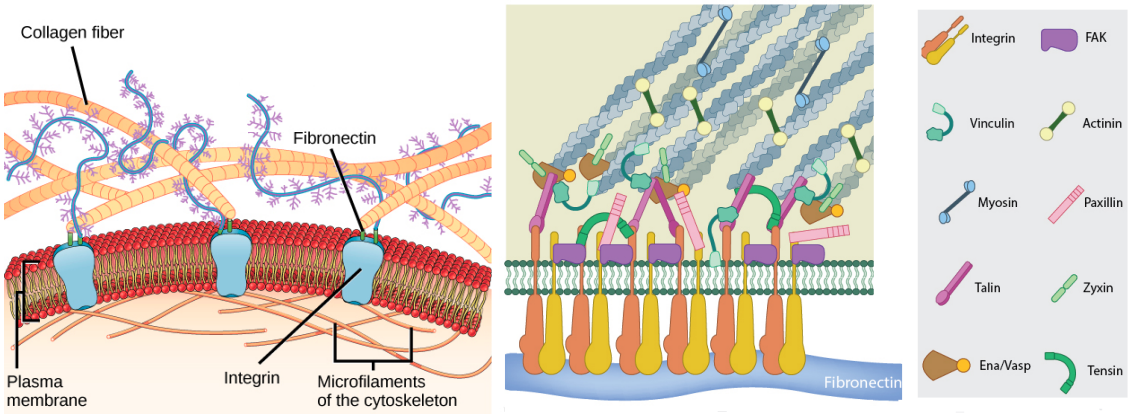

Figure 2.1: Representation of the components involved in cell environment sensing. The figure on the left shows a broader view of the cell-ECM interface, while the figure on the right presents a detailed description of the multiple proteins associated with the cell-ECM adhesions and how they are linked to both the ECM and the actin filaments of the CSK. Adapted from Openstax [1] and MBInfo [2].

and function. Generally, these factors promote fibrosis - the excessive deposition of fibrous connective tissue -, which makes the tissue less elastic, more rigid and generally mechanically weaker than younger or healthier ones, hence affecting the adjacent cells and subsequently promoting age-related diseases, (Kai et al., 2016).

Two main classes of macromolecules can be identified in the ECM: proteoglycans and fibrous proteins. Proteoglycans are molecules formed by glycosaminoglycans chains that are linked to a specific protein core and are extremely hydrophilic, which is essential for hydrogel formation. Thus, they occupy most of the interstitial space as a hydrated gel, which conveys properties to the matrix such as water retention and force-resistance, (Yanagishita, 1993). On the other side, there are four main different types of fibrous proteins: collagens, elastins, fibronectins and laminins. These also impact the matrix's functions and properties.

For example, collagen is the main fibrous protein in the ECM and is its main structural element, providing tensile strength and acting actively in cellular adhesion and motion. Elastin, on the other hand, is a very important protein in tissues that suffer repeated stretch, since it provides recoil. Finally, fibronectin is crucial in directing the ECM's organization and is also a mechanoregulator, as, when exposed to cellular forces, it unfolds, exposing cryptic integrin-binding sites.

2.1.2 Cell-Substrate Adhesions

Interactions of cells with their surroundings are mediated by different types of receptors. Among these, integrins are the best-characterized trans-membrane receptors, having an especially important role in interacting with the ECM and connecting it to the CSK, (Van der Flier and Sonnen-

[1] https://www.openstax.org
[2] https://www.mechanobio.info

berg, 2001). They are heterodimers, composed of an α and a β unit, linked through noncovalent connections, and are known to have large extracellular domains and short cytoplasmatic tails. Integrins function bidirectionally, transferring information from the inside to the cell to the outside, and vice-versa, (Hynes, 2002), and they bind to specific motifs within the matrix protein, like the RGD (Arg-Gly-Asp) motif, recognizing various ligands, such as fibronectin, collagen and laminin, as well as cell surface receptors, (Huttenlocher and Horwitz, 2011).

In spite of being a major part of this link between the ECM and the CSK, integrins are only part of multi-molecular complexes, which include proteins such as talin, vinculin and paxillin, broadly categorized as FAs. Depending on their size, morphology and maturation state, these can be divided into other subclasses, namely nascent adhesions, focal complexes, FAs, and fibrillar adhesions, (Vicente-Manzanares and Horwitz, 2011). FAs grow out of small dot-like adhesion sites, generally called nascent adhesions, that form at the edges of lamellipodia - a type of membrane protrusive structure, (Geiger and Bershadsky, 2001). These complexes later either disappear or mature into FAs, that, subsequently, can also disappear or further mature into fibrillar adhesions, stable structures involved in ECM remodelling, (Gardel et al., 2010).

2.1.3 The Cytoskeleton

The CSK is the cellular component that controls the shape and mechanics of the cell, (Fletcher and Mullins, 2010). It consists of three main types of filaments: intermediate filaments (IF), which provide mechanical strength and resistance to shear stress; microtubules (MT), responsible for determining the positions of organelles and directing intracellular transport; and, finally, actin filaments (AF), that determine the shape of the cell's surface and have an important role in cell migration, (de Mattos Coelho-Aguiar et al., 2015).

Actin monomers, also termed as globular actin (G-actin), under physiological conditions spontaneously polymerize into a helical arrangement, forming long and stable AFs (F-actin), (Pollard and Cooper, 2009). Polymerization can be divided into three sequential phases: nucleation, elongation and a steady-state phase, (Lodish H, 2000), as presented in Fig 2.2. Initially, monomers aggregate in a slow process, forming a stable nucleus of three or four subunits, to which other monomers can bind, elongating the filament in a more rapid mechanism. Based on the polarity of the filaments, which have a barbed (+) end and a pointed (-) end, elongation occurs more favourably at the barbed end, (Pollard and Borisy, 2003). The steady-state is reached when the concentration of available monomers decreases to a critical value and the rate of filament polymerization in the barbed end is equally balanced by filament disassembly in the pointed end. Thus, the filament moves forward but its length is kept constant, in a process usually termed as "treadmilling", (Le Clainche and Carlier, 2008).

Once multiple AFs are formed, bundles of filaments can evolve to create different structures, depending on their number and the types of proteins they attach to, such as myosins or filamins. For instance, protrusive structures can be generated (Mattila and Lappalainen, 2008; King et al., 2016), as well as SFs. SFs are large bundles of crosslinked AFs, usually anchored by FAs at one or both extremities, being classified as ventral or dorsal, accordingly, (Burridge and Wittchen, 2013).

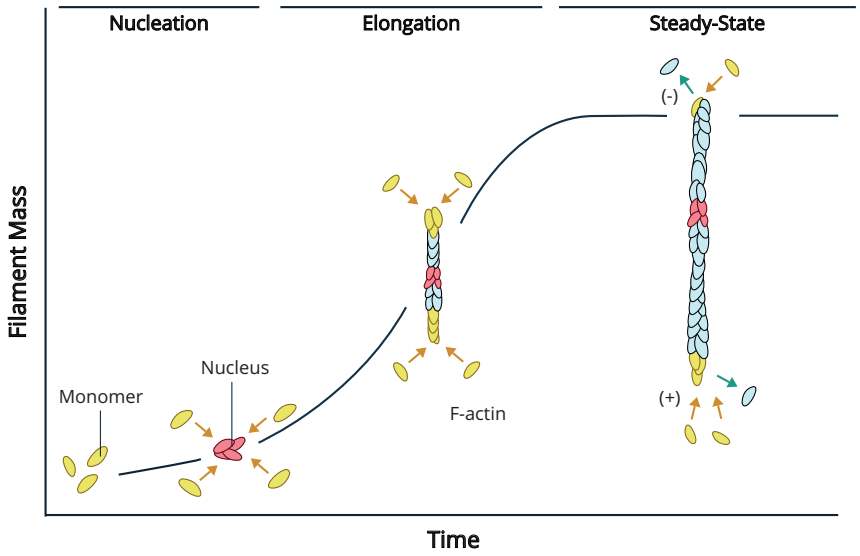

Figure 2.2: Representation of the described AF assembly mechanism. Adapted from (Lodish H, 2000).

However, they can also exist without being anchored and are considered as transverse arcs, in those cases, (Langanger et al., 1986; Naumanen et al., 2008).

SFs have a very relevant ability due to their association with myosin, that results in a sarcomere-like structure: similarly to muscle cells, they can contract, (Katoh et al., 1998). Specifically, in non-muscle cells this contraction mechanism can be explained by the stresses myosin II produces by moving directionally along the AFs, while pulling the filaments, (Dasanayake et al., 2011).

2.1.4 Signaling Pathways

External cues from the environment are recognized by intracellular structures through the activation of signalling pathways, (Devreotes and Horwitz, 2015). For example, cells can sense and move towards gradients of chemoattractants by the activation of G protein-coupled receptors (GPCRs), which in turn initiate signalling cascades that orient the cell in the gradient's direction, and also modulate cell-substrate adhesions to promote migration, (Cotton and Claing, 2009). Likewise, through receptors, cells may respond in similar manners to other types of gradients, such as electrical, gravitational or mechanical, (Cortese et al., 2014). Moreover, signalling networks may induce changes in the structure of adhesions and the CSK, hence influencing their behaviour.

Concerning adhesions, molecules such as talin and paxillin have an important role in determining their turnover rates, through the recruitment of focal adhesion kinase (FAK), (Mitra et al., 2005). FAK, in turn, not only recruits other proteins, which affect the assembly and disassembly of FAs, but also influences the formation of actin structures, through the regulation of Rho-family GTPases, as represented in Fig 2.3.

Rho GTPases are molecules that act as "molecular switches" to control signal transduction, mainly to regulate the remodelling of the actin CSK by affecting downstream effector proteins,

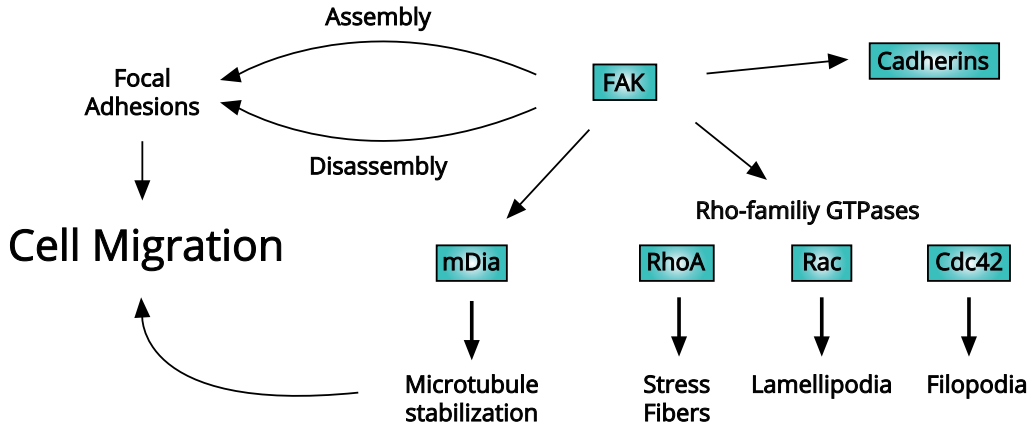

Figure 2.3: Diagram showing the effect of increased concentrations of FAK, that leads to the turnover of FAs and to interactions with the CSK (namely, the stabilization of MTs, as well as the formation of actin structures, influenced by RhoGTPases), which all lead to increased migration levels. In addition, FAK also influences cell-cell adhesions, through interactions with cadherins, proteins that mediate cell-cell junctions. Adapted from (Mitra et al., 2005)

(Ohashi et al., 2017; Raftopoulou and Hall, 2004). There are approximately 20 members of the Rho GTPases family, including RhoA, Rac1 and Cdc42, all of which are important during migration. Rho is associated with the contractility of the cell, the formation of SFs and the assembly of FAs, (Ridley and Hall, 1992), while Rac and Cdc42 induce actin polymerization in the cell front, (Tapon and Hall, 1997).

2.2 Mechanobiology

The effect of forces on biological systems tends to be more easily recognized at larger scales, when thinking about, for instance, how blood flows, how muscles contract and how the vertebrate skeleton allows for structural and locomotory functions. These questions are closely linked to the study of structure and motion and comprise a field of study traditionally denominated as biomechanics, (Hatze, 1974). However, in recent years, a new field in the interface between biology and mechanics has emerged, shifting the focus to smaller spatial scales, specifically to how cells actively respond to mechanical loading, and how it reflects on the tissues' maintenance and adaption mechanisms, (van der Meulen and Huiskes, 2002). This new field is called mechanobiology.

A more formal definition of this subject was provided by Carter et al. (1998), who described it as the study of how mechanical or physical conditions regulate biological processes. For instance, it has been shown experimentally that mechanical loading can promote bone remodelling, (Robling et al., 2006), and that the shape of a cell can influence its growth (Folkman and Moscona, 1978), among multiple other processes, (Eyckmans et al., 2011).

It is not unusual to find two distinct terms to define how forces act upon cells. On one end, there is mechanosensing, or, in other words, how cells sense the mechanical properties of the environment. On the other hand, there is mechanotransduction, or how cells are able to transduce

these signals into a chemical cellular response, (Eyckmans et al., 2011). Nonetheless, these are not static definitions and authors may reference mechanotransduction without disregarding the sensing mechanisms of the cell, or vice-versa. Thus, in this document, it was defined that the term "mechanosensing" would be used to define both the sensing and the transduction processes.

Forces in cells can be classified as active when they are generated by the cell (i.e. forces generated at the cell front by actin polymerization acting against the cellular membrane, or contraction forces exerted by SFs), or passive. Passive forces are related to the mechanical environment cells are located in. Cells that are part of a tissue experience contact and friction forces exerted by other cells and by the ECM, (Choquet et al., 1997) while cells found in a fluid (i.e., blood flow) are exposed to shear flow and pressure, (Tzima et al., 2005). Henceforth, these mechanical properties are important and should be characterized.

In a general manner, the mechanical behaviour of a solid material is defined by its deformation in response to applied forces, (Polacheck and Chen, 2016), which can be written as a function of stress (σ) - the ratio of the force (F) to the area of contact (A) - and strain (ε) - the change in the size of a material due to a force (ΔL) -, (Sugimura et al., 2016). This relationship is captured by Eq 2.1:

$$\sigma = \frac{F}{A} \quad \text{and} \quad \varepsilon = \frac{\Delta L}{L} \tag{2.1}$$

Additionally, in elastic materials the relationship between stress and strain is linear and is given by E, a material constant referred to as Young's modulus, or elastic modulus, defined by Eq 2.2:

$$E = \frac{stress}{stain} = \frac{\sigma}{\varepsilon} \tag{2.2}$$

whereas in nonlinear materials, such as the ECM, it is a function of strain, (Polacheck and Chen, 2016). In linear elasticity, or simplifications of non-linear environments, Hooke's Law ($F = kx$), which is usually used to describe the behaviour of a spring and how its length (x) changes in response to a force (F), which also depends on the stiffness of the spring (k), can be adapted to relate force and displacement in substrates, as described by Eq 2.3:

$$\sigma = E \cdot \varepsilon \tag{2.3}$$

Besides the mechanical properties of the ECM, FAs and SFs are also involved in mechanosensing, as it will be presented throughout this document, with an emphasis on two distinct mechanisms. Regarding FAs, as presented in Fig 2.4, the maturation of FAs, through which adhesions evolve from small nascent adhesions to mature FAs, is promoted by increasing forces, specifically forces exerted by AFs. As forces are applied, the adhesions undergo structural rearrangements

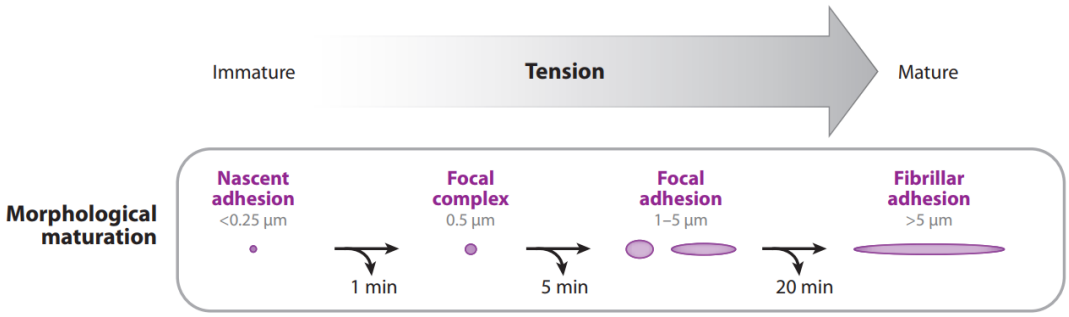

Figure 2.4: Diagram showing the morphological phases of adhesion maturation in response to increasing mechanical tension (gray arrow). At each of these steps, adhesion turnover can occur (curved black arrows) after a certain amount of time (timescale below each arrow). Adapted from: Gardel et al. (2010)

that lead to the recruitment of more proteins to the adhesion complex, promoting its growth, and to actin polymerization, that strengthens the link between FAs and the CSK, (Zaidel-Bar et al., 2004). Interestingly, though, not all types of bonds have their lifetime increased by an increasing load, with the opposite (i.e. an increase in force leading to faster disassembly of the FAs) also being possible, (Kong et al., 2009).

On the other hand, SFs have been shown to be able to adjust the forces they exert in response to substrate stiffness, (Wolfenson et al., 2016). This strengthening mechanism is based on the fibres' contraction level. When fibres are not able to keep shortening because they can no longer deform the substrate, α-actinin is recruited, hence resulting in a reinforcement of the fibre and in an increase in the force values it can exert.

Chapter 3

Cell Migration

Cells can adopt various migration patterns. However, three aspects are ubiquitous to different migration phenotypes: the formation of protrusions, the assembly of adhesions in the area of protrusion, and the retraction of the cell's rear. Thus, this chapter presents an overview of the different migration behaviours, as well as a more detailed explanation of these three mechanisms. In addition, some of the experimental tools used to characterize cell migration are also presented.

3.1 Migration Modes

Cell migration can be performed individually or collectively and it can be further classified according to the morphology of migration patterns, (Friedl and Wolf, 2010). Collective migration tends to be prevalent in physiological phenomena such as tissue regeneration and wound healing, (Mayor and Etienne-Manneville, 2016), and is generally a more complex process. In fact, although the mechanisms involved in both migration types are similar when it comes to motion, collective migration requires an extended chemical and mechanical interaction between cells, to, for instance, maintain tissue organization and propagate signals via cell junctions, (Trepat et al., 2012). Indeed, this increased complexity introduces some difficulty in understanding collective migration and further knowledge of individual cell migration and cell-cell interactions is needed in order to be able to move onto more advanced concepts as such.

Individual migration phenotypes are usually divided into two main groups: mesenchymal and amoeboid migration, as described in Fig 3.1. However, these definitions are extremes of a spectrum, and there are many mechanisms in between that tend to be considered as part of one of the groups, while still sharing some characteristics with the other phenotype, (Friedl and Wolf, 2010).

Amoeboid migration is characterized by rapid movements of the cell and constant changes in cell shape caused by protrusion and retraction, (Lämmermann and Sixt, 2009). Hence, it is the most used cell migration mechanism by highly motile cells, such as neutrophils and lymphocytes, which are present in the inflammatory response, as well as the amoeba, the eponym of the

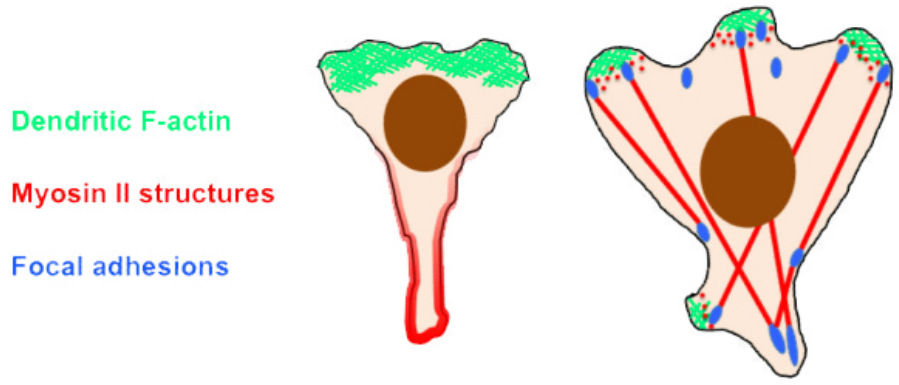

	Amoeboid	Mesenchymal
Migration speed	Fast, ~ 10 μm/min	Slow, < 1 μm/min
Polarity	Well-defined front and rear	Multiple, competing lamellipodia
Adhesion	Relatively weak, mostly intercellular	Strong, mostly ECM with well-defined adhesion complexes
Migration mechanics *in vivo*	Squeezing through pores in matrix/stroma	Traction via adhesion to ECM, matrix degradation as necessary
Organization of actin cytoskeleton	Thick dendritic actin network at the cell front; elsewhere, cortical actomyosin mediates contractility beneath the plasma membrane	Dendritic F-actin in lamellipodia; acto-myosin minifilaments mediate contractility behind the leading edge(s) and form thick stress fibers attached to focal adhesions

Figure 3.1: Comparison of the amoeboid and mesenchymal migration phenotypes. Adapted from (Bear and Haugh, 2014).

phenotype. The rapid movement of the cells is accompanied and facilitated by weak adhesion interactions with the substrate and strong polarization, that allow these cells to generate protrusions and squeeze through pores and small structures, (Lämmermann et al., 2008).

On the other hand, mesenchymal migration is a slower mechanism, commonly used by cells like fibroblasts, in which adhesions are relevant, as are the mechanical and chemical properties of the substrate, (Bear and Haugh, 2014). Moreover, cells may exhibit the ability to degrade the ECM and tend to be less polarized than in amoeboid migration, presenting multiple protrusions.

3.2 The Migration Cycle

Abercrombie (1980) was one of the first to consider separate experiments and compile them into a model proposal for cellular migration, consisting of a four steps cycle: protrusion of the leading edge, adhesion to the substratum, detachment of the adhesions at the cellular rear, and contraction of the cell, that leads to translocation (Figure 3.2). Moreover, although it was only introduced and understood later, a first stage has to occur before this cycle: cellular polarization - the generation

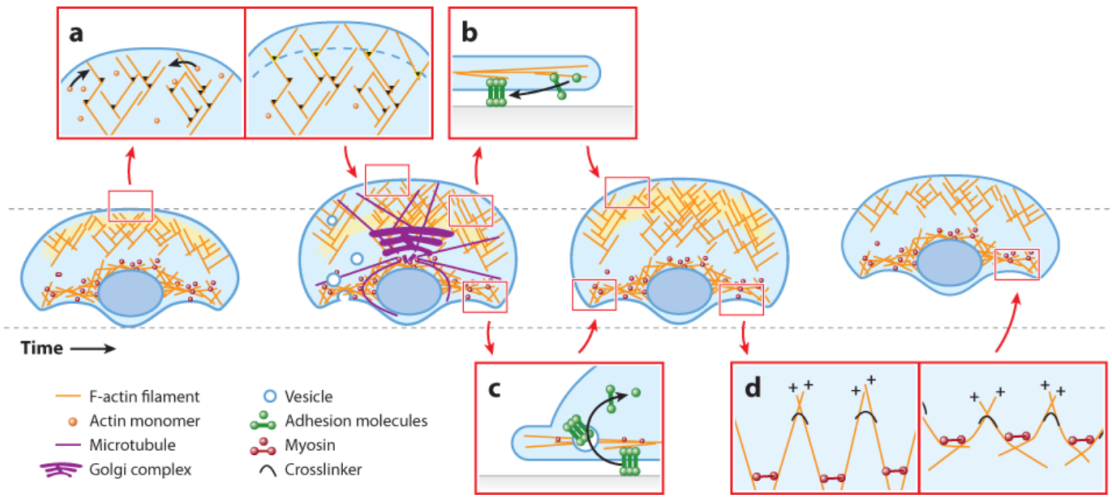

Figure 3.2: Representation of the migration cycle, divided into four steps: (a) protrusion promoted by actin growth; (b) formation of new adhesions; (c) release and recycling of adhesions at the rear; and finally, (d) actin-myosin-powered contraction of the cytoplasm, resulting in forward translocation of the cell body. Source: Danuser et al. (2013)

of cellular asymmetries, that form a well-defined front and rear, (Danuser et al., 2013; St Johnston and Ahringer, 2010). This happens both spontaneously, (Wedlich-Soldner and Li, 2003), and by the influence of extracellular cues.

3.2.1 Protrusion

Protrusion is the first step in the migration cycle, represented by (a) in Figure 3.2, and, in most cases, it involves the extension of cellular membranes to form protrusions such as filopodia and lamellipodia (Lp). Filopodia are long and thin protrusions, composed of tight parallel F-actin bundles, that cells use to probe the environment, (Mattila and Lappalainen, 2008). Lp, on the other hand, are leading-edge fan-shaped protrusions, containing a branched network of short actin filaments, also responsible for advancing on the substrate and sensing its properties, controlling whether the cell moves forward in the direction of the protrusion or if it should retract, (King et al., 2016; Tang and Gerlach, 2017).

The force necessary to move forward and push the cell membrane is provided by the polymerization of AFs against the membrane, (Pollard and Borisy, 2003). Accordingly, in the Lp, agents that potentiate polymerization have an important effect to keep protrusion active. For instance, actin-related protein 2/3 (Arp2/3), a nucleation factor that branches filaments, creates new barbed ends to which monomers can attach to. Similarly, cofflin severs filaments, which also creates new barbed ends, and, in addition, promotes depolymerization at pointed ends, thus generating free monomers that can attach to barbed ends, (Ponti et al., 2004).

3.2.2 Adhesion

During the second step of the cycle, represented by (b), cell adhesions at the front of the cell are formed. Without them, the membrane would resist to actin polymerization, which would promote retrograde actin flow, resulting in a slower protrusion rate, (Huttenlocher and Horwitz, 2011), hence making the migration process less productive.

As explained in the previous chapter, these adhesions start as small structures but mature to become strong and stable FAs, due to the force exerted by SFs on them. The emergence of strong adhesions results in a new area of the cell, the lamella (Lm), becoming visible at this point, (Ponti et al., 2005). This is an area with a width of 10-15 µm where there is almost no retrograde flow, since strong adhesions inhibit this process, and that, thus, has a more stable and less dynamic actin CSK than the Lp. Furthermore, myosin motors are found in the lamella, which makes it an important area for the contraction of the actin CSK, (Geiger et al., 2009).

3.2.3 Contraction

Finally, at the end of the migration cycle, represented by (c) and (d), the adhesions at the rear should detach and the actomyosin CSK should contract, promoting the retraction of the rear and cell body translocation. There is still a lack of knowledge in this area, yet, it has been proposed that the contraction of the CSK promotes the disassembly of cell adhesions by itself, (Crowley and Horwitz, 1995). Microtubules also target some adhesions and lead to their disassembly, alongside dynamin and focal adhesion kinase, (Ezratty et al., 2005), as do some proteolytic enzymes, (Huttenlocher et al., 1997). Furthermore, endocytosis, namely clathrin-mediated endocytosis, promotes recycling of integrins and other molecules present in FAs, thus regulating whether these adhesions persist or not, (Ezratty et al., 2009). It must be noted that coordination between CSK contraction and adhesion disassembly is extremely important to prevent ripping of the adhesions, which can lead to loss of the cell's integrity.

3.3 Characterizing Cell Migration

3.3.1 Imaging Techniques

The first studies on cell migration were based on the observation, and later on the recording, of shape changes, the direction of movement and the extension or retraction of cell protrusions, (Dormann and Weijer, 2006). These studies heavily relied on light microscopy techniques, which were later enhanced by the introduction of specific staining methods and contrast modes, that enable better visualization of specific cell components. Furthermore, technological approaches that can aid in automating the cell migration tracking process, such as image analysis techniques, significantly improved the precision of the process, (Huth et al., 2010). 3D imaging techniques such as confocal and deconvolution microscopy have also been important to both understand changes in the cell's structure, and that of its components, as well as to allow the creation of 3D reconstructions of cells.

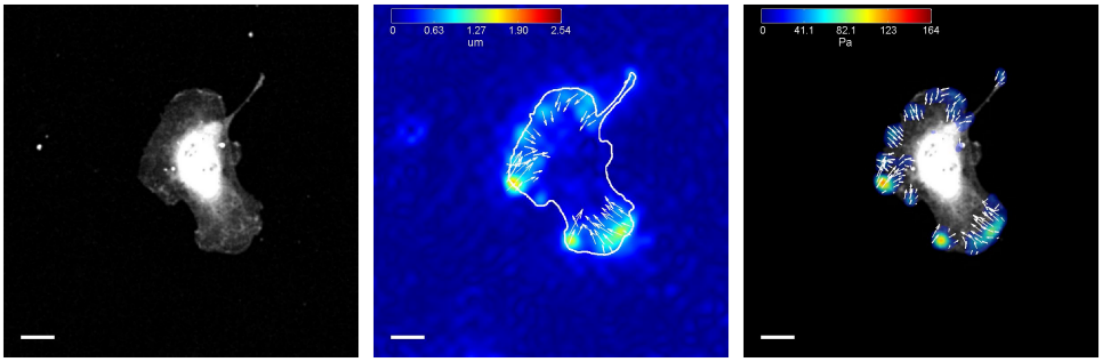

Figure 3.3: HUVEC on a polyacrylamide gel (stiffness 1.5kPa) coated with fibronectin with a concentration of 5µg/ml. Confocal image of the cell (left). Measured bead displacement (middle). Calculated traction values: Color indicates magnitude and arrows direction (right). Image provided by the Mechanobiology and Tissue Engineering group at KU Leuven.

Some examples of more specific techniques include fluorescence recovery after photobleaching (FRAP), commonly used to measure exchange dynamics, (Stephens and Allan, 2003), and that has been used to quantify actin dynamics in protrusions, (Lai et al., 2008), as well as FAs dynamics, (Webb et al., 2003); fluorescence resonance energy transfer (FRET), used to measure conformational changes in proteins and the dynamics of protein-protein interactions, (Periasamy and Day, 1998), enabling advances in the understanding of mechanisms involving RhoGTPases, (Donnelly et al., 2014); and total internal reflection microscopy (TIRF), used to study proteins associated with the plasma membrane, (Renkawitz et al., 2009), hence being used to measure adhesions dynamics, (Webb et al., 2003).

3.3.2 Force Measurement

In addition to visualizing how cells migrate, it is also important to measure the mechanical interactions between migrating cells and the substrate, namely the magnitude and direction of the exerted forces, (Munevar et al., 2001). One notorious example of force-measuring techniques is Traction Force Microscopy (TFM), a technique that calculates the forces cells exert on the surfaces they are located in, by measuring the deformation of the substrate, which can be related to the applied stress, if the mechanical properties of the substrate are known, (Style et al., 2014; Butler et al., 2002), as described in Section 2.2.

To perform this technique, fiducial fluorescent markers are inserted within a flexible substrate that is put under the cell, and their position is tracked, both with and without the cell, thus enabling the displacement's quantification, through particle tracking software, (Muhamed et al., 2017). Alternatively, cells can be cultured on micropatterned pillar substrates, which bend as cells exert forces on them, that can be calculated from the displacement of the tip, (Wang et al., 2002). Fig 3.3 presents an example of how tractions are calculated based on the displacement of markers, for a human umbilical endothelial cell (HUVEC).

Other force-measuring techniques include optical tweezers, (Wang and Ingber, 1995), magnetic twisting cytometry, (Neuman and Nagy, 2008), and Atomic Force Microscopy (AFM), or scanning probe microscopy. The latter consists in applying a controlled amount of force (pico to nano Newton level forces) on cell surfaces, using a cantilever with a sharp tip that probes the cell, (Alonso and Goldmann, 2003; Kuznetsova et al., 2007). In spite of being used mainly as an imaging tool, as it provides 3D images of a substrate's surface topography with sub-nanometer resolution, it can be adapted to act as a force-measuring technique, (Neuman and Nagy, 2008). Furthermore, the tip of the cantilever can be coated with a specific ligand, in order to study certain receptors individually, (Lehenkari and Horton, 1999). This idea of measuring forces at a specific area of the cell has also lead to the development of sophisticated biosensors that can identify how forces influence subcellular components, (Freikamp et al., 2016; Grashoff et al., 2010), being a very relevant advance in the study of mechanosensing.

Chapter 4

Computational Models of Cell Migration

"Essentially, all models are wrong, but some are useful"

— George E. P. Box, Mathematician

In spite of their undeniable value, theoretical and experimental studies have revealed to be insufficient to fully understand cell migration, and biological systems, in general. As a response to this issue, mathematical and engineering strategies were introduced to the biological field to create customizable models which could replicate cell behaviour, with reduced complexity, in order to conduct faster and less expensive studies. Therefore, this chapter aims to provide some basic concepts transversal to cell biology models, giving emphasis to discrete models, and present the state-of-the-art in cell migration modelling.

4.1 Computational Modelling in Cell Biology

In essence, a model is a simplified representation of a system, written as a set of rules. Hence, when building a model, the aim should not be to exactly mimic each component or relationship found in a system, but to distinguish which of them are both necessary and sufficient to describe its behaviour, (Noble, 2002). Of course, simplifications and assumptions should be clearly stated and justified, but they should not be regarded as an impediment, as some knowledge can still be drawn from models that, in some details, may not completely correspond to the reality, (Berro, 2018). For this reason, models may not provide exact answers, but they are a valuable complement to experimental studies.

Brodland (2015) indicates three major steps for the construction of a computational model: developing a concept, translating it into mathematical language and, lastly, converting it into a computational algorithm, or code. Indeed, not all models require to be implemented through a computational approach, as some can be solved analytically. Yet, computational power is an

invaluable tool to simulate complex systems, as was shown by the growth of the biological modelling field upon the technological revolution of the 1970s, when computers became more available, (Brodland, 2004). Henceforth, in this document, more attention is given to computational models.

4.1.1 Continuum vs Discrete Modelling

Traditionally, most computational modelling approaches can be grouped into one of two categories: discrete and continuum models. In continuum models, systems are described by a set of differential equations, solved using numerical methods commonly used in fields like structural mechanics, such as the Finite Element or the Finite Difference Method, (Zienkiewicz et al., 1977). These methods deeply rely upon homogenization techniques, which decrease the complexity of the model but also result in the loss of information at a small scale, (Gardiner et al., 2015). On the other hand, discrete, or agent-based, models are a more recent approach that accounts for the dynamics of spatially distinct entities, normally described by Newtonian laws, (Macal and North, 2005).

The choice of which of these descriptions better suits a specific problem relies on the scale of the problem under study, as well as the extent to which smaller components of the system will be modelled, (Smeets, 2016). As a general rule, if these components have a comparable scale to that of the problem, and the effect of individual components is relevant, then discrete models tend to be more adequate. Contrarily, if the difference in scale is large and the effect of individual components can be averaged and defined as a function, rather than a sum of each individual element, continuum descriptions of the system are justified, (Munjiza, 2004; Spill et al., 2015). In biology, many times continuum models disregard how cells act as individuals, characterizing tissue behaviour through macroscopic properties. More recently, though, multiple continuum models have been built to modulate changes in shape in single cells as a response to mechanical loading and some have even evolved to consider the active nature of cells, (Bansod and Bursa, 2015).

Yet, it is still not possible to account for small subcellular components and molecules, hence discrete models tend to be preferred in cell biology modelling. There is also the possibility to combine the continuum and discrete approaches, offering the reduced complexity of continuous models where detail is not necessary while providing lower scale information to certain parts of the model, (Dallon, 2000; Wakeland et al., 2007).

4.1.2 Agent-Based Models

Agent-based models can be further classified based on how elements interact with each other. Lattice-based models are characterized by elements connected by a spatial grid, or mesh, with a fixed neighbourhood, that allows for efficient computation. In spite of their popularity, mesh-based methods present some limitations, (Belinha, 2014). For instance, they are very dependent on the mesh's quality and may require remeshing to overcome numerical artefacts introduced by a fixed grid.

Particularly in cell biology, the scale of the problem under study is captured by how lattice sites represent cells. Large multicellular systems can be represented through meshes in which each element represents multiple cells, but, if smaller scales are required, a lattice site may be occupied by a single cell, or it can even occupy many of these sites, (Van Liedekerke et al., 2015).

A popular example of a lattice-based approach is the cellular automata model, mostly recognized in biology due to the work of Conway (1970). In his "Game of Life", the author developed a model where the state of a cell is defined by a set of simple rules, dictated based on the cell's neighbours state, resulting in complex behaviours and patterns. Another lattice-based approach used in cell biology is the Cellular Potts Model, in which cell states are defined based on a Monte-Carlo scheme, a technique that uses statistical simulation (i.e. random number sequences are generated and used to run the simulations, (Tenekedjiev et al., 2017)), to employ an energy minimization principle, (Scianna et al., 2013).

Lattice-free models, on the other hand, do not rely on a fixed mesh and are represented by moving nodes, with interactions between nodes being described by forces. Accordingly, the position of the particles can be calculated by solving an equation of motion, (Van Liedekerke et al., 2015), which makes them advantageous to model systems where mechanical interactions are important. Yet, although the disadvantages introduced by a mesh are not present, there is a significant increase in the necessary computational power.

Among lattice-free methods, there are models like the Brownian Dynamics simulations, an approach to study diffusion dynamics, commonly used to describe the assembly of structures such as the actin CSK, (Northrup and Erickson, 1992); Center-Based-Models, in which cells are modelled by their centres, and have an interaction radius, that dictates whether there is repulsion or attraction between two neighbouring cells, (de Back et al., 2019); and Deformable Cell Models (DCM), that describe cells as multiples nodes, connected through viscoelastic elements, providing the cell with a deformable structure with multiple degrees of freedom and, unlike in Center-Based Models, enables the inclusion of models of subcellular structures, (Van Liedekerke et al., 2018).

4.2 Modelling Cell Migration

As stated previously, Abercrombie (1980) introduced one of the first descriptions of the migration cycle, by combining different phenomena that were commonly studied individually, due to their high complexity. Similarly, many authors choose to focus on specific aspects of the migration process, resulting in is a vast and diverse literature on cell migration models that can then be combined to build multiscale models and reflect a comprehensive description of cell migration.

Yet, all of these models share a similarity: they rely on physical and conservation laws such as force balance and mass conservation laws, (Danuser et al., 2013). Concerning forces, it has been described in Chapter 2 that there are active and passive forces acting on a cell. Thus, models should account for the interactions a cell has with the substrate or with other cells, such as drag and friction forces, as well as internal forces for processes the model may consider, accounting for the fact that forces should be balanced and add up to 0, (Tanimoto and Sano, 2014).

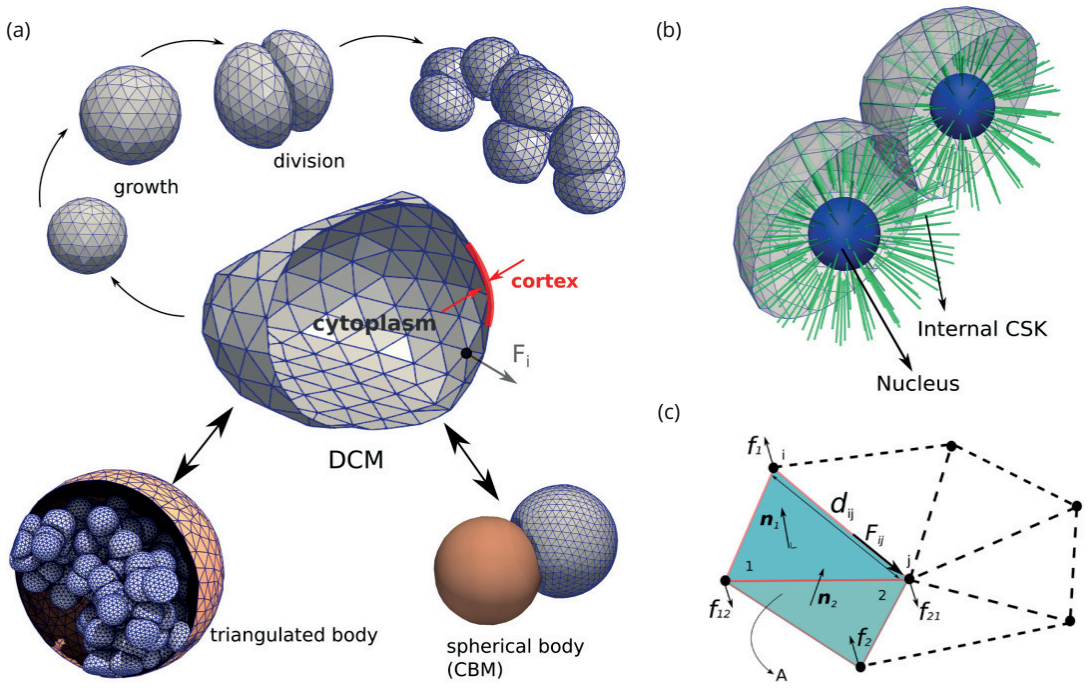

Figure 4.1: Representation of a DCM. (a) showcases the model's ability to grow and divide into multiple cells, as well as the types of interactions it supports (i.e. triangulated bodies and surfaces). (b) presents possible model extensions, to consider organelles in addition to the the cell cortex. (c) gives a detailed view of the way nodes are connected to form a triangulated mesh.. Adapted from (Van Liedekerke et al., 2015, 2018).

The effect of these forces on cell displacement is given by the equation of motion, which is based on Newton's second law, with Stoke's drag, written as Eq 4.1:

$$\vec{F} = m\vec{a} + \zeta\vec{v} \tag{4.1}$$

Inertial forces ($m\vec{a}$) can be neglected, as the environment in which cells live is characterized by a low Reynolds number, (Purcell, 1977), and motion is dominated by viscous forces. Accordingly, Eq 4.1, becomes a first-order equation for the position, that, for complex systems, can be solved by numerical methods, such as, for example, the Euler method, (Butcher, 2016).

Particularly, when modelling a cell through a DCM, as nodes are connected by viscoelastic connections, modelled through Kelvin-Volgt elements (i.e. a spring and a dashpot), the forces introduced by that system, specifically the springs, usually considered to be linear, and dashpots, have to be accounted for, (Özkaya et al., 2017). These forces are given by Eq 4.2:

$$\vec{F} = k(d - d^0) + \gamma\vec{v} \tag{4.2}$$

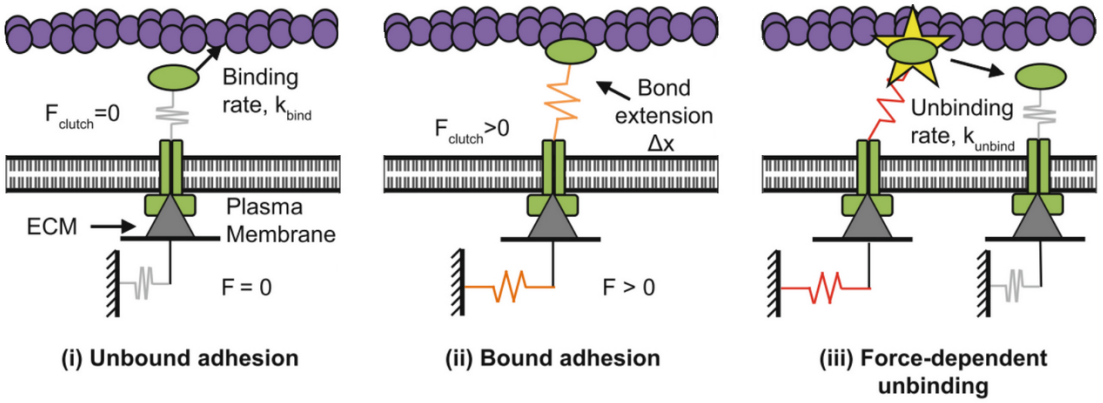

Figure 4.2: Representation of adhesion complexes (green) as molecular clutches that bind F-actin bundles (purple) to the ECM, through a connection modelled as a Hookean spring. (i) represents an unbound adhesion, disconnected from F-actin but bound to the ECM. As there is no force applied on the adhesion (F_{clutch}), the ECM is not deformed and the traction force on the substrate ($F_{substrate}$)) is zero. There is, however, a binding rate k_{bind} to which adhesions bind to the F-actin bundle, leading to (ii). Here, adhesions bind to the CSK, which applies a force on them, deforming the springs, and the force is transmitted to the substrate. Finally, (iii) represents how adhesions detatch based on an unbinding rate (k_{unbind}), which can be influenced by force, hence relaxing the load on the adhesion and the substrate. Source: (Prahl and Odde, 2018)

where the first term describes the force introduced by the spring, as already explained in Section 2.2, and the second characterizes the force introduced by the dashpot, with γ being the dissipation level and $\vec{v}$ is the relative velocity between nodes. Additionally, models can be developed with non-linear descriptions of the springs, such as the Finitely Extensible Nonlinear Elastic model, to better capture the nature of some materials, (Odenthal et al., 2013).

4.2.1 Cell Adhesions

Cell adhesions have been modelled as "clutches" that connect the actin CSK to the ECM, (Chan and Odde, 2008). To do so, adhesion complexes can be represented by a Hookean spring, connected in series to a deformable substrate, also modelled as an elastic spring, (Schwarz et al., 2006). The highly dynamic association and dissociation kinetics of cell adhesions can be described by stochastic events, using characteristic association and dissociation rates. Nonetheless, since it has been shown that force has a large effect on the dissociation of adhesions, models have been developed to adapt to this new idea of mechanosensing. Fig 4.2 presents a representation of this type of systems.

An early model of cell adhesion, that, to this day, is still one of the most relevant pieces of work in the area, was described by Bell (1978). It consists of a theoretical framework to study adhesion between cells mediated by reversible bonds, although it can be also applied to cells and a substrate, and it provided the conclusion that, with increasing force, the rate of dissociation of an adhesion exponentially increases, hence decreasing its lifetime. It was later introduced by Dembo

et al. (1988) that, despite being counter-intuitive, the opposite behaviour is also possible, i.e. the lifetime of an adhesion can be extended by force.

Therefore, adhesions can be classified according to how they respond to force. When force decreases the lifetime of an adhesion, it is classified as a "slip" bond. Contrarily, when force stabilizes the adhesion, thus increasing its lifetime, it is termed as a "catch" bond, (Dembo et al., 1988). In addition, a transition between "catch" and "slip" behaviours has been observed in some adhesions and it has been modelled, (Pereverzev et al., 2005). In these cases, force has a biphasic effect on lifetime. It starts by strengthening the adhesions, yet increasingly higher forces actually lead to detachment. Consequently, the longest lifetimes occur at an intermediate force.

The interaction between "slip" and "catch" behvaiours to define the dissociation rate (k_{off})in an adhesion i influenced by both modes can be captured by the the sum of two exponentials, each corresponding to a bond type, (Bangasser et al., 2013), as described by Equation 4.3:

$$k_{off,i} = k^0_{off} \exp[F_i/F_b] + k^0_{off,c} \exp[-F_i/F_b] \tag{4.3}$$

where F_i represents the force on an adhesion, k^0_{off} and $k^0_{off,c}$ are the dissociation and catch rate when no force is applied, and F_b and F_c are the characteristic rupture and catch force, respectively. Accordingly the first exponential refers to the slip behaviour, with force increasing the dissociation rate, whereas the second defines the catch portion of the bond, where force lowers the dissociation rate. The balance between the two terms is also given by force: when the force on the adhesion is low, the catch portion of the model dominates, yet, when it is high, the slip portion takes over, (Bangasser et al., 2013).

4.2.2 Actomyosin Contraction

The contraction of the CSK has been largely attributed to force transmission in SFs. Therefore, models have been built to consider a simple representation of a filament as a prestressed viscoelastic element connecting two adhesions or a single adhesion and an intracellular structure, such as the nucleus, (Hwang et al., 2012; Gouget et al., 2016). However, more complex models have been introduced, considering SFs as a series of discrete elements, namely a linear elastic spring, a linear viscous dashpot, and an active contractile unit all connected in parallel, (Chapin et al., 2014).

4.2.3 Protrusion and Other Dynamics

Protrusion caused by actin-filament dynamics, for example, started by being modelled through ratchet models, like the work proposed by Peskin et al. (1993), in which the growth and bending of actin filaments produced a force that was applied to the cellular membrane, pushing it and promoting protrusion. Nonetheless, the viscoelastic properties of actin are not defined by these models, hence creating a gap that was later resolved by new models, (Marcy et al., 2004). More current solutions tend to include both these aspects, in order to provide a more approximate view of what happens in reality, (Zimmermann et al., 2010). Mechanisms that do not rely on actin to

form protrusions, such as the formation of blebs and pressure-driven membrane extension, have also been modelled, (Bergert et al., 2012; Schreiber et al., 2010; Tozluoğlu et al., 2013).

4.2.4 Whole-Cell Models

One of the first and most influential whole-cell models was proposed by DiMilla et al. (1991), and considered cytoskeletal force generation, cell polarization and dynamic adhesion, with cell mechanics being characterized through a viscoelastic-solid discrete model. With this piece of work, it was concluded that there is a biphasic dependence on adhesiveness and contractility, meaning that both too-weak and too-strong adhesions, or contractions, affect migration negatively and that optimal migration efficiency is found at an intermediate level of these variables. In addition, their results were later confirmed experimentally, (Palecek et al., 1997; Rajagopalan et al., 2004).

Years later, Alt and Dembo (1999), developed a framework to study amoeboid migration through a continuum, two-phase fluid model with moving boundaries, that also considered interactions between the actin cytoskeleton and membrane proteins. Running 1D simulations of the model, the authors realized that, despite its simplicity, the model was able to produce typical features of cell motility, such as the existence of traction forces between cells and the substrate, ruffle formation and protrusion/retraction cycles. A similar continuum approach was introduced by Gracheva and Othmer (2004), but it additionally accounted for active forces promoted by actin polymerization and contraction.

Keratocytes have also been of interest to modellers, due to their simplicity: they have highly persistent migration patterns and do not present FAs nor SFs, although they have a contractile actin CSK, (Sambeth and Baumgaertner, 2001; Keren et al., 2008; Lieber et al., 2013). Nonetheless, models of keratocytes can still reach a high complexity level, when they consider multiple processes. For instance, Rubinstein et al. (2005) proposed a model that considers protrusion at the front of the cell, caused by actin polymerization, the mechanics of the actin network and contraction at the rear of the cell.

More recently, 3D models started gaining more attention. However, due to their increased complexity, many models decrease the system's complexity by modelling cells as vectors or spheroids, (Parkhurst and Saltzman, 1992), or by replicating 3D migration over a flat surface. For instance, Allena (2013) and Zeng and Li (2011) both present continuum models of 3D cells migrating over a substrate, but neither fully capture contraction of the actin CSK or the dynamic behaviour of FAs.

Kim et al. (2013) introduced some of the most advanced 3D models for cell spreading and migration behaviours, considering a deformable cortex, FAs dynamics, lamellipodia protrusion, CSK and nucleus remodelling, as well as actin contraction. Additionally, efforts have been made by the same group to account for a truly 3D environment, with surrounding ECM, and to include the idea of mechanosensing by adding rigidity sensing strategies in filopodia, (Kim et al., 2018).

Chapter 5

Methodology

5.1 Computational Model

The proposed computational model consists of a 3D migrating cell placed on a rigid substrate plane (see Fig 5.1). It results from the combination of a DCM model used to characterize the cortex of a cell and its contact with the substrate, previously developed by Odenthal et al. (2013), with additional methods to model the cell's anatomy and subcellular components. In addition, the models for the subcellular components were extended to consider mechanosensing, resulting in two possible mechanisms for each component, one without mechanosensing and one with.

The model was implemented through the particle-based framework Mpacts [1], developed by the Mechatronics, Biostatistics and Sensors (MeBioS) division of KU Leuven, which consists of a collection of C++ modules connected through a Python interface. Model parameters are listed along with their values and source of estimation in Appendix A. Formulation and implementation of the model are presented next.

5.1.1 Deformable Cell Model

The DCM used was originally built to describe the dynamics of initial cell spreading on a flat surface using red blood cells. However, here a non-specific cell should be considered and the system is initialized such that the cell is already spread at the begining of the simulation. At the start of the simulation, the cell is not in contact with the substrate, being in a round state, and the first simulated minutes, (T_{spread}), correspond to the cell becoming attached to the substrate, acquiring a spread state. From this point in time, the migration mechanisms start having a more relevant effect. Thus, in this study, since the focus is on migration and the spreading events are already well-characterized in (Odenthal et al., 2013), the initial period will not be considered.

The modelled cell is generated by subdividing an icosahedron and projecting the nodes onto a sphere with a radius (r_{cell}) of 8 µm, (Van Liedekerke et al., 2010), which, using five subdivisions, corresponds to a total of 2562 nodes. These nodes are connected, forming a mesh of 5120 triangles that represents the actin cortex of the cell underlying the cell membrane. Accordingly, in order to

[1] (http://dem-research-group.com)

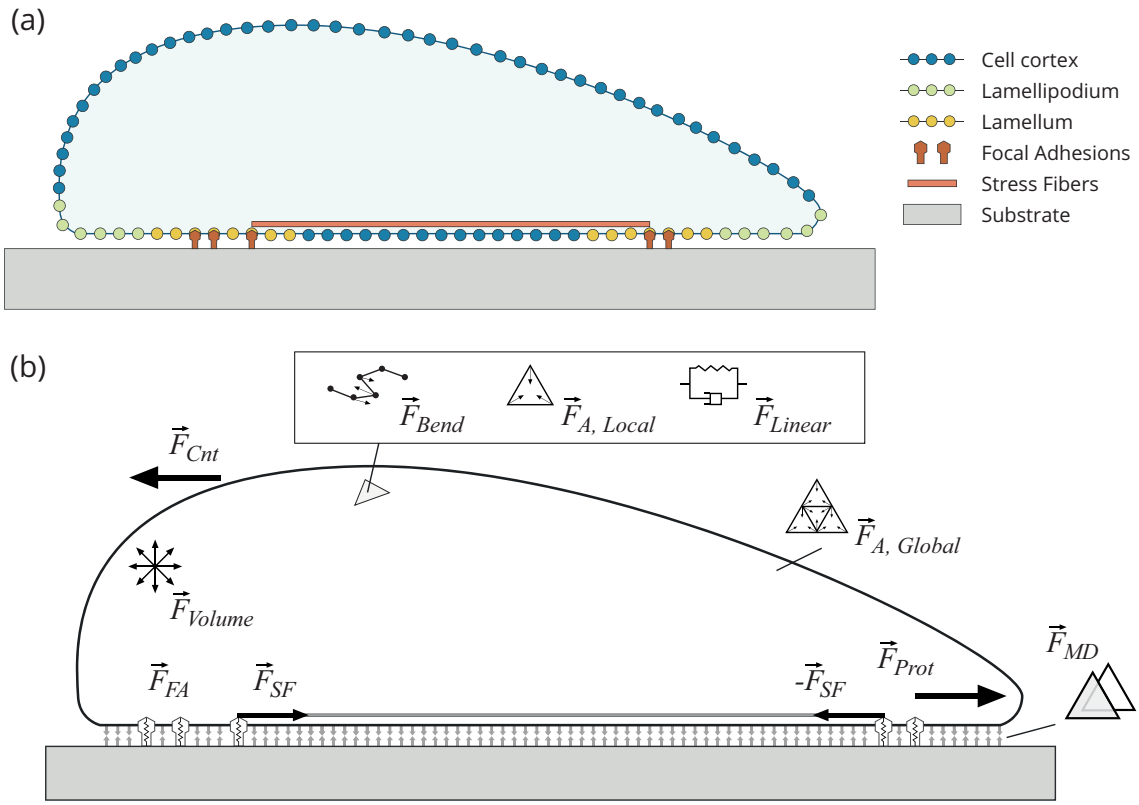

Figure 5.1: Diagram of the proposed computational model, with a visual description of the forces acting on the cell cortex ($\vec{F}_{Volume}$, $\vec{F}_{Bend}$, $\vec{F}_{A,\ Local}$, $\vec{F}_{Linear}$, $\vec{F}_{A,\ Global}$), the contact forces between the cell cortex and the substrate ($\vec{F}_{MD}$), the forces acting on subcellular components ($\vec{F}_{FA}$, $\vec{F}_{SF}$) and the forces introduced by the protrusion mechanisms at the cell front ($\vec{F}_{Prot}$, $\vec{F}_{Cnt}$).

capture the cell's viscoelastic behaviour, nodes are connected via Kelvin-Voigt elements, (Özkaya et al., 2017). A linear elastic spring is used, with Equation 5.1 describing the magnitude of the force acting on two vertices nodes, i and j:

$$F_{Linear} = k_{cortex}(d_{ij} - d^*_{ij}) \tag{5.1}$$

where d_{ij} and d^*_{ij} are the actual distance and the equilibrium distance between nodes i and j, and k_{cortex} is the spring constant of the cellular cortex. On the other hand, the magnitude of the force contributed by the dashpot is described by Equation 5.2:

$$F_{Dashpot} = -c\vec{n}_{ij} \cdot \vec{v}_{ij} \tag{5.2}$$

where c is the damping constant and $\vec{n}_{ij} \cdot \vec{v}_{ij}$ the projection of the velocity along the connecting axis between nodes i and j.

Additional forces defining mesh geometry include a local triangle area conservation ($F_{A,local}$),

a global cell area conservation ($F_{A,global}$), a cell volume conservation (F_{Volume}), and a resistance to bending based on the angle between the two planes defined by neighboring triangles (F_{Bend}). A mathematical description of these forces can be found in (Odenthal et al., 2013).

5.1.2 Substrate

The rigid plane substrate consists of two concentric rectangles of different dimensions and properties. The larger rectangle has dimensions of 170×45 μm^2 ($l_{ECM} \times w_{ECM}$) and the smaller inner rectangle has dimensions of 165×40 μm^2 ($l_{lig} \times w_{lig}$). Cell adhesion is only enabled in the inner rectangle. Both rectangles are triangulated using right isosceles triangles with area of 2.102 μm^2, in order to compute and record information on local forces and on the area of interaction between the cell and the substrate.

5.1.3 Cell Anatomy

The cell-substrate interface of the modeled cell includes two distinct parts, more specifically a lamellipodium and a lamellum, that dictate where the cell can potentially protrude and where FAs can be formed, respectively. The classification of the nodes into these areas is done based on the concentration of actin, $[G]$. Considering that actin polimerizes near the edge of the cell, it is necessary to identify the edges, which in the model correspond to triangles only partially in contact with the substrate, and set them as sources of this protein. Resembling retrograde flow, a diffusion constant (D_{actin}) defines how actin diffuses to other triangles. At every triangle actin is degradated. Accordingly, as triangles that are not at the edges of the cell only dissipate actin, without generating it, there is a gradient of actin concentration that is highest at the edge and decays along the bottom and top surfaces of the cell. The change in concentration of actin at each triangle is given by Equation 5.3:

$$\frac{\delta [G]_{\Delta i}}{\delta t} = k_{gen,\Delta i} - k_{deg}[G]_{\Delta i} - D_{actin} \oint \nabla \left(\frac{[G]_{\Delta i}}{A_{\Delta i}} \right) dl \tag{5.3}$$

where $k_{gen,\Delta i}$ is the rate at which actin is generated per surface area unit at the edge triangles of the cell, and k_{deg} the rate at which actin is degraded in all triangles. The third term in the right-hand side of the question corresponds to the change in concentration of actin at triangle i with area $A_{\Delta i}$ due to diffusion across the sides of the triangle l.

Having the actin concentration values, which is checked at every time point, classification is done by setting two threshold values for the Lp and Lm areas, $[G]_{Lp}$ and $[G]_{Lm}$: if $[G]_{\Delta i} > [G]_{Lp}$ then the triangle is part of the Lp, and if $[G]_{Lp} > [G]_{\Delta i} > [G]_{Lm}$ then the triangle is part of the Lm. Due to how the forces are balanced in the model, the cell adopts a more rounded state at the back, which induces a decrease in the size of the lamella. Therefore, to avoid an excessive reduction, the thresholds for the back of the cell were adjusted.

As actin polymerization promotes the extension of the cell membrane and the formation of protrusive structures, a force F_{prot} is applied to the triangles in the Lp based on its $[G]_{\Delta i}$ value,

to mimick this behaviour. However, acknowledging the polarization process cells go by, which causes the front of the cell to extend, and not other regions, this force is only applied to the triangles located at the front of the cell. A factor (k_{prot}) is defined to adjust the force value based on concentration, in a relationship defined by Eq 5.4.

$$\vec{F}_{prot,i} = \frac{k_{prot}[G]_{\Delta i}}{|\nabla[G]_{\Delta i}|}\nabla[G]_{\Delta i} \tag{5.4}$$

$\vec{F}_{prot}$ should not cause migration to occur, though, but only promote the extension of the cortex of the cell. Accordingly, a force $\vec{F}_{cnt}$ is applied to the cell's nodes, in the opposite direction, to counter the effect of the protrusion force, as described by Equation 5.5:

$$\vec{F}_{Cnt,i} = \frac{-1}{n_{nodes}}\sum_{j=0,i}\vec{F}_{Prot,i} \tag{5.5}$$

To confirm that the protrusion forces were not having a significant effect on migration, the force exerted by the Lp was quantified. $[G]_{\Delta}$ values range between 0.28 and 1.5 molecules/μm^2, with the average value of $|F_{prot}|$ per triangle being about 0.12 nN. As each triangle has an area of 1 μm^2, and the entire Lp amounts to an area of approximately 160 μm^2, the front Lp exerts 18.5 nN. Indeed, per triangle, the protrusion force nears experimentally observed maxima (0.15 nN), (Gardel et al., 2008), and is one order of magnitude lower than that exerted at a FA by the CSK.

5.1.4 Cell Adhesions

Two types of adhesions are modeled: non-specific adhesions and FAs. Non-specific adhesions are attributed to integrin-ligand bonds, which, without reinforcement, are transient, weak and evenly distributed. Accordingly, they are modeled by triangle-triangle attraction when a minimum distance is met, and scaled by the area of interaction, as described by the Maugis-Dugdale theory, (Maugis, 1992). An in-depth description of how Maugis-Dugdale theory has been applied in this context can be found (Odenthal et al., 2013), but a brief summary is provided. In this theory, interactions are described based on spherical overlap, so interaction force ($\vec{F}_{MD}$) between a surface and its surroundings, which ensures cell spreading, is computed as the interactions between two spheres corresponding to two triangles in contact. These spheres have a Young's modulus (E_c and E_s for cell and substrate respectively) and a Poisson's ratio (ν_c and ν_s for cell and substrate respectively). Curvatures are defined by fitting a sphere to each triangle. Maugis-Dugdale theory includes both a Hertzian elastic interaction for a radius of interaction a (based on sphere overlap), and an extended radius b (where $b > a$) in which an attraction potential is defined. The attraction constant for this potential is defined for cell-substrate (W_{cs}).

Regarding the FAs, they are represented by Hookean springs, more specificaly a system of two springs in series connecting a point in the substrate j to a cell node i . One of the springs represents

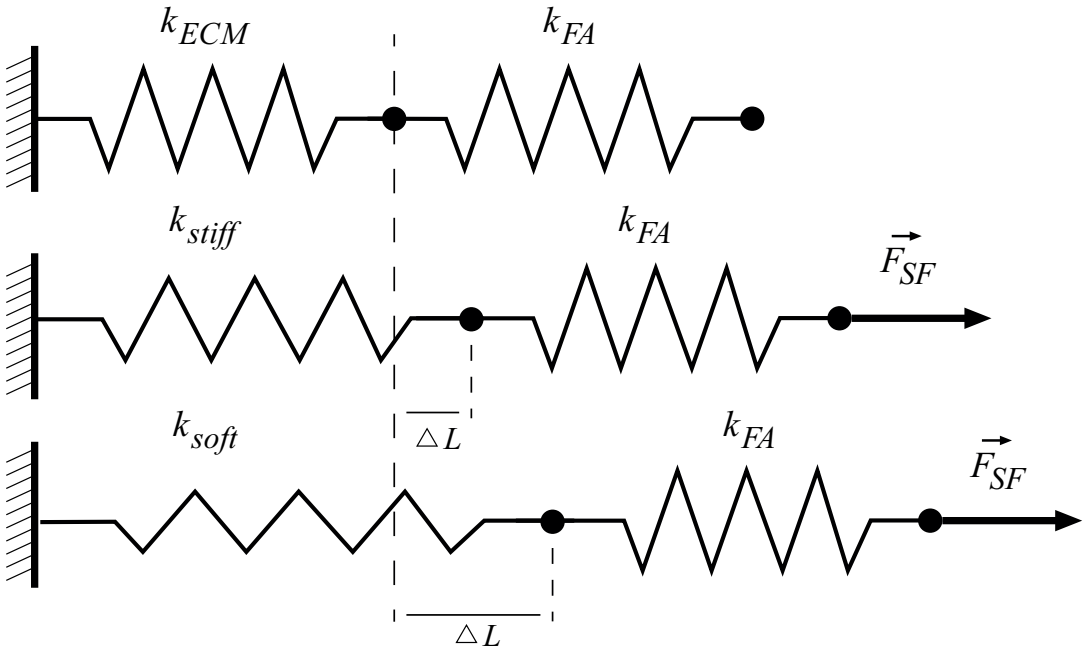

Figure 5.2: Spring system representing the deformable ECM and the FA connecting it to a node of the cell boundary. The figure shows how the system deforms by application of force through a SF, ($\vec{F}_{SF}$). Assuming that $k_{FA} \gg k_{ECM}$, depending on the stiffness of the ECM, different deformations are expected for the same exerted force.

the FA while the other represents the ECM, and the force carried by the system at node i ($\vec{F}_{FA,i}$) is described by Equation 5.6:

$$\vec{F}_{FA,i} = \left(\frac{1}{k_{FA}} + \frac{1}{k_{ECM}}\right)^{-1} \left((L_{FA,0} + L_{ECM,0}) - L\right) \vec{n}_{ji} \tag{5.6}$$

where $L_{FA,0}$ and $L_{ECM,0}$ are the equilibrium lengths of the FA and the ECM ligand fiber, respectively, and L is the length at each corresponding time step. $\vec{n}_{ij}$ is the unit vector in the axis that runs from point in the substrate j and node i. Finally, k_{FA} and k_{ECM} are the spring stiffnesses for the FA and the ECM, respectively. Here, adhesions are considered to represent strong and mature FAs, with the forces applied being able to deform the ECM. Thus, the assumption that $k_{FA} \gg k_{ECM}$ is made, which means that the system's force response will be dictated by the substrate stiffness. Fig 5.2 presents how this system responds in function of the force exerted by the SFs.

FAs can be formed by a node in the Lm area, if in proximity of a binding target, that is, any point of the inner rectangle of the substrate, as long as it is within a distance ($L_{FA,max}$) of 0.075 µm the plane. Moreover, formation and disassembly of adhesions is implemented as a stochastic process, with assembly being determined by a binding rate ($r_{on,FA}$), that dictates how often adhesions are formed on average. Likewise, a rate dictates how often adhesions are disassembled ($r_{off,FA,i}$). Due to the polarization of the cell, this disassembly rate in the back Lm is twice as large as the rate in the front Lm. Once a FA is disassembled, in case it has lived for a minimum period of time

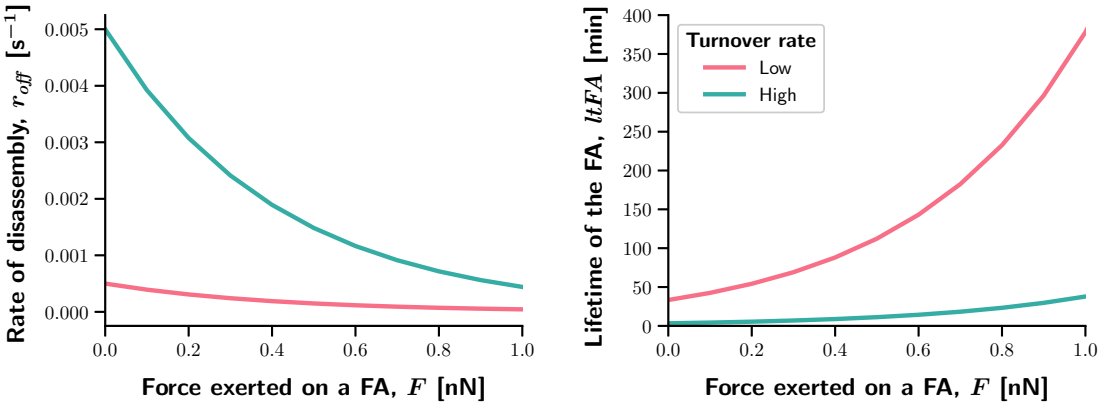

Figure 5.3: Evolution of the FAs rate of disassembly (left) and lifetime (right), in response to force, based on the implemented mechanosensing mechanism. As the model aims to replicate a "catch" bond, the disassembly rate decreases exponentially with increasing force, meaning that force stabilizes the FAs, and increases their lifetime.

lt_{mat}, the corresponding node undergoes a time period, termed refractory (lt_{ref}), representative of the time it takes for that area of the cortex to be able to form a new adhesion. In addition, there is a maximum force a FA can endure (F_{rup}), rupturing when that value is reached. In that case, the FA detaches and enters the refractory time period.

5.1.4.1 Mechanosensing of the FAs

The first mechanosensing strategy to be introduced is an extension to the disassembly rate of the FAs. Rather than being kept as a constant value, this rate is made dependent on the magnitude of the force carried by the adhesion. More specifically, replicating findings that show that FAs transduce the force applied on them and recruit proteins that stabilize the adhesion, (Elosegui-Artola et al., 2016), the rate of disasssembly is set to decrease in response to increases in force. The exact relation between these two variables is captured by Equation 5.7, which is based on modeling of catch bonds, (Bangasser et al., 2013):

$$r_{off,FA,i} = r^0_{off,FA} \exp\left[-\frac{\zeta_{FA}\left\|\vec{F}_{FA,i}\right\|}{F_c}\right] \tag{5.7}$$

where r^0_{off} signifies the rate of disassembly when no force is carried by and adhesion, and ζ_{FA} and F_c are parameters that control the effect in magnitude that mechanosensing has on the rate of disassembly.

5.1.5 Stress Fibers

SFs connect two discrete adhesions and apply on them a pair of opposite and equal forces, which pull the adhesions together, simulating the effect of myosin II motors sliding along the antiparallel

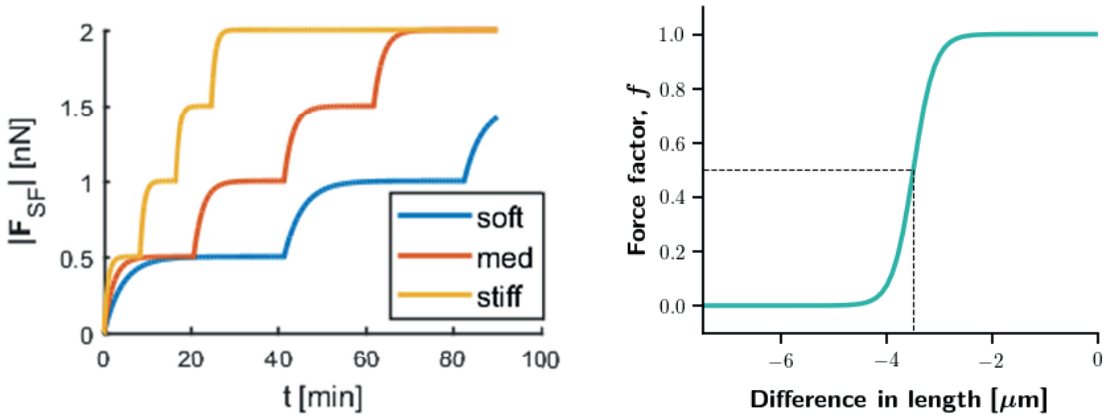

Figure 5.4: Representation of the modelled mechanosensing mechanism for the SFs (left), with fibers being able to exert more force as a response to their ability to deform the substrate (i.e. in stiffer substrates SFs contract less and strengthen faster than in softer substrates). The figure on the right presents the force adjustment function implemented to describe the relaxation of the SFs upon large contraction levels.

actin bundles of the SFs. These forces have a set force magnitude (F_{am}, where *am* stands for actomyosin) and are applied until the SFs are removed. Removal of the SFs occurs when they become detached on both ends. In order to be created, a potential fiber connecting two random adhesions needs to meet all of the following conditions:

1. The selected adhesions are not bound to an existing fiber;
2. The fiber has a minimum initial length (L^0_{fib}) of 8 µm;
3. The angle formed by the fiber and the long side of the rectangular pattern (θ_{fib}) is not greater than $\pi/10$ rad.

The last two conditions were set based on the model's geometry and observations found in the literature stating that fibers will only form along the long axis of a rectangular underlying pattern, (McCain et al., 2012; Polio et al., 2012).

5.1.5.1 Mechanosensing of the SFs

The second mechanosensing mechanism proposed is based on the work by Wolfenson et al. (2016) and extends the model to consider fiber maturation, or, in other words, a fiber's ability to recruit α-actinin molecules to FAs when it can no longer deform the substrate, resulting in an increase in the force the fiber can exert. Accordingly, stiffer substrates, which are more difficult to deform, will promote maturation, and, consequently, higher tractions will be generated.

In order to implement this strategy, the length of a particular fiber f is monitored at every time step, and a threshold (L_{thr}) was set to define the minimum value the change in length can assume.

Once it falls below that threshold, it is assumed that the distance between adhesions has ceased to decrease and that the fiber will be reinforced, to be able to exert more force. Henceforth, the factor by which the force is multiplied ($n_{str,f}$) is increased. The force exerted by stress fiber f on node i, when connecting nodes i and j, is described in Equation 5.8:

$$\vec{F}_{SF,i} = n_{str,f} F_{am} \vec{n}_{ij} \tag{5.8}$$

where $\vec{n}_{ij}$ is the unit vector in the axis that runs from node i to node j. When a fiber is formed, the value for $n_{str,f}$ is set as 1, and it is increased by the value of 1 every time the change in length of the fiber reaches the defined threshold. Yet, a maximum of 5 is set to $n_{str,f}$, as there is a limit to the force exerted by a SF.

5.1.6 Fiber Contraction and Cell Detachment

As fibers are able to exert more force, it is expected that the associated FAs, when able to mature with force, will live for long periods of time. However, as further discussed in Appendix B.2, once the cell's rear is retracted, excessive adhesion to the substrate actually hinders the cell's ability to migrate. Accordingly, in concordance with the idea that fiber strain induces the reorganization of the CSK, i.e. the disassembly of existing SFs and assembly of new ones, (Sato et al., 2005), the model was extended to overcome this issue. Hence, a factor f, by which force is multiplied, is introduced in Eq 5.8, to decrease the force exerted by the fiber in response to a change in length. f is modeled as a logistic curve: for a small change in the fiber's length, the factor is kept at a value of 1, allowing for contraction to promote the SFs strengthening, but, for a shortening value F_{f50}, the factor is halved and then decays to 0, so that force no longer extends the adhesions' lifetime. A representation of this function in terms of the change in length is presented in Fig 5.4 (b) and it can be defined by Eq 5.9:

$$f = \frac{1}{1 + \exp\left(-\mu\left(\Delta L_{fib} + F_{f50}\right)\right)} \; ; \; \Delta L = L_{fib}(t) - L_{fib,0} \tag{5.9}$$

where ΔL represents the difference between a fibers length at a time t, ($L_{fib}(t)$), and its initial length, ($L_{fib,0}$), and μ is the steepness of force decay with shortening. Adding this factor to 5.8, the equation becomes Eq 5.10:

$$\vec{F}_{SF,i} = n_{str,f} F_{am} f \vec{n}_{ij} \tag{5.10}$$

When a retraction event occurs in mesenchymal cells, the back of the cell is retracted and, subsequently, the cell has the ability to extend its edge, moving forward. However, if the FAs at the front of the cell are stabilized and do not detach, the nodes at the front of the cell do not have the flexibility to advance in space and create new adhesions at the front. In other words, the cell

becomes stuck. Consequently, to avoid this from happening, the number of deleted fibers in the last 60 seconds is tracked, and a threshold $nFib_{thr}$ is set to define a full retraction event. If the number of deleted fibers is larger than this threshold, all the FAs are deleted, in order to allow the cell to spread again and, consequently, move forward.

5.1.7 Equation of Motion

Given that cells live in environments with a low Reynolds number, (Purcell, 1977), inertial forces are negligible. Thus, the equation of motion of each node i takes the form of Equation 5.11:

$$\sum_{conn.\ j} \vec{F}_{Linear,i} + \vec{F}_{A\ Local,i} + \vec{F}_{A\ Global,i} + \vec{F}_{Volume,i} + \vec{F}_{Bend,i} + \sum_{triangles\ l} \vec{F}_{MD,i} + \vec{F}_{FA,i} + \vec{F}_{SF,i} + \vec{F}_{Prot,i} + \vec{F}_{Cnt,i} = \sum_{conn.\ j} c(\vec{v}_i - \vec{v}_j) + \sum_{triangles\ l} (\Gamma_{substrate,norm}\vec{v}_{norm,i} + \Gamma_{substrate,tan}\vec{v}_{tan,i}) + \sum_{triangles\ l} \Gamma_{cell}\vec{v}_i + \Gamma_{liquid}\vec{v}_i \tag{5.11}$$

The left-hand side contains the sum of all forces acting on a node. The linear force due to the springs in the Kelvin-Voigt model are summed for each node over all connections (conn.). For the Maugis-Dugdale force, as it acts on the triangles in the mesh, forces are transfixed to the nodes, (Odenthal et al., 2013). The right-hand side of the equation shows how proportionality between the sum of forces acting on node i and its velocity ($\vec{v}_i$) is determined by the drag acting on the node. This corresponds to dissipation of the actin cortex by all dampers j connected to node i, friction due to contact with triangles the other cell (Γ_{cell}) or with the substrate in the direction normal ($\Gamma_{substrate,norm}$) and tangential ($\Gamma_{substrate,tan}$) to the contact, and stoke's drag (Γ_{liquid}). For contact with the substrate, friction is calculated separately in the normal and tangential directions to the contact to ensure cells do not detach form the substrate. To calculate the friction due to contact with triangles, friction coefficients ($\Gamma_{substrate}$ and Γ_{cell}) are weighed according to distance of node to the contact point, (Odenthal et al., 2013).

Equation 5.11 is a first order differential equation that couples the movements of all nodes. The system is solved iteratively for the velocities using the conjugate gradient method. The positions of the nodes are updated by using a forward Euler scheme, (Tijskens et al., 2003). A time step of 0.05 s was used in all simulations.

5.2 Post-Processing

The analysis of the outputs returned by the computational model presented in 5.1 was conducted using two distinct frameworks, with different purposes. At an initial stage, data visualization and exploration was primarily done in Paraview [2], a piece of software specialized in large data visualization and analysis. Furthermore, in order to complement the observations made in this stage, and to further characterize the insights obtained about how the model was behaving, a quantitative data analysis was performed in Python.

[2] https://www.paraview.org/

In this analysis, six metrics were extensively studied: the displacement of the cell, the actual lifetime of the FAs, the strengthening factor of the SFs, the number of FAs, the number of ruptured FAs (FAs that disassembled due to a value of force higher than F_{rup}) and the traction exerted by the cell on the substrate. All of the aforementioned metrics at each recorded time point are direct outputs of the model, with the exception of displacement and traction, which require further calculations.

Displacement is obtained through the position of the centre of mass of the nodes in the cell-substrate interface for each time point of the simulation. As the simulated cell moves along an axis, in this case, the x-axis, displacement was calculated by measuring the differences between the cell's x-coordinates at consecutive time points, and summing up their values. In terms of traction, values are obtained for each substrate triangle based on the sum of forces ($\vec{F}$) acting on FAs bound to that triangle, as described by Equation 5.12:

$$\vec{T}_{tri,i} = \frac{1}{A_{\Delta,i}} \sum_{j=0,\ n_{FA,j}} \vec{F}_i \tag{5.12}$$

where $\vec{T}_{tri,i}$ is the traction value on a triangle i, $A_{tri,i}$ is the area of that triangle and $n_{FA,j}$ is the number of FAs bound to the triangle. Total traction, the metric that will be studied in detail, is given by the sum of the magnitude of the tractions for all substrate triangles.

A representative value of each metric for the total time of the simulation was also calculated, as to ease comparisons between samples. Since both the displacement of the cell and the number of ruptured FAs are cumulative quantities, their representative value is the value at the end of the simulation. For the remaining metrics, as they are average values of the existing FAs and SFs at a certain time point, the representative value is computed for the time periods where the migration step is stabilized. When there is no detachment of the cell (see Sec 5.1.6), this period corresponds to the last 800 minutes of the simulation, for which the mean value of each metric is computed. Contrarily, when cells are forced to detach, their migration step is stabilized before detachment, but, upon that event, it is interrupted and cells need time to rebuild structures and reach the stabilized state once again. Thus, the best representation of their stabilized Lm is in the moments immediately before the cell is detached, and the representative value is given by the average of values immediately before all the detachment events the cell undergoes.

5.3 Study Design

This study aims to understand how the maturation of FAs and the strengthening of the SFs affect force exertion and displacement in a migrating cell. Thus, different stiffness values ($kECM$) and FAs disassembly rates ($r^0_{off,FA}$) were selected to study how cells respond to substrates with different properties. Although the rate of disassembly is not a property of the substrate, it can be thought of as representative of the affinity the cell has with the substrate: cells with long-lived adhesions should be able to adhere to the substrate better, whereas cells with short-lived adhesions should

Table 5.1: Values for substrate stiffness ($kECM$) and FAs disassembly rate ($r^0_{off,FA}$) used in the study. In addition, disassembly rates were converted into lifetime values.

Parameter	Values	Units
$kECM$	[0.001, 0.0035, 0.012, 0.0416, 0.1443, 0.5]	$\mathrm{N\,m^{-1}}$
$r^0_{off,FA}$	[0.0005, 0.0023, 0.0108, 0.05]	$\mathrm{s^{-1}}$
$ltFA_0$	[0.3, 1.5, 7.2, 33.3]	min

adopt a less spread state. The chosen values can be found in Table 5.1, which also includes the corresponding lifetime values to the presented disassembly rates, as they are more easily interpreted. The conversion of disassembly rates, ($r^0_{off,FA}$), to lifetime values, ($ltFA_0$), was done through Eq 5.13:

$$ltFA_0 = \frac{-1}{\ln(1 - r^0_{off,FA})} \tag{5.13}$$

Similarly, substrate stiffness values ($kECM$) can be converted to the Young's modulus of the substrate (E_{ECM}), which is more commonly referenced in the literature, using Eq 5.14:

$$E_{ECM} = \frac{kECM(1-\nu)^2}{D} \tag{5.14}$$

where ν is the Poisson's ratio of the substrate, which was set as 0.5, and D is the diameter of the contact area of the FA with the substrate, assumed to be 1 μm, (Mitrossilis et al., 2009). This results in a range of 0.25-125 kPa for the selected values of $kECM$.

The stiffness values and disassembly rates chosen consist of values equally spaced in a logarithmic space, in order to cover a wide range of values found in the literature, (Berginski et al., 2011; Mitrossilis et al., 2009; Stehbens and Wittmann, 2014). Combining the six $kECM$ values with the four $r^0_{off,FA}$ rates, a set of twenty-four simulations was built, with each simulation running for 24 simulated hours. Due to the stochastic nature of the model, four additional sets were run, so that results for the same settings could be compared.

In order to characterize the effect of each mechanosensing mechanism, this exact study structure was run for the four possible combinations of the two mechanisms: the maturation of the FAs, (FA_{mat}), and the strenghtening of the SFs, (SF_{str}). Classifying whether the mechanisms are active or not through $[ON]$ and $[OFF]$ states, the four conditions can be defined as:

1. $FA_{mat}[OFF]/SF_{str}[OFF]$ - None of the mechanisms is active;
2. $FA_{mat}[ON]/SF_{str}[OFF]$ - Only the maturation of the FAs is active;
3. $FA_{mat}[OFF]/SF_{str}[ON]$ - Only the strengthening of the SFs is active;

4. $FA_{mat}[ON]/SF_{str}[ON]$ - Both mechanisms are active;

The computational resources and services used were provided by the VSC (Flemish Supercomputer Center), funded by the Research Foundation - Flanders (FWO) and the Flemish Government – department EWI. Simulations were run using an Intel Xeon Processor E5-2680 v3 on nodes, each with 2.7 GB of memory, taking a total of 25 hours to run (24 hours for the simulation itself and 1 additional hour to process the results)

Chapter 6

Results and Discussion

6.1 A First Look into the Simulated Cells

As stated in the Methodology (see Section 5.2), the proposed model simulates cells that move along an axis. Thus, to illustrate this with actual results, Fig 6.1 (a) showcases the general motion of a migrating cell. However, despite this similarity, not all cells shared the exact same migration patterns. Actually, two migration modes could be identified, based on the different ways in which the retraction of the cellular rear occurs. Also in the Methodology, it has been explained that it is expected that a collective rupture of the FAs in the cells' rear occurs, causing the back of the cell to retract. Indeed, some of the cells adopted this behaviour, but others presented a more continuous retraction process, as seen in Fig 6.1 (b).

Cells with continuous retraction were classified as presenting "progressive retraction". Their associated displacement curve is relatively smooth, meaning that, from one time point to another, there was not a large difference in displacement. Cell shape does not change significantly between time points, either, and the number of FAs and traction levels are low, with barely any rupture of FAs (Fig 6.1 (c1)), promoting the idea that there is a balance between the assembly and turnover of FAs. Hence, these cells can be thought as low-adhered cells, that constantly move forward without changing its shape, similarly to keratocytes, (Lee et al., 1993).

On the other hand, retraction events promoted by the collective rupture of FAs (i.e., "collective" retraction) are represented by a displacement curve with step-like behaviour, indicating that, rather than a continuous motion, the cell stalled for some minutes, to then abruptly move forward, resembling the migration patterns of a mesenchymal cell, (Friedl and Wolf, 2010). Analyzing the remaining metrics for this migration mode, (Fig 6.1 (c2)), contrarily to what was seen for "progressive" retraction, there was no balance between assembly and turnover of FAs. Instead, there was a cyclic process where assembly started by having dominance, but, at a certain time point, a large collective rupture occurred. The cell was then forced to detach and entered a refractory period (see 5.1.6), with the cycle restarting at the end of said period.

It must be noted that the retraction patterns described here serve solely as examples of the two principal observed migration phenotypes. Many times, cells did not maintain one of the migration

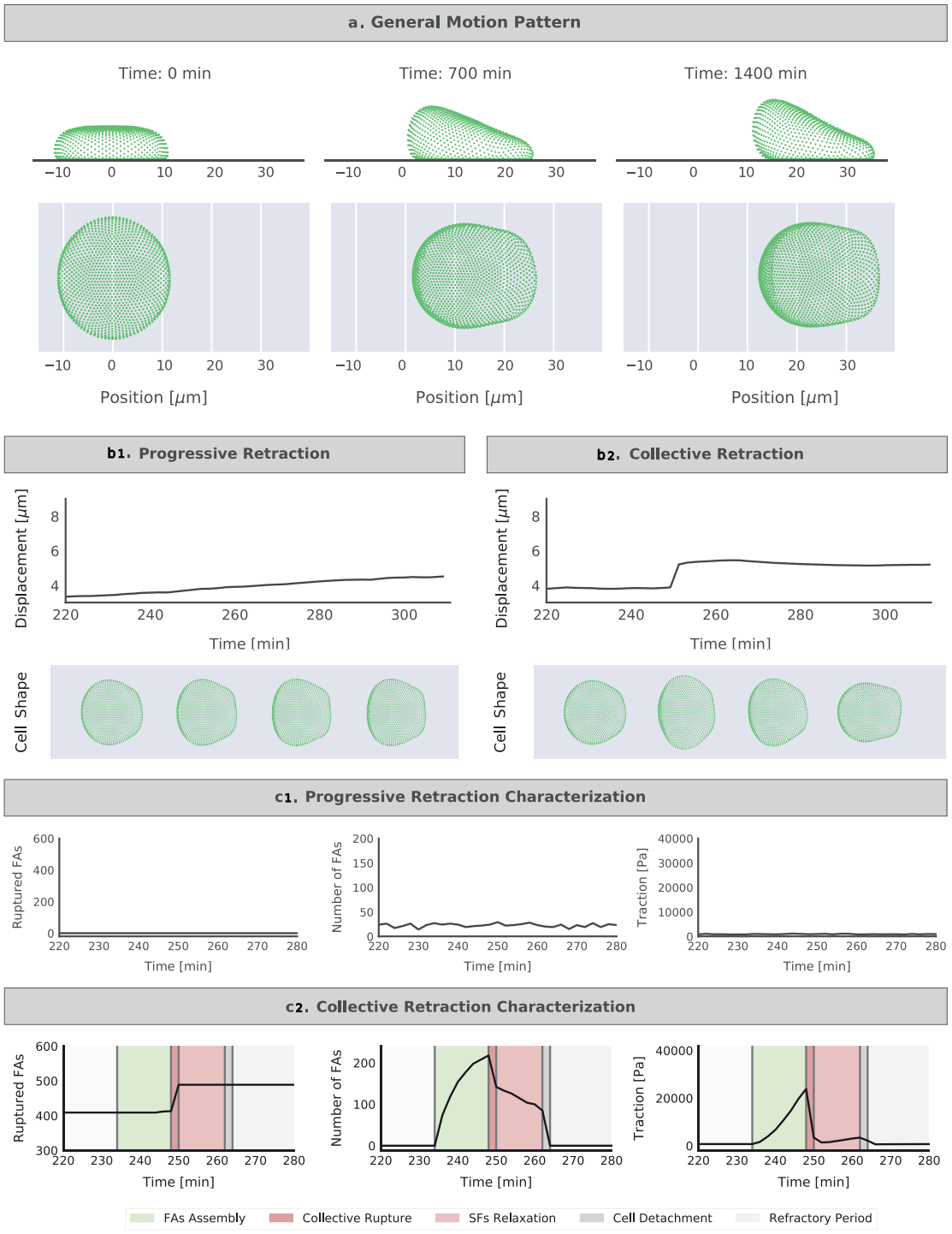

Figure 6.1: (a) Representation of the position of the cell's cortex (side and top view) at different time points (representing the beginning, middle and end of the simulation), to showcase the cell's motion through time.; (b) Example representations of the cell's displacement and shape for the two identified migration modes: progressive retraction ($FA_{mat}[ON]/SF_{str}[ON]$, $kECM$ = 0.0416, $ltFA_0$ = .3) and collective retraction ($FA_{mat}[ON]/SF_{str}[ON]$, $kECM$ = 0.5, $ltFA_0$ = 33.3); (c) Representations of the number of ruptured FAs, number of FAs and traction values for both migration modes.

modes throughout the entire simulation, and the adopted phenotype was heavily dependent on the conditions and parameters of the simulation. Nonetheless, an extended analysis will not be done in this section and will be present in the following sections.

In addition to studying how a cell moves, quantifying how much cells move is one of the most important questions to be answered, as it will reveal which conditions and parameters lead to displacement and which impair the migration mechanisms. Final displacement was calculated based on the difference between the position of the cell's centre of mass at the end and the beginning of the simulation. Accordingly, Fig 6.2 provides a representation of two extremes of the migration spectrum (i.e., a cell that does not migrate and one of the fastest cells), accompanied by their respective final displacement value. It also presents all the final displacement values obtained for the four conditions, to be analyzed in the sections to follow.

The negative value (seen in the figure on the right) does not indicate that the cell has migrated "backwards". In reality, the cell remained attached to the substrate and the changes in its shape, due to the forces that counteract protrusion, led its centre of mass to shift to the back. Hence, this value is more representative of changes in cell shape than of displacement, and, throughout this discussion, all samples with a negative final displacement value should be regarded as non-migrating cells.

Finally, in terms of migration speed, it is apparent that the simulated cells are slower than what is seen in nature. Selecting the cell that migrated the most in the 24 hour simulated period, (22 µm) the corresponding speed is 0.015 µm/min. In the literature, on the other hand, slow mesenchymal cells have been characterized by speed values of 0.1-0.5 µm, (Friedl et al., 1998; Wu et al., 2013). This is caused by limitations of the model, to be further presented and discussed. Therefore, it will not be possible to directly compare the simulated results to actual results, but the patterns found should match experimental observations.

6.2 Force-Independent Adhesions

6.2.1 When Fibers Cannot Mature, Excessive Adhesion Hinders Migration

Analyzing the results for $FA_{mat}[OFF]/SF_{str}[OFF]$, all the migrating cells present a "progressive retraction" migration mode. Also, from the final displacement values, it can be concluded that higher stiffness values tend to lead to more displacement. Yet, it is also apparent that this effect is limited by the expected lifetime of the FAs. To better understand why these two variables are causing these effects, Fig 6.3 presents the results obtained for the other analyzed metrics, with focus on traction.

Starting by confirming the assumptions of this condition, undoubtedly, there is no strengthening of the SFs, and the only difference in the lifetime of the FAs is introduced by the $ltFA_0$ variable. Although the lifetime of the adhesions, in this condition, was static and was not influenced by other metrics, it produced some interesting outcomes. It is well-established that a finely tuned balance

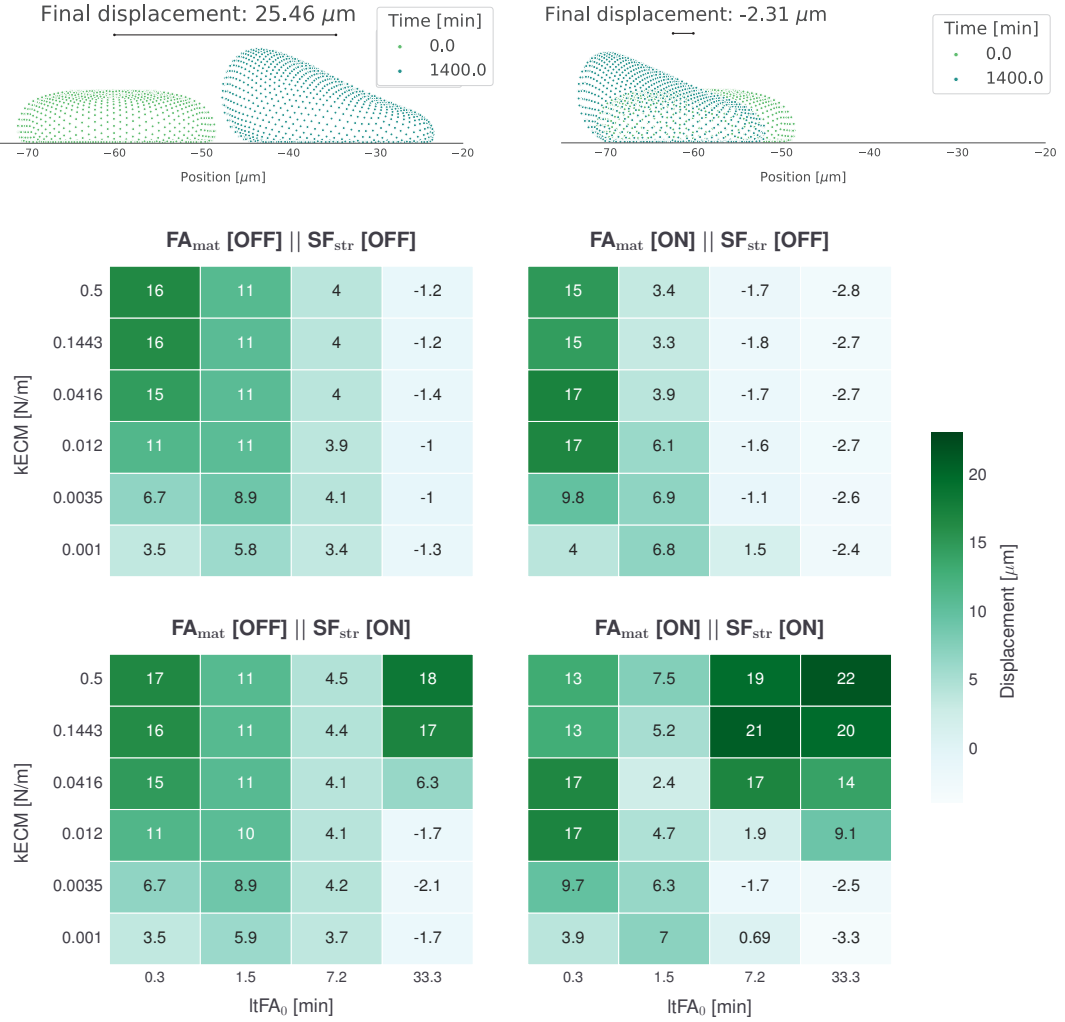

Figure 6.2: The top figure presents two examples of final displacement for two samples representative of the fastest (left, $FA_{mat}[ON]/SF_{str}[ON]$, $kECM$ = 0.5, $ltFA_0$ = 33.3) and slowest (right, $FA_{mat}[ON]/SF_{str}[ON]$, $kECM$ = 0.0035, $ltFA_0$ = 33.3) cells. The bottom figure presents heatmaps for the mean final displacement values for the four conditions (considering the 5 replicates), in terms of the expected lifetime of the FAs ($ltFA_0$) and the stiffness of the ECM ($kECM$). Regarding the effect of FA_{mat}, given by the comparison of $FA_{mat}[OFF]/SF_{str}[OFF]$ and $FA_{mat}[ON]/SF_{str}[OFF]$ (top row of the figure), the results are not indicative of a significant change in behaviour due to the maturation of the FAs. On the other hand, comparing $FA_{mat}[OFF]/SF_{str}[OFF]$ and $FA_{mat}[OFF]/SF_{str}[ON]$ (left column), which reveals the effect of SF_{str}, cells start migrating for a $ltFA_0$ of 33.3 min. Finally, considering both mechanisms, present in $FA_{mat}[ON]/SF_{str}[ON]$, in high $ltFA_0$ and high $kECM$ migration occurs over a larger range of parameter space.

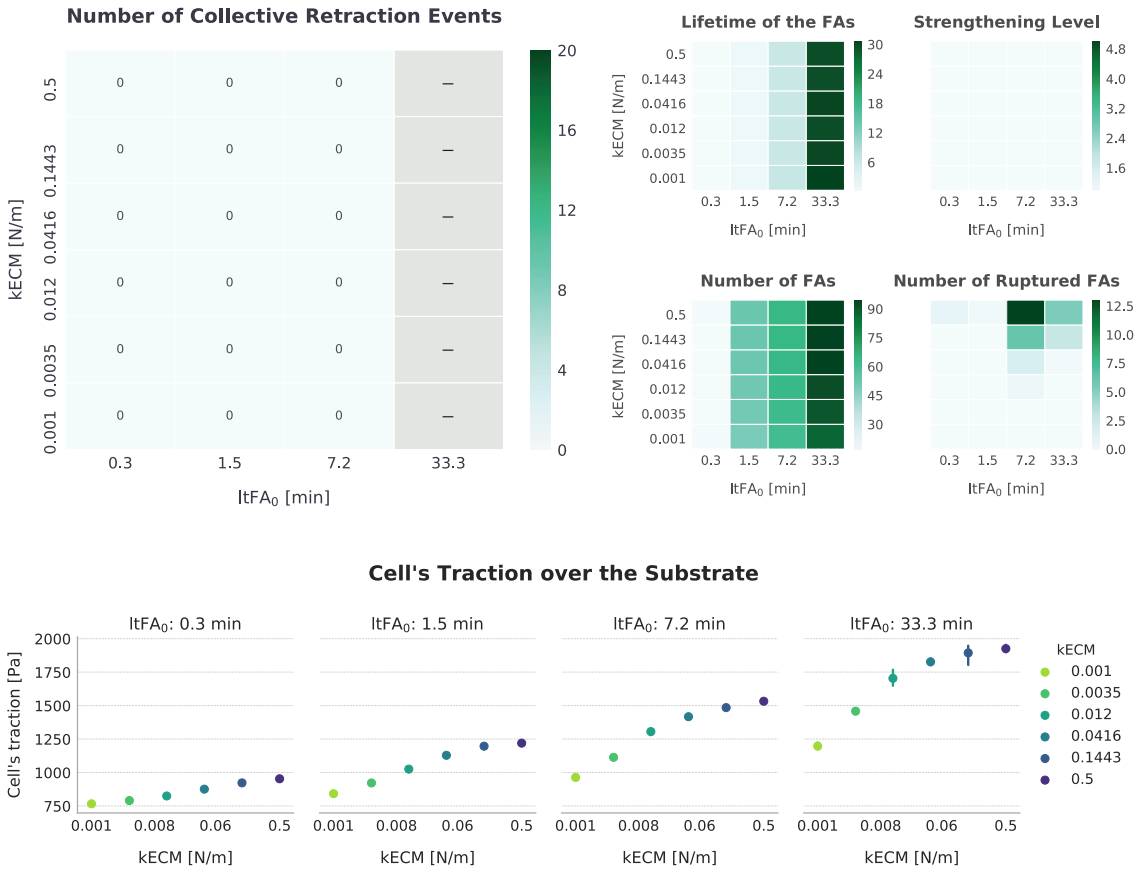

Figure 6.3: Summarized results for $FA_{mat}[OFF]/SF_{str}[OFF]$. The top figure presents a heatmap number of collective retraction events, with gray cells corresponding to samples with no displacement, showing that there is no collective rupture for this condition, and all cells adopt a "progressive" retraction phenotype. In addition, the figure presents a summarized view of the actual lifetime of the FAs, the strengthening level of the SFs, the number of FAs and the number of ruptured FAs. The bottom figure presents an errorbar with the obtained traction values for each sample (presenting the mean value and the standard error of the mean for the five replicates).

between assembly and disassembly of FAs is required for migration to occur. Henceforth, having in mind that with high formation rates and low turnover rates cells become stably adhered to the substrate instead of moving forward, (Nagano et al., 2012), the obtained results appear to be coherent with this idea.

There is only significant migration for cells with a high turnover rate of FAs ($ltFA_0 \leq 1.5$ min). In contrast, for lifetime values closer to those found in the literature (20-40 min), (Berginski et al., 2011; Stehbens and Wittmann, 2014), the number of FAs is higher and the adhesions hinder migration. Thus, the results indicate that, in normal conditions for a mesenchymal cell ($ltFA_0$ = 33.3 min), migration is not possible with the inexistence of mature FAs and strengthened SFs. However, for specific conditions, specifically when the adhesions live for less time, migration occurs without the need for these structures. This is seen in nature, usually for cells that have an amoeboid migration phenotype, or faster cells such as keratocytes, that have small, few FAs and

rarely present SFs, (Lämmermann and Sixt, 2009; Lee and Jacobson, 1997). However, it has also been observed that mesenchymal cells may start presenting shorter-lived adhesions, in response to changes in the environment, (Paňková et al., 2010), impairing the ability of SFs to strengthen, as that process requires time.

Although the main aspects of migration have already been explained, the effect of stiffness has not yet been presented, and it should be studied. The effect on the number of FAs is not very noticeable, but a slight increase in number of FAs with increasing substrate stiffness was identified, which can be explained by a reduction in the size of the lamella in lower stiffnesses. With less nodes capable of forming FAs, it is reasonable that the number of FAs decreases. This reduction is caused since cells are able to deform the substrate, adopting a more round, less spread state, (Wells, 2008). Regarding the number of ruptured FAs, the values are very low, but it is not surprising that there are more ruptured FAs in substrates with high stiffness values, and for longer-lived adhesion, as both promote an increase in the force exerted by the cell.

Furthermore, there is an increase in traction with increasing stiffness values, as it has been shown by previous studies, (Lo et al., 2000). Going back to displacement, for low-lived adhesions, this increase is simultaneous with an increase in migration. Additionally, the only cases where, for the same stiffness, an increase in lifetime results in more displacement, also present an increase in traction (i.e., $ltFA_0 = 0.3; kECM = 0.001$ and $kECM = 0.0035$). Hence, it seems like, in these cases, higher tractions are associated with more migration, and, actually, for cells with low adhesion to the substrate, this behaviour has been described in the literature, (Onochie et al., 2019). Still, from the results obtained for long-lived adhesions, it is concluded that high tractions, per se, do not translate into more movement.

It is important to note that the number of FAs, which is representative of the area of the cell adhered to the substrate and has been shown to increase for longer-lived adhesions, also has a role in traction: more adhered cells are able to exert more forces and exert higher traction. Henceforth, it is concluded that cell traction is a function of both the stiffness of the substrate and the lifetime of the FAs, (Califano and Reinhart-King, 2010), and that it is difficult to quantify the effect of each of one. In conclusion, traction by itself is not sufficient to predict the displacement of the cell, but understanding the causes behind the differences in traction, i.e. the balance between adhesiveness and the stiffness of the substrate, is helpful in understanding why a cell migrates or not.

6.2.2 The Strengthening of Stress Fibers Enables Collective Retraction, but Requires Long-Lived Adhesions and High Stiffnesses

Regarding the results for Condition $FA_{mat}[OFF]/SF_{str}[ON]$ (see Fig 6.4), all cells adopted the "progressive retraction" phenotype and, for most samples, there was a great similarity to the displacement values discussed in the previous section. Thus, this is indicative that SFs require certain settings to actually affect migration. Nonetheless, when displacement values differ, namely for an expected lifetime of 33.3 min and stiffness values ≥ 0.0418 N/m, the difference is very significant, as displacement values are not only restored, but higher values are being reached. Moreover,

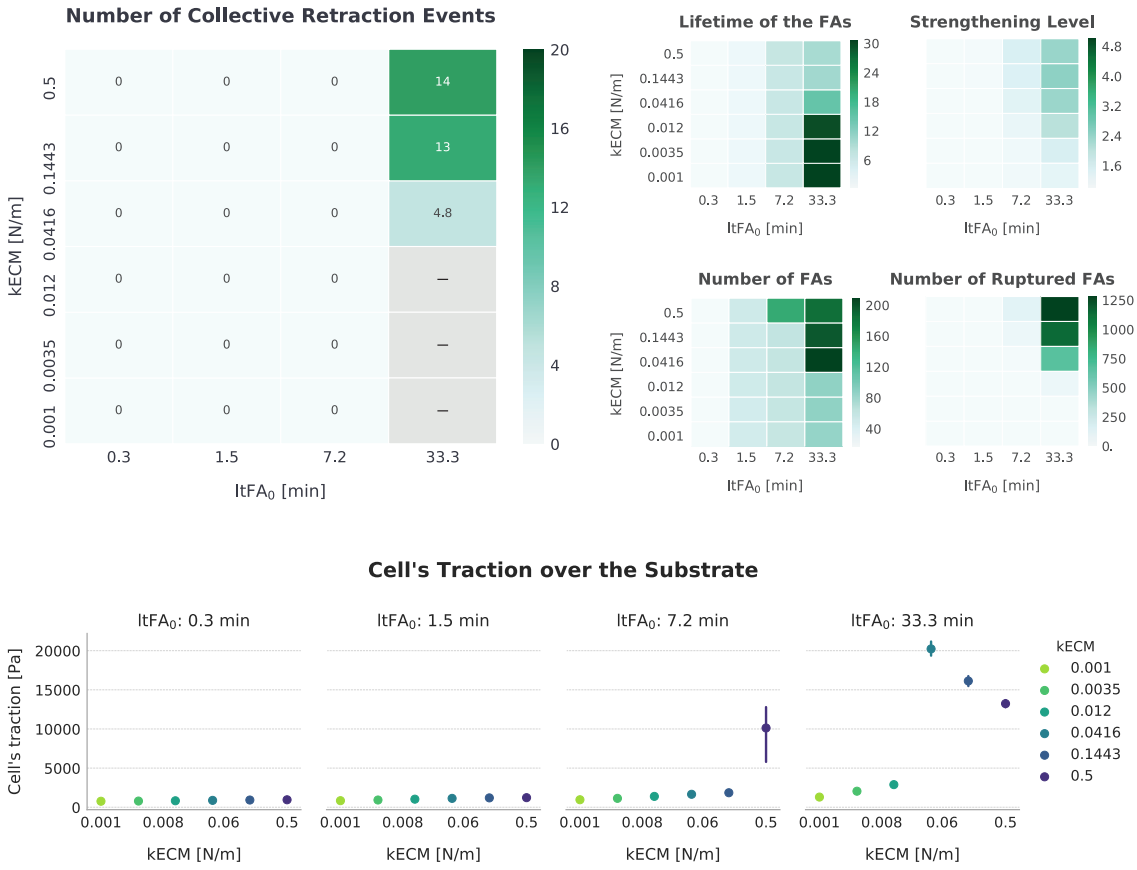

Figure 6.4: Summarized results for $FA_{mat}[OFF]/SF_{str}[ON]$. It can be seen that "collective" retraction occurs for the three highest stiffness values of samples with $ltFA_0$ = 33.3 min, resulting from an increase in the strengthening level of the SFs. This new behaviour has significant effects on the remaining metrics, introducing an interesting trend in the lifetime of the FAs and the exerted traction: as stiffness increases, both these metrics decrease in value.

in these cases, cells migrate using a collective retraction mode, as suggested by the high rupture levels and the decrease in the lifetime of the adhesions, promoted by an increase in force. In other words, FAs do not only disappear, but they are forced to disassemble before the end of their expected lifetime is reached. This behaviour has been described as a cyclic process termed as "load-and-fail", where high values of force are built and ultimately lead to the rupture of multiple adhesions, (Bangasser et al., 2013).

Considering how the strengthening mechanism was implemented (described in 5.1.5), the results here indicate that, for low-lived adhesions ($ltFA_0$ smaller than 7.2 min), SFs are able to keep contracting, without reaching a stalling period, which keeps them from being reinforced. In other words, the strengthening mechanism is not immediate and depends on stiffness, as it has been presented in the Methodology (see Fig 5.1.5). Accordingly, it makes sense that SFs are usually not found in cells with short-lived adhesions, (Lämmermann and Sixt, 2009), although they present contractile actin structures.

As SFs take less time to be strengthened, collective rupture also occurs sooner, and there are more retraction events, as indicated by the increase in the number of ruptured FAs and confirmed by measuring the number of retraction events. This is why there is a decrease in traction, the number of FAs and the lifetime of the FAs with increasing stiffness. Interestingly, some authors have described that, for certain cell types, substrates with high stiffness values may cause a decrease in the exerted tractions, (Chan and Odde, 2008), but it has been associated with a decrease in the cell's speed, which is not seen in the results for the proposed model. Furthermore, this behaviour has been captured by "molecular clutch" models that consider a "catch-slip" behaviour for the adhesions, (Bangasser et al., 2013), which attribute the decrease in traction to the "slip" part of the model (i.e. as force increases, adhesions disassemble before force can build up to generate high tractions). In the case of the proposed model, this is not true, though, as adhesions are modeled solely as "catch" bonds.

To further illustrate the effect introduced by the activation of the strengthening mechanism for the SFs, Fig 6.5 provides a representation of the displacement values for both conditions (i.e. $FA_{mat}[OFF]/SF_{str}[OFF]$ and $FA_{mat}[OFF]/SF_{str}[ON]$), overlapped. In addition, it presents heatmaps for the differences in values between the mentioned conditions, for all the other metrics, confirming what has been stated.

6.2.3 Summary

The two presented conditions have revealed why two different migration modes are seen, presenting two different ways traction influences migration. On one side, there are cells with fibers that cannot mature, either because of the strengthening mechanism not being active or because they do not live for the necessary amount of time. In this case, adhesions that live for long periods of time induce an adhered state that is associated to higher tractions, keeping the cell from moving forward. However, stiffness also leads to an increase in traction, but results in increases in displacement. Thus, for this migration phenotype, characterized by a "progressive" retraction of the back, there has to be a fine balance between the ability to attach to the substrate, in order to be able to exert traction forces, which are promoted by the substrate stiffnes, and the turnover rate of the adhesions, so that these adhesions do not become hindering to migration.

On the other hand, a very different behaviour is seen for cells with fibers that mature. Here, long-lived adhesions are actually essential for displacement to occur, as they use the time that adhesions live for to build force, enabling the rupture of the FAs located at the cell's rear, thus promoting a "collective" retraction phenotype. Furthermore, stiffness has an important role in determining the rate at which retraction events occur, which in turn leads to a decrease in the exerted traction, because adhesions are ruptured before they can exert higher values of force.

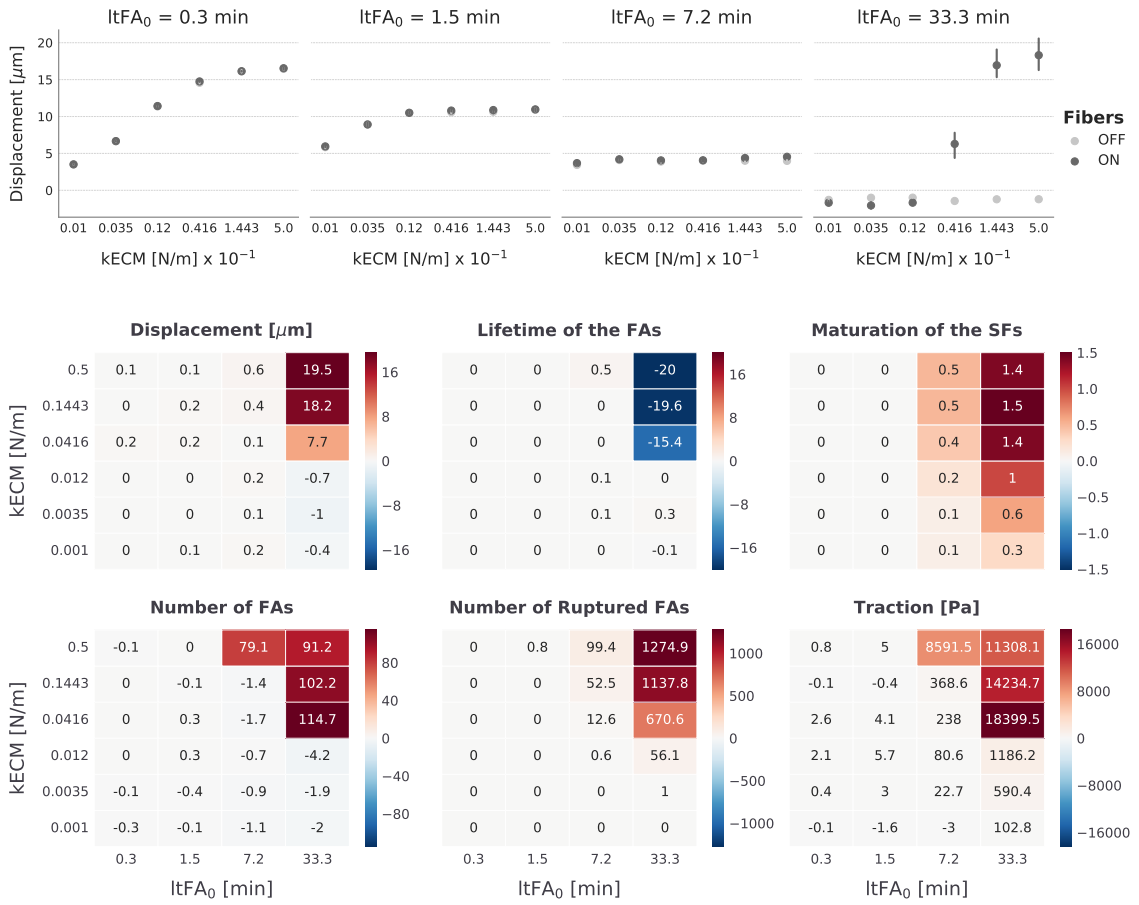

Figure 6.5: Representation of the effect introduced by the strengthening of SFs. (a) presents the errorbars for the final displacement values of the conditions with no maturation of the adhesions: $FA_{mat}[OFF]/SF_{str}[OFF]$ (light gray) and $FA_{mat}[OFF]/SF_{str}[ON]$ (dark gray), highlighting how strengthening only has an effect on displacement for $ltFA_0$ = 33.3 min and $kECM \geq 0.416$ N/m. (b) represents the differences between the two conditions for all the other metrics in study, further confirming that significant differences are only seen for high lifetimes and high stiffness values.

6.3 Introducing Force-Dependent Lifetimes

6.3.1 Maturation of FAs without Strengthening of SFs Further Inhibits the Cells' Migration Ability, Specially on High Stiffness Substrates

Observing the heatmaps in Fig 6.2, the displacement values for $FA_{mat}[ON]/SF_{str}[OFF]$, for the most part, can be easily compared to the results obtained for $FA_{mat}[OFF]/SF_{str}[OFF]$, if it is kept in mind that the actual lifetime of the adhesions is being extended by force. As stated in Section 6.2.1, both increasing stiffness values and increasing expected lifetimes promote a spread adhered state, reflected by an increase in the number of FAs and in the forces exerted on the substrate. Accordingly, having in mind that the maturation of the FAs is promoted by force, both variables will promote an extension of the actual lifetime of FAs, represented in Fig 6.6. Therefore, the same progressive retraction migration mode is adopted, and the same pattern of excessive adhesion can

be seen, yet, it is extended to lower expected lifetimes, (i.e., whereas $FA_{mat}[OFF]/SF_{str}[OFF]$ there was migration for $ltFA_0$ = 7.2, and it was only for $ltFA_0$ = 33.3 that migration stalled, here migration stalls at $ltFA_0$ = 7.2), and to higher stiffness values (i.e., for $ltFA_0$ = 0.3 min, it is seen that the two highest stiffness values have an hindering effect on displacement).

Regarding other metrics, it is not surprising that there is no strengthening of the SFs, nor that the number of FAs and the traction levels are increasing with both $ltFA_0$ and $kECM$, with higher magnitude than for $FA_{mat}[OFF]/SF_{str}[OFF]$. It is, nonetheless, worth-mentioning that the trend in rupture also seems to have shifted to lower expected lifetimes of the FAs, and longer-lived adhesions are promoting less rupture, which is surprising. Yet, a possible explanation to this behaviour is that, although there is more force being exerted for high $ltFA_0$, this force is being distributed through many FAs, so the force a single adhesion has to withstand is actually smaller than when there are less FAs, and does not reach the rupture force.

Therefore, from the results for this condition, it can be concluded that, although there are more FAs and more force being applied, it is still not enough to promote collective rupture. Thus, maturation of the FAs, per se, does not introduce any new behaviour. On the contrary, it only amplifies patterns that were already described for the samples with neither maturation of adhesions nor strengthening of the SFs.

6.3.2 Combining Both Mechanosensing Strategies Enables Collective Retraction in Physiological Conditions

Analyzing the results when both mechanisms are implemented (i.e. $FA_{mat}[ON]/SF_{str}[ON]$), Fig 6.2 shows that the observed effect of each mechanism independently is still seen when implemented together. In other words, collective retraction was visible once again, due to the strengthening of the SFs, and it was shifted to lower expected lifetimes, by the influence of the maturation of the FAs. Accordingly, the parameter space became dominated by "collective" retraction. Furthermore, it is interesting to note that the highest displacement values for all the simulations were obtained for this condition, with very high displacements being seen for expected lifetimes that almost did not have displacement for other conditions.

The emergence of "collective" retraction at a large area of the parameter space is very relevant, as it shows that adhesions that were expected to live for short periods of time, through the maturation of FAs, become able to live for longer periods. This is more similar to what happens in nature, since most adhesions disassemble before reaching an expected lifetime such as 33.3 min, and actually require maturation to reach lower disassembly rates.

Additionally, as seen in Fig 6.7, the values for the traction, the strengthening level and the number of FAs, in samples that adopt a collective retraction migration mode, presented a decrease due to stiffness as it was seen for $FA_{mat}[OFF]/SF_{str}[ON]$. Moreover, a biphasic trend became apparent, instead of having very low traction values for low stiffness values, bearing more similarities to trends seen in nature. For instance, considering that the results correspond to stiffness values

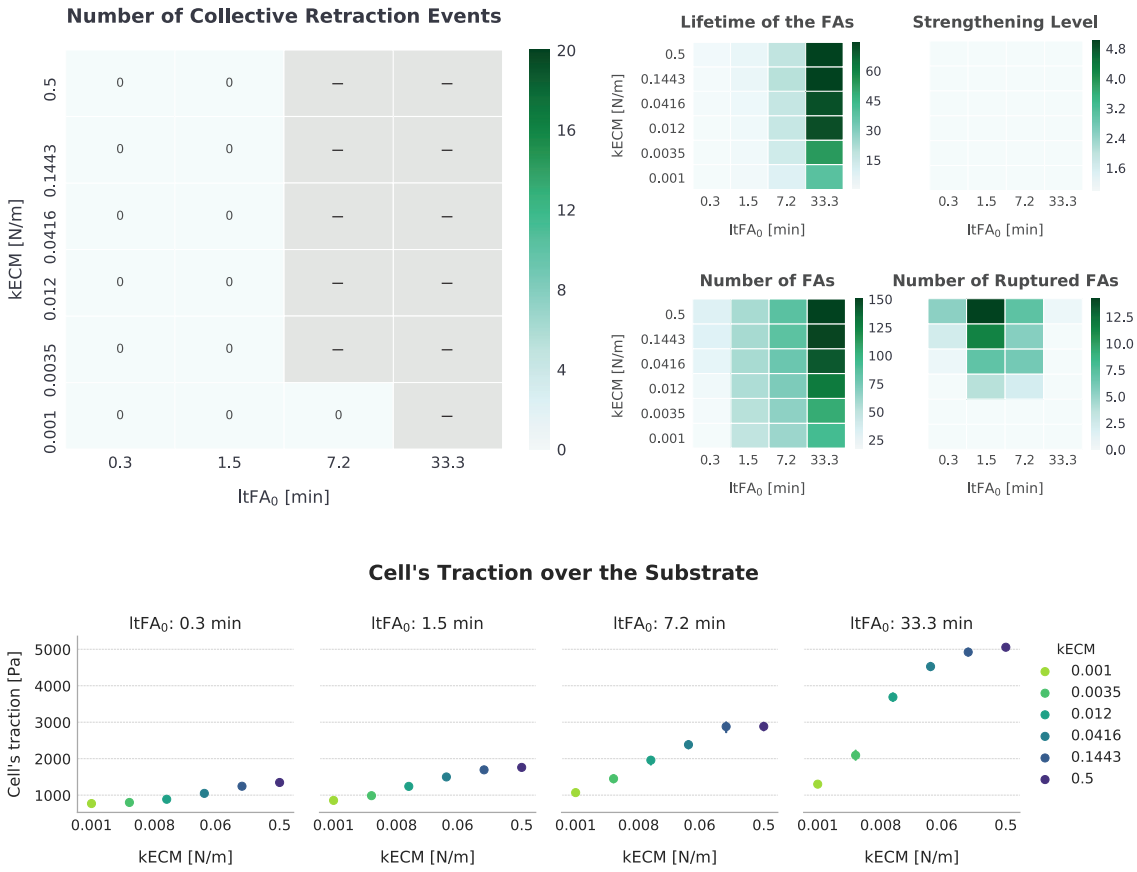

Figure 6.6: Summarized results for $FA_{mat}[ON]/SF_{str}[OFF]$. The observed patterns are more similar to $FA_{mat}OFF/SF_{str}OFF$, with no samples presenting "collective" retraction events, and more samples being unable to displace, due to an excessive adhered state.

of 0.25-125 kPa, the results for traction exerted by the cell can be compared to those reported for Bovine Aortic Endothelial (BAE) cells by Califano and Reinhart-King (2010).

This newly observed apparent increase in traction relates to a period of "frictional slippage", in which high forces cannot be built because of the soft stiffness of the ECM, that allows for deformation of the substrate, and also due to the fact that adhesions may disassemble before a high value of force is achieved. On the other hand, for higher stiffness values, the "load-and-fail" cycle is dominant.

The model described by Bangasser et al. (2013), as mentioned when analyzing condition $FA_{mat}[OFF]/SF_{str}[ON]$, presents a period of "frictional slippage" subsequently to the "load-and-fail" behaviour, as the "slip" part of the model leads to increases in force resulting in higher disassembly rates, hence making adhesions disappear before force can be built. However, as the proposed model only consists of a "catch" bond behaviour, this description does not apply and the biphasic effect of stiffness on traction is promoted by higher rates of the "load-and-fail" cycle.

Furthermore, for all the samples with the two lowest stiffness values, the effect of the SFs is not significant enough to translate into changes in displacement, hence reinforcing the idea that

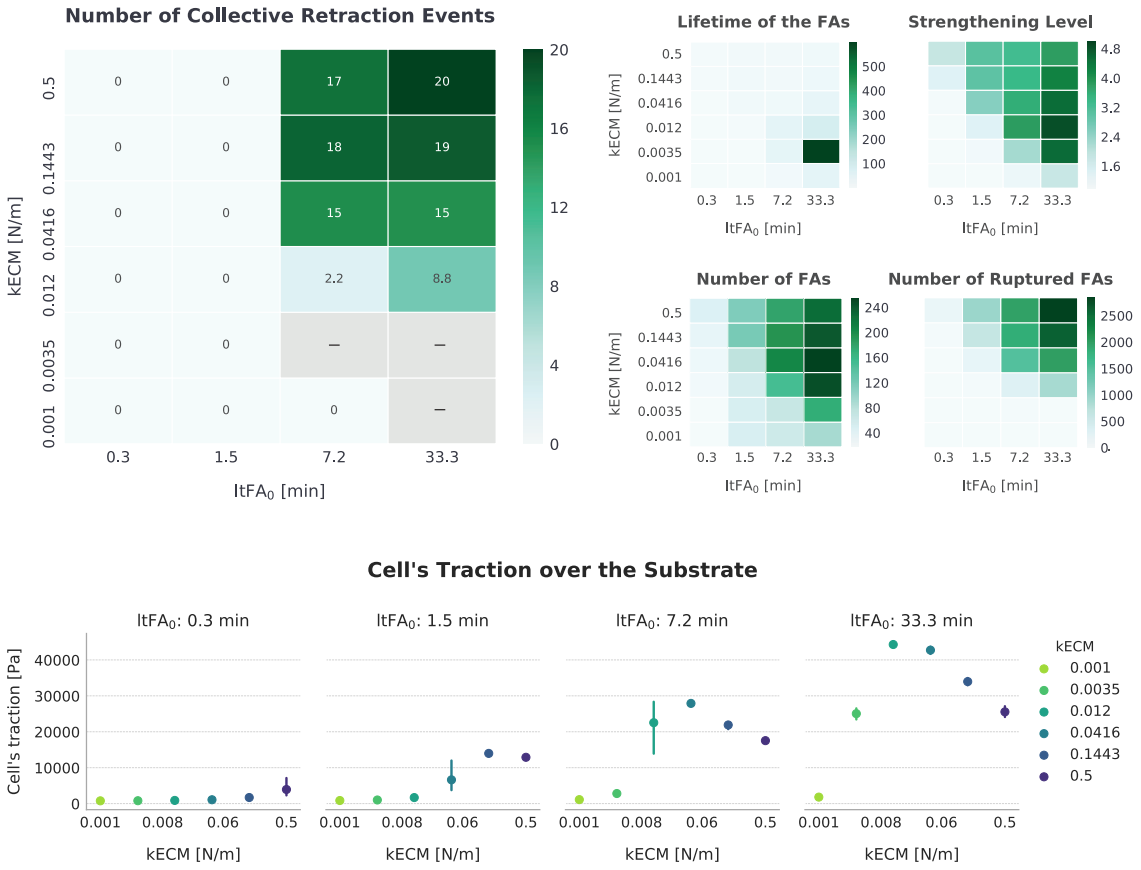

Figure 6.7: Summarized results for $FA_{mat}[ON]/SF_{str}[ON]$. "Collective" retraction events become more relevant due to the maturation of the FAs, with changes in the remaining metrics appearing in a larger area of the parameter space.

SFs need high stiffnesses for their strengthening to have an effect. For a set of samples in particular ($ltFA0 = 33.3$ min, $kECM = 0.0035$ N/m), this is particularly evident: there are high traction values, but they are not enough to promote rupture. Thus, adhesions only become stabilized by force, without being forced to rupture, leading to a peak in the actual lifetime of the FAs.

Fig 6.8 highlights the differences in metrics between conditions $FA_{mat}[ON]/SF_{str}[OFF]$ and $FA_{mat}[ON]/SF_{str}[ON]$, in a similar manner to what was done in Fig 6.5.

6.3.3 Summary

The analysis and comparison of the results for the conditions with FAs capable of maturing (i.e. $FA_{mat}[ON]/SF_{str}[OFF]$ and $FA_{mat}[ON]/SF_{str}[ON]$), alongside the insights gathered previously in this discussion, enabled the characterization of how the maturation of FAs affects migration, being concluded that it can have both a positive or a negative effect, depending on the migration phenotype. For the "progressive" retraction phenotype, excessive adhesion limits displacement, because forces can never reach a critical value to promote collective rupture, given that there is no strengthening of the SFs. As high stiffness values promote the maturation of the FAs, and,

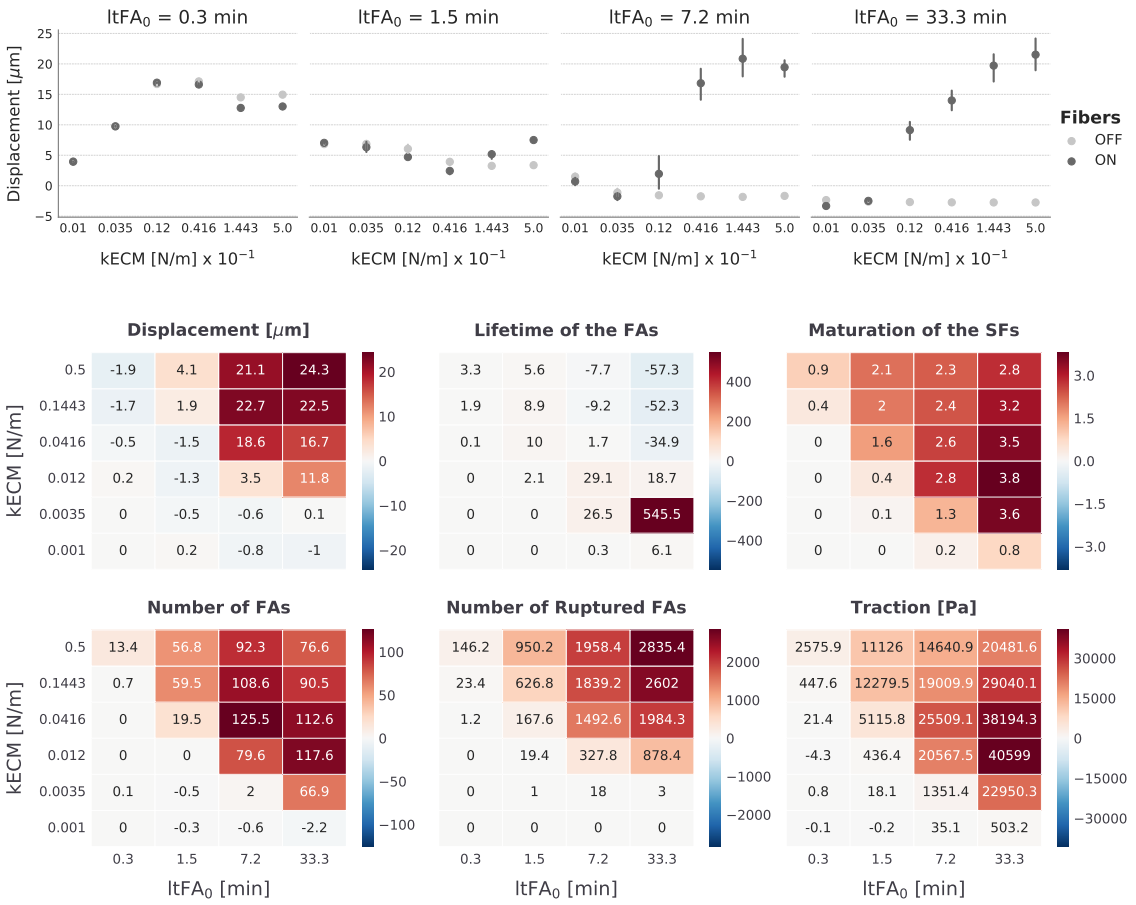

Figure 6.8: Representation of the effect introduced by the maturation of the FAs. (a) presents the errorbars for the final displacement values of the conditions with maturation of the adhesions: $FA_{mat}[ON]/SF_{str}[OFF]$ (light gray) and $FA_{mat}[ON]/SF_{str}[ON]$ (dark gray). (b) represents the differences between the two conditions for all the other metrics in study.

subsequently, their stabilization, it was observed that, for the first time in this study, stiffness could actually limit displacement. Finally, in terms of traction, the values follow a similar trend to the "progressive" retraction phenotype with no mature FAs, but values become higher, as the cells are more adhered to the susbtrate.

On the other hand, for "collective" retraction, the maturation of the FAs is actually benefitial, as long-lived adhesions provide the required time for SFs to mature. Accordingly, specially for FAs that have an intermediate turnover rate and attached too much to be able to move with fast velocities in a "progressive" retractiton phenotype, maturation processes allow for adhesions to live long enough for cells to start adopting a "collective" retraction phenotype.

Chapter 7

Conclusions and Future Work

In this thesis, a computational approach has been used to study how mechanosensing strategies influence the way migrating cells exert traction on a substrate, and how that reflects on the cell's migration abilities. Henceforth, it has been shown how computational tools can be used to replicate biological studies, providing flexibility to customize the model to adapt to specific settings and test a new hypothesis. Particularly, it was possible to study the effect of adhesion maturation and fibre strengthening on migration, which, experimentally, would require very advanced sensors and settings that are complex to be replicated.

Moreover, interesting biological insights have been gathered, which relate to ideas found in the literature but also present some new interpretations. More specifically, it has been shown how the stiffness of the substrate and the expected lifetime of FAs influence cell displacement in different conditions, namely when considering the maturation of the FAs and the strengthening of SFs. Furthermore, the simulated results have shown different behaviours not only in terms of cell speed, but also on the adopted migration phenotype, with two different migration modes being identified: "progressive" and "collective" retraction of the cellular rear.

These migration modes have significantly different dependences on traction. In "progressive" retraction, promoted by the lack of strengthened SFs, migration is optimal for lower traction values, as high traction is highly associated with an adhered state, that cells are not able to overcome. Thus, in this case, the maturation of the FAs is not beneficial to migration. Contrarily, in "collective" retraction, enabled by the existence of strengthened SFs, much higher values of traction are exerted, as fibres are strengthened and actually rupture adhesions due to the force they exert, but migration occurs with faster cell speeds. Also, here maturation of FAs permits the extension of the adhesions' lifetimes, which can be used by the SFs to strengthen and build up force, to enter the "load-and-fail" cycle described in the last section of the discussion. It is noteworthy that the proposed model, by modelling adhesions as having a "catch" bond behaviour (i.e. adhesions are stabilized by force), instead of a "catch-slip" bond as seen on other studies, has captured the same biphasic trend in traction due to stiffness, but not a biphasic trend in displacement.

However, quantitatively, the results obtained for the cell speed are distant from values found in the literature, with the simulated cells being significantly slower than what is seen in nature or in

other models. The main model limitation that is leading to this shortcoming is the model's inability to extend the front of the cell so a new Lm can form simultaneously with retraction. In fact, in nature, it is seen that the cellular membrane can protrude while adhesions are still attached, and it was originally expected that the proposed model could replicate this behaviour. As the cellular rear retracted, the front would also protrude, and the front of the cell would become more distant to the cell adhesions. Accordingly, the nodes would probably no longer be part of the Lm, and, thus, the associated adhesions would disappear. However, the front of the cell is not expanding for the necessary extent, hence adhesions are not detaching. Consequently, to overcome this issue, the properties of the cortex model could be adjusted to permit more flexibility of the nodes to flow over the cellular front and move the cell edge farther away from the cell's centre. Alternatively, it was chosen to include a mechanism to impose detachment of the cell upon the retraction of the cellular rear, which is an artificial approach and should be regarded as a limitation of the model.

In addition, still considering how the model was implemented, there is an area of the cell (namely, the cell body between the front and rear lamella) that is not able to contract, and that, in proportion to the rest of the cell area, may be too large. Hence, there is a limit to how much cells can contract and, if the cells were made larger and the model was adjusted to accommodate with that change, perhaps cells could contract, and subsequently move, more. Additionally, when measuring the number of retraction events, it has been seen that retraction events were separated by a time period very similar to the refractory period during which cells are not able to create new adhesions. Hence, the value for the refractory time could be further studied, in order to be decreased, and allow for a higher rate of retraction events, while still promoting the cell spreading that enables the cell to move forward.

Finally, it must be stated that not all the simulated settings are easy to replicate *in vitro*, and, although it is a disadvantage not to be able to directly compare the simulated results to actual experiments, it also provides a good view of what can be achieved through computational modelling, to unravel mechanisms. For instance, experimentally it would not be possible to directly replicate the different rates of disassembly of the FAs of a cell. However, different substrates and cells have different binding affinities, and cells with high disassembly rates can be thought of as cells that have low affinity to the substrate, being able to move without attaching too much. Regarding the mechanosensing mechanisms, though, it is more difficult to think of cells that are able to have strengthened SFs without mature FAs, for example. Nevertheless, studies could still be implemented with the inhibition of small molecules required in these processes, thus preventing them from occurring.

Consequently, it is important to look into this study as an exploration of how the proposed model responds to different model extensions, and as an effort to understand exactly these modifications affect the model, which was achieved successfully.

Appendix A

Parameters Used in the Simulations

The parameters used in the simulations, alongside their values and source of estimation, are presented in Tables A.1 and A.2, corresponding to the spreading and migration parts of the simulations, respectively. For the second part of the simulation, the parameters that are not presented in the corresponding table keep the same value that was presented for the first part.

Table A.1: List of Parameters Used in the First Period of the Simulation (Spreading)

Type	**Parameter**	**Description**	**Value**	**Units**	**Source**
Simulation	Δt	Timestep	0.05	s	-
	T_{spread}	Spreading time	4	min	-
	T_{end}	Total simulation time	736	min	-
	T_{rec}	Recording time	120	s	-
Cell geometry	r_{cell}	Cell radius	8.0×10^{-6}	m	-
Substrate geometry	l_{ECM}	Substrate plane length	170×10^{-6}	m	-
	w_{ECM}	Substrate plane width	45×10^{-6}	m	-
	l_{Lig}	Ligand pattern length	165.0×10^{-6}	m	-
	w_{Lig}	Substrate plane width	40×10^{-6}	m	-
Cell mechanics	E_c	Young's modulus of the cell cortex	2×10^{4}	Pa	(Odenthal et al., 2013)
	ν_c	Poisson's ratio of the cell cortex	0.4	-	(Odenthal et al., 2013)
	k_{cortex}	Stiffness of the cell cortex	3.0×10^{-5}	N/m	(Pontes et al., 2017)
	$k_{b,\ cortex}$	Cortex bending constant	1.0×10^{-16}	N/m	Trial runs
	$k_{V,\ cell}$	Cortex volume constraint	10	Pa	Trial runs
	$k_{A,\ cortex}$	Cortex local area constraint	1.0×10^{-3}	N/m	Trial runs
	$k_{d,\ cortex}$	Cortex global area constraint	1.0×10^{-3}	N/m	Trial runs
	c	Cortex damping	2.0×10^{-3}	Ns/m	Trial runs
Substrate mechanics	E_s	Young's modulus of the substrate	1.0×10^{-5}	Pa	-

Type	Parameter	Description	Value	Units	Source
	ν_s	Poisson's ratio of the substrate	0.5	-	-
Contact	η	Viscosity of the medium	1.0×10^2	Pas	Trial runs
	W_{cs}	Cell-substrate adhesions constant	1.0×10^2	N/m	-
	$\Gamma_{cs,\,n}$	Cell-substrate normal friction	1.0×10^{10}	Pas/m	Trial runs
	$\Gamma_{cs,\,t}$	Cell-substrate tangential friction	0.0	Pas/m	Trial runs
Cell anatomy	D_{actin}	Actin diffusion coefficient	8.0×10^{-14}	s^{-1}	Interpolated from (Fischer et al., 2009)
	k_{gen}	Actin generation rate	1.18×10^{11}	$m^{-2}\,s$	Interpolated from (Delorme et al., 2007; Fischer et al., 2009)
	k_{deg}	Actin degradation rate	0.016	s^{-1}	Interpolated from (Delorme et al., 2007; Fischer et al., 2009)
	$[G]_{Lp,\,front}$	Actin threshold concentration for the front Lp	2.5×10^{11}	-	Interpolated from (Delorme et al., 2007; Fischer et al., 2009), trial runs
	$[G]_{Lp,\,back}$	Actin threshold concentration for the back Lp	5.0×10^{11}	-	Interpolated from (Delorme et al., 2007; Fischer et al., 2009), trial runs
	$[G]_{Lm}$	Actin threshold concentration for the Lm	6.0×10^9	-	Interpolated from (Delorme et al., 2007; Fischer et al., 2009)
Focal adhesions	k_{ECM}	Spring stiffness of the substrate	1.0×10^{-2}	$N\,m^{-1}$	Trial runs
	k_{FA}	Spring stiffness of the FAs	1.0×10^{-2}	$N\,m^{-1}$	Trial runs
	$L_{ECM,\,0}$	Equilibrium length of the substrate	2.59×10^{-8}	m	-
	$L_{FA,\,0}$	Equilibrium length of the FAs	0.1×10^{-9}	m	-

Type	Parameter	Description	Value	Units	Source
	$L_{FA,max}$	Maximum distance between nodes to form an adhesion	7.5×10^{-8}	m	-
	$r_{on,FA}$	Rate of assembly of FAs	0.0	-	-
	$r_{off,FA}$	Rate of disassembly of FAs at zero force	1.0×10^{-3}	-	-
	ζ	FAs mechanosensing parameter	8.5	-	Trial runs
	lt_{ref}	Refractory period for FAs	1800.0	s	-
	lt_{mat}	Required lifetime to enter a refractory period	600.0	s	-
Stress fibers	L^0_{fib}	Minimum initial potential fiber length	8.0×10^{-6}	m	-
	θ_{fib}	Fiber orientation	0.3142	-	Trial runs
	$nFib_{thr}$	Number of deleted fibers to define a retraction event	15	-	Trial runs
	F_{f50}	Difference in fibers length that leads to force decay	3.5×10^{-6}	-	Trial runs
	μ	Slope of the force decay function	5.0×10^{6}	-	Trial runs
Cellular forces	F_{am}	Reference actomyosin force	5.0×10^{-10}	N	Interpolated from (Moore et al., 2010)

Table A.2: List of Parameters Used in the Second Period of the Simulation (Migration)

Type	**Parameter**	**Description**	**Value**	**Units**	**Source**
Cell mechanics	E_c	Young's modulus of the cell cortex	1.0×10^{5}	Pa	(Odenthal et al., 2013)
	k_{cortex}	Spring stiffness of the cell cortex	2.9×10^{-4}	N/m	Trial runs
	$k_{b,\ cortex}$	Bending rigidity of the cell cortex	8.0×10^{-16}	N/m	Trial runs
	$k_{V,\ cell}$	Volume constraint for the cell	8.5	Pa	Trial runs
	$k_{A,\ st\ cortex}$	Area constraint for the cortex	5.0×10^{-4}	N/m	Trial runs
	$k_{A,\ cm\ cortex}$	Area constraint for the cortex	5.0×10^{-1}	N/m	Trial runs
	$k_{d,\ cortex}$	Global area constraint for the cortex	1.0×10^{-8}	N/m	Trial runs
Contact	η	Viscosity of the medium	5.0×10^{4}	Pa s	Trial runs
	W_{cs}	Cell-substrate adhesions constant	2.5×10^{-4}	N/m	Trial runs
	$\Gamma_{cs,\ n}$	Cell-substrate normal friction	5.0×10^{11}	Pa s/m	Trial runs
	$\Gamma_{cs,\ t}$	Cell-substrate normal friction	1.0×10^{4}	Pa s/m	Trial runs
Focal adhesions	k_{FA}	Spring stiffness of the FAs	1.0×10^{3}	N m^{-1}	(Bangasser et al., 2013)
	$r_{on,FA}$	Rate of assembly of FAs at zero force	5.0×10^{-3}	s^{-1}	(Kaverina et al., 1999)
Cellular forces	F_{am}	Reference actomyosin force	$1.0 \times 10^{-9}.0$	N	Trial runs

Appendix B

Model Optimization

As of the start of this dissertation, the proposed model still did not include the SFs relaxation nor the cell detachment mechanisms. Consequently, the simulated cells presented very low migration speeds, with two main issues being identified as possible causes to this problem: the retraction of the back was not efficient, and the front of the cells was not detaching. Therefore, this appendix aims to present the preliminary work developed in this context. It must be noted that all the adjustments were done while running studies with the settings for the $FA_{mat}[ON]/SF_{str}[ON]$ condition.

B.1 Stress Fibers' Strengthening Optimization

As the retraction of the cell's back was occurring slowly, it was proposed that an increase in the number of SFs or in the exerted force could lead to faster retraction events and, consequently, to faster migration. Therefore, in order to test this hypothesis, simulations were run with higher values for the actomyosin force ($\vec{F}_{am}$).

Ultimately, it was concluded, and further confirmed through studies that aimed to characterize the contraction and strengthening of a single SF, that the problem was not the basal $\vec{F}_{am}$ value, but the fact that strengthening was taking too long to occur, due to some flaws in the model's implementation. For once, the timestep used in the simulations was too high. Yet, it was also shown that the threshold referenced in 5.1.5, used to detect when fibre contraction stalls, was too low and not representative of the stalling period, as the values started fluctuating around a certain value minutes before the threshold was reached.

Fig B.1 presents the evolution of the results obtained in these preliminary studies, based on the introduction of each of these adjustements. It is possible to see that the decrease in the timestep indeed decreased the fluctuations, but there was still an artefact at low difference values. Yet, by making the threshold higher, and scaling it according to force, it was not only possible to make strengthening events equally spaced in time but also substantially faster, which, indeed, resulted in faster retraction of the cellular rear.

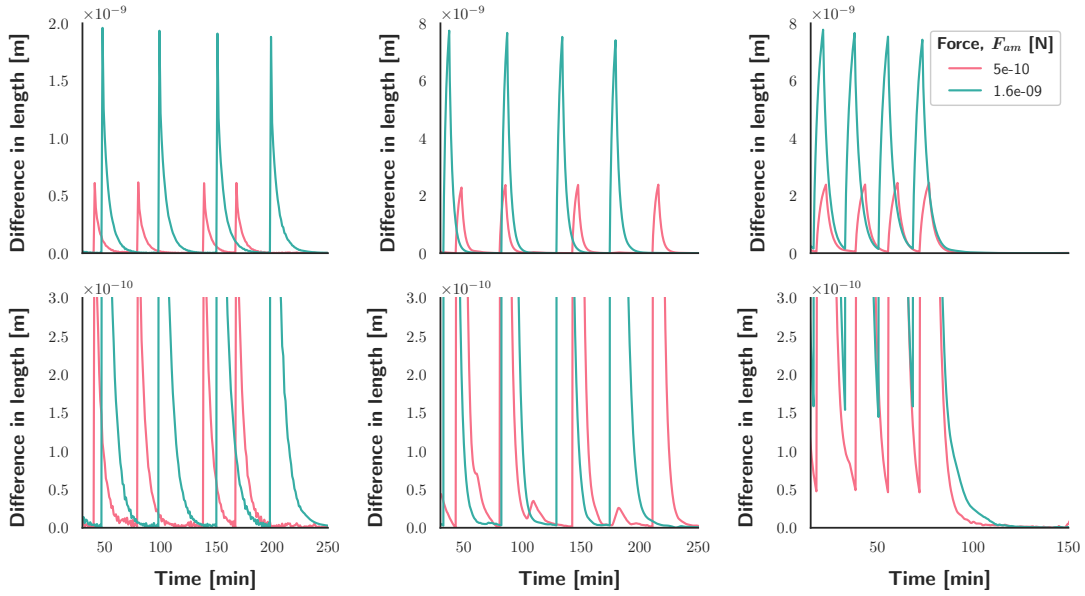

Figure B.1: Results obtained for the difference in length for a single SF, before the implementation of new adjustments (left), after the implementation of a lower timestep (centre), and after the implementation of both a lower timestep and a higher and scalable difference threshold (right). Values are expected to peak when a fibre contracts, as it leads to a large change in length. Subsequently, values should drop, showcasing that contraction is becoming more difficult to achieve, until they start fluctuating around a value, indicating that the length of the fibre has stabilized and strengthening should occur, hence resetting this cycle. Observing the results from left to right, it is possible to see that, initially, it was taking too long to reach this threshold, and, consequently, to fully strengthen the SF (around 170 min for low forces and around 210 for high forces). However, as adjustments were implemented, the strengthening events started occurring faster and were no longer influenced by the magnitude of the actomyosin force (taking less than 100 minutes for both force values to fully strengthen the fibre).

B.2 Fiber Relaxation and Cell Detachment

Despite the improvements mentioned in the previous section, in order to efficiently migrate, a cell still needs to, upon the retraction of its rear, be able to extend its front and create new adhesions in that area, promoting the adhesions at the front Lm to detach. However, the proposed model was not able to replicate this behaviour and an extension had to be implemented to overcome this issue. A balance needed to be reached: the contraction of the fibres had to lead to an increase in force so that the cell's rear could retract; but, once SFs had contracted enough to promote this behaviour, they should no longer exert high force values.

The strategy proposed to model this seemingly contradictory effect was based on the scaling of the exerted force through a logistic function written in terms of the fibres' shortening. The idea was that, to a certain extent of contraction, the new function would maintain a value close to 1, so it would not have a significant effect on the exerted force. Yet, when a determined contraction value was reached, the output of the logistic would quickly drop, assuming a value of 0 for larger

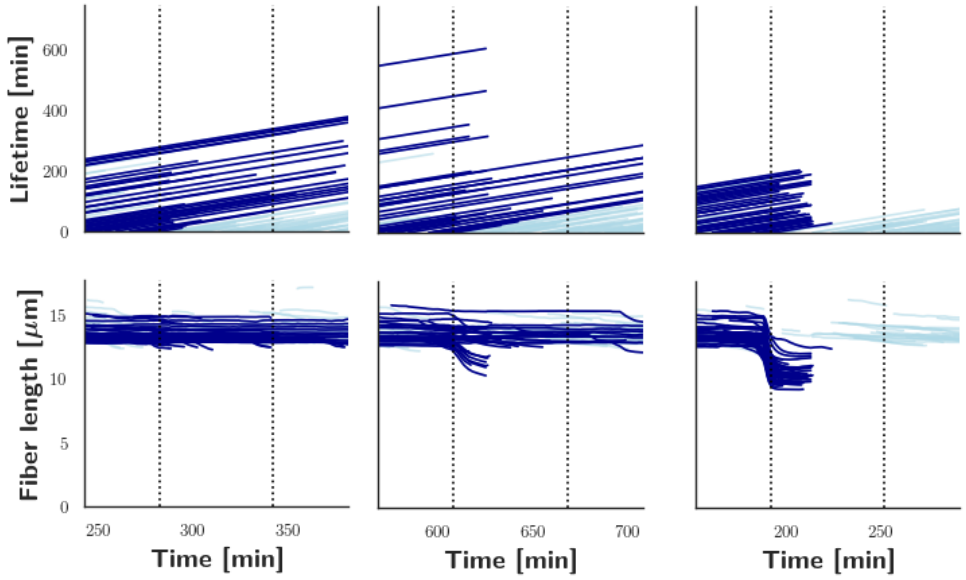

Figure B.2: Examples of the results obtained for the preliminary studies aimed to define a strategy to delete the existing fibres, upon the retraction of the cellular rear. Each line represents the lifetime and length of a single fibre, with dark blue lines corresponding to fibres that existed before the collective retraction (represented by the first dashed line) and light blue lines corresponding to fibres that appeared after that time point, or fibres that were deleted before the retraction. The results show how many of the fibres do not shorten to the extent required to be deleted, living for long periods of time (over 60 min, marked by the second dashed line) after the retraction. Moreover, even when fibres are deleted, it is apparent that new fibres form shortly after the retraction, thus meaning that there are adhesions blocking the cell from moving forward.

contractions. In this case, the logistic function would be dominant over the strengthening factor and force would decrease, hence making disassembly of the adhesions more probable.

Given the general form of the logistic function, described by Eq B.1:

$$F(x) = \frac{1}{1 + \exp\left(-k(x - x_0)\right)} \tag{B.1}$$

where k determines the steepness of the curve and x_0 is the x coordinate at which the function's value is halved, some studies had to be conducted to find adequate values for these parameters, and to optimize the model according to this new extension. Adapting this function to the problem in study, it became Eq 5.9.

Trials were run to tune the model according to this extension. Nonetheless, the results provided by these studies indicated that, upon contraction, not all fibres were deleted, as it can be seen in Fig B.2. To test if the number of deleted fibres could be increased, an alternative equation with the logistic term as a function of the fractional shortening of fibres was also tested. Nonetheless, further preliminary studies (not shown) indicated that using the difference in length was more effective.

Given that, despite the efforts to make the fibres be deleted based on a decrease in force, fibres still lived for a significant amount of time, the strategy referenced in 5.1.6 to delete fibres based on a maximum lifetime, was introduced. In addition, it was concluded that, even when existing adhesions disappear, if new ones are assembled before the cell is able to extend its front, migration will still be hindered. Thus, the idea that cells should enter a period in which they were not able to form new adhesions, being allowed to spread, in a similar way to what happens at the beginning of the simulation, also explained in 5.1.6, was presented.

References

Abercrombie, M. (1980). The croonian lecture, 1978-the crawling movement of metazoan cells. *Proc. R. Soc. Lond. B*, 207(1167):129–147.

Allena, R. (2013). Cell migration with multiple pseudopodia: temporal and spatial sensing models. *Bulletin of mathematical biology*, 75(2):288–316.

Alonso, J. L. and Goldmann, W. H. (2003). Feeling the forces: atomic force microscopy in cell biology. *Life sciences*, 72(23):2553–2560.

Alt, W. and Dembo, M. (1999). Cytoplasm dynamics and cell motion: two-phase flow models. *Mathematical biosciences*, 156(1-2):207–228.

Bangasser, B. L., Rosenfeld, S. S., and Odde, D. J. (2013). Determinants of maximal force transmission in a motor-clutch model of cell traction in a compliant microenvironment. *Biophysical journal*, 105(3):581–592.

Bansod, Y. D. and Bursa, J. (2015). Continuum-based modelling approaches for cell mechanics. *World Academy of Science, Engineering and Technology, International Journal of Biological, Biomolecular, Agricultural, Food and Biotechnological Engineering*, 9(9):969–980.

Bear, J. E. and Haugh, J. M. (2014). Directed migration of mesenchymal cells: where signaling and the cytoskeleton meet. *Current opinion in cell biology*, 30:74–82.

Belinha, J. (2014). Meshless methods in biomechanics. *Bone Tissue Remodelling Analysis*.

Bell, G. I. (1978). Models for the specific adhesion of cells to cells. *Science*, 200(4342):618–627.

Bergert, M., Chandradoss, S. D., Desai, R. A., and Paluch, E. (2012). Cell mechanics control rapid transitions between blebs and lamellipodia during migration. *Proceedings of the National Academy of Sciences*, 109(36):14434–14439.

Berginski, M. E., Vitriol, E. A., Hahn, K. M., and Gomez, S. M. (2011). High-resolution quantification of focal adhesion spatiotemporal dynamics in living cells. *PloS one*, 6(7):e22025.

Berro, J. (2018). "essentially, all models are wrong, but some are useful"—a cross-disciplinary agenda for building useful models in cell biology and biophysics. *Biophysical reviews*, 10(6):1637–1647.

Brodland, G. W. (2004). Computational modeling of cell sorting, tissue engulfment, and related phenomena: A review. *Applied Mechanics Reviews*, 57(1):47–76.

Brodland, G. W. (2015). How computational models can help unlock biological systems. In *Seminars in cell & developmental biology*, volume 47, pages 62–73. Elsevier.

Burridge, K. and Wittchen, E. S. (2013). The tension mounts: stress fibers as force-generating mechanotransducers. *J Cell Biol*, 200(1):9–19.

Butcher, J. C. (2016). *Numerical methods for ordinary differential equations*. John Wiley & Sons.

Butler, J. P., Tolic-Nørrelykke, I. M., Fabry, B., and Fredberg, J. J. (2002). Traction fields, moments, and strain energy that cells exert on their surroundings. *American Journal of Physiology-Cell Physiology*, 282(3):C595–C605.

Califano, J. P. and Reinhart-King, C. A. (2010). Substrate stiffness and cell area predict cellular traction stresses in single cells and cells in contact. *Cellular and molecular bioengineering*, 3(1):68–75.

Carter, D. R., Beaupré, G. S., Giori, N. J., and Helms, J. A. (1998). Mechanobiology of skeletal regeneration. *Clinical Orthopaedics and Related Research®*, 355:S41–S55.

Caton, R. Contributions to the cell-migration theory. *Journal of anatomy and physiology*, 5 Pt 1:35–420.7.

Chan, C. E. and Odde, D. J. (2008). Traction dynamics of filopodia on compliant substrates. *Science*, 322(5908):1687–1691.

Chapin, L., Edgar, L., Blankman, E., Beckerle, M., and Shiu, Y. (2014). Mathematical modeling of the dynamic mechanical behavior of neighboring sarcomeres in actin stress fibers. *Cellular and molecular bioengineering*, 7(1):73–85.

Choquet, D., Felsenfeld, D. P., and Sheetz, M. P. (1997). Extracellular matrix rigidity causes strengthening of integrin–cytoskeleton linkages. *Cell*, 88(1):39–48.

Conway, J. (1970). The game of life. *Scientific American*, 223(4):4.

Cortese, B., Palama, I. E., D'Amone, S., and Gigli, G. (2014). Influence of electrotaxis on cell behaviour. *Integrative Biology*, 6(9):817–830.

Cotton, M. and Claing, A. (2009). G protein-coupled receptors stimulation and the control of cell migration. *Cellular signalling*, 21(7):1045–1053.

Crowley, E. and Horwitz, A. F. (1995). Tyrosine phosphorylation and cytoskeletal tension regulate the release of fibroblast adhesions. *The Journal of cell biology*, 131(2):525–537.

Dallon, J. C. (2000). Numerical aspects of discrete and continuum hybrid models in cell biology. *Applied Numerical Mathematics*, 32(2):137–159.

Danuser, G., Allard, J., and Mogilner, A. (2013). Mathematical modeling of eukaryotic cell migration: insights beyond experiments. *Annual review of cell and developmental biology*, 29:501–528.

Dasanayake, N. L., Michalski, P. J., and Carlsson, A. E. (2011). General mechanism of actomyosin contractility. *Physical review letters*, 107(11):118101.

de Back, W., Zerjatke, T., and Roeder, I. (2019). Statistical and mathematical modeling of spatiotemporal dynamics of stem cells. In *Stem Cell Mobilization*, pages 219–243. Springer.

de Lucas, B., Pérez, L. M., and Gálvez, B. G. (2018). Importance and regulation of adult stem cell migration. *Journal of cellular and molecular medicine*, 22(2):746–754.

de Mattos Coelho-Aguiar, J., Andreiuolo, F., Gebhardt, H., Geraldo, L. H., Pontes, B., Matias, D. I. L., Balça-Silva, J., Aguiar, D. P., do Carmo, A., Lopes, M. C., et al. (2015). The role of the cytoskeleton in cell migration, its influence on stem cells and the special role of gfap in glial functions. In *The Cytoskeleton in Health and Disease*, pages 87–117. Springer.

Delorme, V., Machacek, M., DerMardirossian, C., Anderson, K. L., Wittmann, T., Hanein, D., Waterman-Storer, C., Danuser, G., and Bokoch, G. M. (2007). Cofilin activity downstream of pak1 regulates cell protrusion efficiency by organizing lamellipodium and lamella actin networks. *Developmental cell*, 13(5):646–662.

Dembo, M., Torney, D., Saxman, K., and Hammer, D. (1988). The reaction-limited kinetics of membrane-to-surface adhesion and detachment. *Proceedings of the Royal Society of London. Series B. Biological Sciences*, 234(1274):55–83.

Devreotes, P. and Horwitz, A. R. (2015). Signaling networks that regulate cell migration. *Cold Spring Harbor perspectives in biology*, 7(8):a005959.

DiMilla, P., Barbee, K., and Lauffenburger, D. (1991). Mathematical model for the effects of adhesion and mechanics on cell migration speed. *Biophysical journal*, 60(1):15–37.

Donnelly, S. K., Bravo-Cordero, J. J., and Hodgson, L. (2014). Rho gtpase isoforms in cell motility: Don't fret, we have fret. *Cell adhesion & migration*, 8(6):526–534.

Dormann, D. and Weijer, C. J. (2006). Imaging of cell migration. *The EMBO journal*, 25(15):3480–3493.

Elosegui-Artola, A., Oria, R., Chen, Y., Kosmalska, A., Pérez-González, C., Castro, N., Zhu, C., Trepat, X., and Roca-Cusachs, P. (2016). Mechanical regulation of a molecular clutch defines force transmission and transduction in response to matrix rigidity. *Nature cell biology*, 18(5):540.

Eyckmans, J., Boudou, T., Yu, X., and Chen, C. S. (2011). A hitchhiker's guide to mechanobiology. *Developmental cell*, 21(1):35–47.

Ezratty, E. J., Bertaux, C., Marcantonio, E. E., and Gundersen, G. G. (2009). Clathrin mediates integrin endocytosis for focal adhesion disassembly in migrating cells. *The Journal of cell biology*, 187(5):733–747.

Ezratty, E. J., Partridge, M. A., and Gundersen, G. G. (2005). Microtubule-induced focal adhesion disassembly is mediated by dynamin and focal adhesion kinase. *Nature cell biology*, 7(6):581.

Fischer, R. S., Gardel, M., Ma, X., Adelstein, R. S., and Waterman, C. M. (2009). Local cortical tension by myosin ii guides 3d endothelial cell branching. *Current Biology*, 19(3):260–265.

Fletcher, D. A. and Mullins, R. D. (2010). Cell mechanics and the cytoskeleton. *Nature*, 463(7280):485.

Fletcher, D. A. and Theriot, J. A. (2004). An introduction to cell motility for the physical scientist. *Physical Biology*, 1(1):T1.

Folkman, J. (1995). Angiogenesis in cancer, vascular, rheumatoid and other disease. *Nature medicine*, 1(1):27.

Folkman, J. and Moscona, A. (1978). Role of cell shape in growth control. *Nature*, 273(5661):345.

Frantz, C., Stewart, K. M., and Weaver, V. M. (2010). The extracellular matrix at a glance. *J Cell Sci*, 123(24):4195–4200.

Freikamp, A., Cost, A.-L., and Grashoff, C. (2016). The piconewton force awakens: quantifying mechanics in cells. *Trends in cell biology*, 26(11):838–847.

Friedl, P. and Wolf, K. (2010). Plasticity of cell migration: a multiscale tuning model. *The Journal of cell biology*, 188(1):11–19.

Friedl, P., Zänker, K. S., and Bröcker, E.-B. (1998). Cell migration strategies in 3-d extracellular matrix: Differences in morphology, cell matrix interactions, and integrin function. *Microscopy research and technique*, 43(5):369–378.

Gardel, M. L., Sabass, B., Ji, L., Danuser, G., Schwarz, U. S., and Waterman, C. M. (2008). Traction stress in focal adhesions correlates biphasically with actin retrograde flow speed. *J cell Biol*, 183(6):999–1005.

Gardel, M. L., Schneider, I. C., Aratyn-Schaus, Y., and Waterman, C. M. (2010). Mechanical integration of actin and adhesion dynamics in cell migration. *Annual review of cell and developmental biology*, 26:315–333.

Gardiner, B. S., Wong, K. K., Joldes, G. R., Rich, A. J., Tan, C. W., Burgess, A. W., and Smith, D. W. (2015). Discrete element framework for modelling extracellular matrix, deformable cells and subcellular components. *PLoS computational biology*, 11(10):e1004544.

Geiger, B. and Bershadsky, A. (2001). Assembly and mechanosensory function of focal contacts. *Current opinion in cell biology*, 13(5):584–592.

Geiger, B., Spatz, J. P., and Bershadsky, A. D. (2009). Environmental sensing through focal adhesions. *Nature reviews Molecular cell biology*, 10(1):21.

Gouget, C. L., Hwang, Y., and Barakat, A. I. (2016). Model of cellular mechanotransduction via actin stress fibers. *Biomechanics and modeling in mechanobiology*, 15(2):331–344.

Gracheva, M. E. and Othmer, H. G. (2004). A continuum model of motility in ameboid cells. *Bulletin of mathematical biology*, 66(1):167–193.

Grashoff, C., Hoffman, B. D., Brenner, M. D., Zhou, R., Parsons, M., Yang, M. T., McLean, M. A., Sligar, S. G., Chen, C. S., Ha, T., et al. (2010). Measuring mechanical tension across vinculin reveals regulation of focal adhesion dynamics. *Nature*, 466(7303):263.

Hatze, H. (1974). The meaning of the term" biomechanics". *Journal of biomechanics*, 7(2):189.

Heck, T., Vargas, D. A., Smeets, B., Ramon, H., Van Liedekerke, P., and Van Oosterwyck, H. (2019). The role of actin protrusion dynamics in cell migration through a degradable viscoelastic extracellular matrix: Insights from a computational model. *BioRxiv*, page 697029.

Huth, J., Buchholz, M., Kraus, J. M., Schmucker, M., Von Wichert, G., Krndija, D., Seufferlein, T., Gress, T. M., and Kestler, H. A. (2010). Significantly improved precision of cell migration analysis in time-lapse video microscopy through use of a fully automated tracking system. *BMC cell biology*, 11(1):24.

Huttenlocher, A. and Horwitz, A. R. (2011). Integrins in cell migration. *Cold Spring Harbor perspectives in biology*, 3(9):a005074.

Huttenlocher, A., Palecek, S. P., Lu, Q., Zhang, W., Mellgren, R. L., Lauffenburger, D. A., Ginsberg, M. H., and Horwitz, A. F. (1997). Regulation of cell migration by the calcium-dependent protease calpain. *Journal of Biological Chemistry*, 272(52):32719–32722.

Hwang, Y., Gouget, C. L., and Barakat, A. I. (2012). Mechanisms of cytoskeleton-mediated mechanical signal transmission in cells. *Communicative & integrative biology*, 5(6):538–542.

Hynes, R. O. (2002). Integrins: bidirectional, allosteric signaling machines. *cell*, 110(6):673–687.

Izquierdo-Álvarez, A., Vargas, D. A., Jorge-Peñas, Á., Subramani, R., Vaeyens, M.-M., and Van Oosterwyck, H. (2019). Spatiotemporal analyses of cellular tractions describe subcellular effect of substrate stiffness and coating. *Annals of biomedical engineering*, 47(2):624–637.

Jansen, K. A., Donato, D. M., Balcioglu, H. E., Schmidt, T., Danen, E. H., and Koenderink, G. H. (2015). A guide to mechanobiology: where biology and physics meet. *Biochimica et Biophysica Acta (BBA)-Molecular Cell Research*, 1853(11):3043–3052.

Jorge-Penas, A., Izquierdo-Alvarez, A., Aguilar-Cuenca, R., Vicente-Manzanares, M., Garcia-Aznar, J. M., Van Oosterwyck, H., de Juan-Pardo, E. M., Ortiz-de Solorzano, C., and Muñoz-Barrutia, A. (2015). Free form deformation–based image registration improves accuracy of traction force microscopy. *PloS one*, 10(12):e0144184.

Kai, F., Laklai, H., and Weaver, V. M. (2016). Force matters: biomechanical regulation of cell invasion and migration in disease. *Trends in cell biology*, 26(7):486–497.

Katoh, K., Kano, Y., Masuda, M., Onishi, H., and Fujiwara, K. (1998). Isolation and contraction of the stress fiber. *Molecular Biology of the Cell*, 9(7):1919–1938.

Kaverina, I., Krylyshkina, O., and Small, J. V. (1999). Microtubule targeting of substrate contacts promotes their relaxation and dissociation. *The Journal of cell biology*, 146(5):1033–1044.

Keren, K., Pincus, Z., Allen, G. M., Barnhart, E. L., Marriott, G., Mogilner, A., and Theriot, J. A. (2008). Mechanism of shape determination in motile cells. *Nature*, 453(7194):475.

Kim, M.-C., Neal, D. M., Kamm, R. D., and Asada, H. H. (2013). Dynamic modeling of cell migration and spreading behaviors on fibronectin coated planar substrates and micropatterned geometries. *PLoS computational biology*, 9(2):e1002926.

Kim, M.-C., Silberberg, Y. R., Abeyaratne, R., Kamm, R. D., and Asada, H. H. (2018). Computational modeling of three-dimensional ecm-rigidity sensing to guide directed cell migration. *Proceedings of the National Academy of Sciences*, 115(3):E390–E399.

King, S. J., Asokan, S. B., Haynes, E. M., Zimmerman, S. P., Rotty, J. D., Alb, J. G., Tagliatela, A., Blake, D. R., Lebedeva, I. P., Marston, D., et al. (2016). Lamellipodia are critical for haptotactic sensing and response. *J Cell Sci*, pages jcs–184507.

Kong, F., García, A. J., Mould, A. P., Humphries, M. J., and Zhu, C. (2009). Demonstration of catch bonds between an integrin and its ligand. *The Journal of cell biology*, 185(7):1275–1284.

Kuznetsova, T. G., Starodubtseva, M. N., Yegorenkov, N. I., Chizhik, S. A., and Zhdanov, R. I. (2007). Atomic force microscopy probing of cell elasticity. *Micron*, 38(8):824–833.

Lai, F. P., Szczodrak, M., Block, J., Faix, J., Breitsprecher, D., Mannherz, H. G., Stradal, T. E., Dunn, G. A., Small, J. V., and Rottner, K. (2008). Arp2/3 complex interactions and actin network turnover in lamellipodia. *The EMBO journal*, 27(7):982–992.

Lamalice, L., Le Boeuf, F., and Huot, J. (2007). Endothelial cell migration during angiogenesis. *Circulation research*, 100(6):782–794.

Lämmermann, T., Bader, B. L., Monkley, S. J., Worbs, T., Wedlich-Söldner, R., Hirsch, K., Keller, M., Förster, R., Critchley, D. R., Fässler, R., et al. (2008). Rapid leukocyte migration by integrin-independent flowing and squeezing. *Nature*, 453(7191):51.

Lämmermann, T. and Sixt, M. (2009). Mechanical modes of 'amoeboid'cell migration. *Current opinion in cell biology*, 21(5):636–644.

Langanger, G., Moeremans, M., Daneels, G., Sobieszek, A., De Brabander, M., and De Mey, J. (1986). The molecular organization of myosin in stress fibers of cultured cells. *The Journal of cell biology*, 102(1):200–209.

Lauffenburger, D. A. and Horwitz, A. F. (1996). Cell migration: a physically integrated molecular process. *Cell*, 84(3):359–369.

Le Clainche, C. and Carlier, M.-F. (2008). Regulation of actin assembly associated with protrusion and adhesion in cell migration. *Physiological reviews*, 88(2):489–513.

Lee, J., Ishihara, A., Theriot, J. A., and Jacobson, K. (1993). Principles of locomotion for simple-shaped cells. *Nature*, 362(6416):167.

Lee, J. and Jacobson, K. (1997). The composition and dynamics of cell-substratum adhesions in locomoting fish keratocytes. *Journal of Cell Science*, 110(22):2833–2844.

Lehenkari, P. and Horton, M. (1999). Single integrin molecule adhesion forces in intact cells measured by atomic force microscopy. *Biochemical and biophysical research communications*, 259(3):645–650.

Lieber, A. D., Yehudai-Resheff, S., Barnhart, E. L., Theriot, J. A., and Keren, K. (2013). Membrane tension in rapidly moving cells is determined by cytoskeletal forces. *Current biology*, 23(15):1409–1417.

Liu, X., Vargas, D. A., Lü, D., Zhang, Y., Zaman, M. H., and Long, M. (2014). Computational modeling of stem cell migration: A mini review. *Cellular and Molecular Bioengineering*, 7(2):196–204.

Lo, C.-M., Wang, H.-B., Dembo, M., and Wang, Y.-l. (2000). Cell movement is guided by the rigidity of the substrate. *Biophysical journal*, 79(1):144–152.

Lodish H, Berk A, Z. S. e. a. (2000). *Section 18.2, The Dynamics of Actin Assembly*. New York: W. H. Freeman.

Luster, A. D., Alon, R., and von Andrian, U. H. (2005). Immune cell migration in inflammation: present and future therapeutic targets. *Nature immunology*, 6(12):1182.

Lysaght, M. J., Jaklenec, A., and Deweerd, E. (2008). Great expectations: private sector activity in tissue engineering, regenerative medicine, and stem cell therapeutics. *Tissue Engineering Part A*, 14(2):305–315.

Macal, C. M. and North, M. J. (2005). Tutorial on agent-based modeling and simulation. In *Proceedings of the Winter Simulation Conference, 2005.*, pages 14–pp. IEEE.

Marcy, Y., Prost, J., Carlier, M.-F., and Sykes, C. (2004). Forces generated during actin-based propulsion: a direct measurement by micromanipulation. *Proceedings of the National Academy of Sciences*, 101(16):5992–5997.

Mattila, P. K. and Lappalainen, P. (2008). Filopodia: molecular architecture and cellular functions. *Nature reviews Molecular cell biology*, 9(6):446.

Maugis, D. (1992). Adhesion of spheres: the jkr-dmt transition using a dugdale model. *Journal of colloid and interface science*, 150(1):243–269.

Mayor, R. and Etienne-Manneville, S. (2016). The front and rear of collective cell migration. *Nature reviews Molecular cell biology*, 17(2):97.

McCain, M. L., Lee, H., Aratyn-Schaus, Y., Kléber, A. G., and Parker, K. K. (2012). Cooperative coupling of cell-matrix and cell–cell adhesions in cardiac muscle. *Proceedings of the National Academy of Sciences*, 109(25):9881–9886.

Mehlen, P. and Puisieux, A. (2006). Metastasis: a question of life or death. *Nature reviews cancer*, 6(6):449.

Mitra, S. K., Hanson, D. A., and Schlaepfer, D. D. (2005). Focal adhesion kinase: in command and control of cell motility. *Nature reviews Molecular cell biology*, 6(1):56.

Mitrossilis, D., Fouchard, J., Guiroy, A., Desprat, N., Rodriguez, N., Fabry, B., and Asnacios, A. (2009). Single-cell response to stiffness exhibits muscle-like behavior. *Proceedings of the National Academy of Sciences*, 106(43):18243–18248.

Mogilner, A., Wollman, R., and Marshall, W. F. (2006). Quantitative modeling in cell biology: what is it good for? *Developmental cell*, 11(3):279–287.

Moore, S. W., Roca-Cusachs, P., and Sheetz, M. P. (2010). Stretchy proteins on stretchy substrates: the important elements of integrin-mediated rigidity sensing. *Developmental cell*, 19(2):194–206.

Muhamed, I., Chowdhury, F., and Maruthamuthu, V. (2017). Biophysical tools to study cellular mechanotransduction. *Bioengineering*, 4(1):12.

Munevar, S., Wang, Y.-l., and Dembo, M. (2001). Traction force microscopy of migrating normal and h-ras transformed 3t3 fibroblasts. *Biophysical journal*, 80(4):1744–1757.

Munjiza, A. A. (2004). *The combined finite-discrete element method*. John Wiley & Sons.

Nagano, M., Hoshino, D., Koshikawa, N., Akizawa, T., and Seiki, M. (2012). Turnover of focal adhesions and cancer cell migration. *International journal of cell biology*, 2012.

Naumanen, P., Lappalainen, P., and Hotulainen, P. (2008). Mechanisms of actin stress fibre assembly. *Journal of microscopy*, 231(3):446–454.

Neuman, K. C. and Nagy, A. (2008). Single-molecule force spectroscopy: optical tweezers, magnetic tweezers and atomic force microscopy. *Nature methods*, 5(6):491.

Nishida, N., Yano, H., Nishida, T., Kamura, T., and Kojiro, M. (2006). Angiogenesis in cancer. *Vascular health and risk management*, 2(3):213.

Noble, D. (2002). The rise of computational biology. *Nature Reviews Molecular Cell Biology*, 3(6):459.

Northrup, S. H. and Erickson, H. P. (1992). Kinetics of protein-protein association explained by brownian dynamics computer simulation. *Proceedings of the National Academy of Sciences*, 89(8):3338–3342.

Odenthal, T., Smeets, B., Van Liedekerke, P., Tijskens, E., Van Oosterwyck, H., and Ramon, H. (2013). Analysis of initial cell spreading using mechanistic contact formulations for a deformable cell model. *PLoS computational biology*, 9(10):e1003267.

Ohashi, K., Fujiwara, S., and Mizuno, K. (2017). Roles of the cytoskeleton, cell adhesion and rho signalling in mechanosensing and mechanotransduction. *The Journal of Biochemistry*, 161(3):245–254.

Onochie, O. E., Zollinger, A., Rich, C. B., Smith, M., and Trinkaus-Randall, V. (2019). Epithelial cells exert differential traction stress in response to substrate stiffness. *Experimental eye research*, 181:25–37.

Özkaya, N., Leger, D., Goldsheyder, D., and Nordin, M. (2017). *Mechanical Properties of Biological Tissues*, pages 361–387. Springer International Publishing, Cham.

Palecek, S. P., Loftus, J. C., Ginsberg, M. H., Lauffenburger, D. A., and Horwitz, A. F. (1997). Integrin-ligand binding properties govern cell migration speed through cell-substratum adhesiveness. *Nature*, 385(6616):537.

Paňková, K., Rösel, D., Novotnỳ, M., and Brábek, J. (2010). The molecular mechanisms of transition between mesenchymal and amoeboid invasiveness in tumor cells. *Cellular and molecular life sciences*, 67(1):63–71.

Parkhurst, M. R. and Saltzman, W. M. (1992). Quantification of human neutrophil motility in three-dimensional collagen gels. effect of collagen concentration. *Biophysical journal*, 61(2):306–315.

Pereverzev, Y. V., Prezhdo, O. V., Forero, M., Sokurenko, E. V., and Thomas, W. E. (2005). The two-pathway model for the catch-slip transition in biological adhesion. *Biophysical journal*, 89(3):1446–1454.

Periasamy, A. and Day, R. N. (1998). Visualizing protein interactions in living cells using digitized gfp imaging and fret microscopy. In *Methods in cell biology*, volume 58, pages 293–314. Elsevier.

Peskin, C. S., Odell, G. M., and Oster, G. F. (1993). Cellular motions and thermal fluctuations: the brownian ratchet. *Biophysical journal*, 65(1):316–324.

Polacheck, W. J. and Chen, C. S. (2016). Measuring cell-generated forces: a guide to the available tools. *Nature methods*, 13(5):415.

Polio, S. R., Rothenberg, K. E., Stamenović, D., and Smith, M. L. (2012). A micropatterning and image processing approach to simplify measurement of cellular traction forces. *Acta biomaterialia*, 8(1):82–88.

Pollard, T. D. and Borisy, G. G. (2003). Cellular motility driven by assembly and disassembly of actin filaments. *Cell*, 112(4):453–465.

Pollard, T. D. and Cooper, J. A. (2009). Actin, a central player in cell shape and movement. *Science*, 326(5957):1208–1212.

Pontes, B., Monzo, P., and Gauthier, N. C. (2017). Membrane tension: a challenging but universal physical parameter in cell biology. In *Seminars in cell & developmental biology*, volume 71, pages 30–41. Elsevier.

Ponti, A., Machacek, M., Gupton, S., Waterman-Storer, C., and Danuser, G. (2004). Two distinct actin networks drive the protrusion of migrating cells. *Science*, 305(5691):1782–1786.

Ponti, A., Matov, A., Adams, M., Gupton, S., Waterman-Storer, C., and Danuser, G. (2005). Periodic patterns of actin turnover in lamellipodia and lamellae of migrating epithelial cells analyzed by quantitative fluorescent speckle microscopy. *Biophysical journal*, 89(5):3456–3469.

Prahl, L. S. and Odde, D. J. (2018). Modeling cell migration mechanics. In *Biomechanics in Oncology*, pages 159–187. Springer.

Purcell, E. M. (1977). Life at low reynolds number. *American journal of physics*, 45(1):3–11.

Raftopoulou, M. and Hall, A. (2004). Cell migration: Rho gtpases lead the way. *Developmental biology*, 265(1):23–32.

Rajagopalan, P., Marganski, W. A., Brown, X. Q., and Wong, J. Y. (2004). Direct comparison of the spread area, contractility, and migration of balb/c 3t3 fibroblasts adhered to fibronectin-and rgd-modified substrata. *Biophysical journal*, 87(4):2818–2827.

Renkawitz, J., Schumann, K., Weber, M., Lämmermann, T., Pflicke, H., Piel, M., Polleux, J., Spatz, J. P., and Sixt, M. (2009). Adaptive force transmission in amoeboid cell migration. *Nature cell biology*, 11(12):1438.

Ridley, A. J. and Hall, A. (1992). The small gtp-binding protein rho regulates the assembly of focal adhesions and actin stress fibers in response to growth factors. *Cell*, 70(3):389–399.

Robling, A. G., Castillo, A. B., and Turner, C. H. (2006). Biomechanical and molecular regulation of bone remodeling. *Annu. Rev. Biomed. Eng.*, 8:455–498.

Rubinstein, B., Jacobson, K., and Mogilner, A. (2005). Multiscale two-dimensional modeling of a motile simple-shaped cell. *Multiscale Modeling & Simulation*, 3(2):413–439.

Sambeth, R. and Baumgaertner, A. (2001). Locomotion of a two dimensional keratocyte model. *Journal of Biological Systems*, 9(03):201–219.

Sato, K., Adachi, T., Matsuo, M., and Tomita, Y. (2005). Quantitative evaluation of threshold fiber strain that induces reorganization of cytoskeletal actin fiber structure in osteoblastic cells. *Journal of biomechanics*, 38(9):1895–1901.

Scarpa, E. and Mayor, R. (2016). Collective cell migration in development. *J Cell Biol*, 212(2):143–155.

Schreiber, C. H., Stewart, M., and Duke, T. (2010). Simulation of cell motility that reproduces the force–velocity relationship. *Proceedings of the National Academy of Sciences*.

Schwarz, U. S., Erdmann, T., and Bischofs, I. B. (2006). Focal adhesions as mechanosensors: the two-spring model. *Biosystems*, 83(2-3):225–232.

Scianna, M., Preziosi, L., and Wolf, K. (2013). A cellular potts model simulating cell migration on and in matrix environments. *Mathematical Biosciences & Engineering*, 10(1):235–261.

Smeets, B. (2016). From single cell mechanics and intercellular forces to collective aggregate dynamics individual cell-based modeling of cell cultures for tissue engineering.

Spill, F., Guerrero, P., Alarcon, T., Maini, P. K., and Byrne, H. M. (2015). Mesoscopic and continuum modelling of angiogenesis. *Journal of mathematical biology*, 70(3):485–532.

St Johnston, D. and Ahringer, J. (2010). Cell polarity in eggs and epithelia: parallels and diversity. *Cell*, 141(5):757–774.

Stehbens, S. J. and Wittmann, T. (2014). Analysis of focal adhesion turnover: a quantitative live-cell imaging example. In *Methods in cell biology*, volume 123, pages 335–346. Elsevier.

Stephens, D. J. and Allan, V. J. (2003). Light microscopy techniques for live cell imaging. *science*, 300(5616):82–86.

Style, R. W., Boltyanskiy, R., German, G. K., Hyland, C., MacMinn, C. W., Mertz, A. F., Wilen, L. A., Xu, Y., and Dufresne, E. R. (2014). Traction force microscopy in physics and biology. *Soft matter*, 10(23):4047–4055.

Sugimura, K., Lenne, P.-F., and Graner, F. (2016). Measuring forces and stresses in situ in living tissues. *Development*, 143(2):186–196.

Tabata, Y. (2003). Tissue regeneration based on growth factor release. *Tissue engineering*, 9(4, Supplement 1):5–15.

Tang, D. D. and Gerlach, B. D. (2017). The roles and regulation of the actin cytoskeleton, intermediate filaments and microtubules in smooth muscle cell migration. *Respiratory research*, 18(1):54.

Tanimoto, H. and Sano, M. (2014). A simple force-motion relation for migrating cells revealed by multipole analysis of traction stress. *Biophysical journal*, 106(1):16–25.

Tapon, N. and Hall, A. (1997). Rho, rac and cdc42 gtpases regulate the organization of the actin cytoskeleton. *Current opinion in cell biology*, 9(1):86–92.

Tenekedjiev, K. I., Nikolova, N. D., and Kolev, K. (2017). *Applications of Monte Carlo simulation in modelling of biochemical processes*. Intech.

Tijskens, E., Ramon, H., and De Baerdemaeker, J. (2003). Discrete element modelling for process simulation in agriculture. *Journal of sound and vibration*, 266(3):493–514.

Tozluoğlu, M., Tournier, A. L., Jenkins, R. P., Hooper, S., Bates, P. A., and Sahai, E. (2013). Matrix geometry determines optimal cancer cell migration strategy and modulates response to interventions. *Nature cell biology*, 15(7):751.

Trepat, X., Chen, Z., and Jacobson, K. (2012). Cell migration. *Comprehensive Physiology*, 2(4):2369.

Tzima, E., Irani-Tehrani, M., Kiosses, W. B., Dejana, E., Schultz, D. A., Engelhardt, B., Cao, G., DeLisser, H., and Schwartz, M. A. (2005). A mechanosensory complex that mediates the endothelial cell response to fluid shear stress. *Nature*, 437(7057):426.

Van der Flier, A. and Sonnenberg, A. (2001). Function and interactions of integrins. *Cell and tissue research*, 305(3):285–298.

van der Meulen, M. C. and Huiskes, R. (2002). Why mechanobiology?: A survey article. *Journal of biomechanics*, 35(4):401–414.

Van Liedekerke, P., Neitsch, J., Johann, T., Warmt, E., Grosser, S., Valverde, I. G., Kaes, J., Hoehme, S., and Drasdo, D. (2018). Quantifying the mechanics and growth of cells and tissues in 3d using high resolution computational models. *bioRxiv*, page 470559.

Van Liedekerke, P., Palm, M., Jagiella, N., and Drasdo, D. (2015). Simulating tissue mechanics with agent-based models: concepts, perspectives and some novel results. *Computational particle mechanics*, 2(4):401–444.

Van Liedekerke, P., Tijskens, E., Ramon, H., Ghysels, P., Samaey, G., and Roose, D. (2010). Particle-based model to simulate the micromechanics of biological cells. *Physical Review E*, 81(6):061906.

Vicente-Manzanares, M. and Horwitz, A. R. (2011). Adhesion dynamics at a glance. *J Cell Sci*, 124(23):3923–3927.

Viegas, S., Ladeira, C., Costa-Veiga, A., Perelman, J., and Gajski, G. (2017). Forgotten public health impacts of cancer–an overview. *Archives of Industrial Hygiene and Toxicology*, 68(4):287–297.

Wakeland, W., Macovsky, L., and An, G. (2007). A hybrid simulation model for studying acute inflammatory response. In *Proceedings of the 2007 spring simulation multiconference-Volume 2*, pages 39–46. Society for Computer Simulation International.

Wang, N. and Ingber, D. E. (1995). Probing transmembrane mechanical coupling and cytomechanics using magnetic twisting cytometry. *Biochemistry and Cell Biology*, 73(7-8):327–335.

Wang, N., Ostuni, E., Whitesides, G. M., and Ingber, D. E. (2002). Micropatterning tractional forces in living cells. *Cell motility and the cytoskeleton*, 52(2):97–106.

Webb, D. J., Brown, C. M., and Horwitz, A. F. (2003). Illuminating adhesion complexes in migrating cells: moving toward a bright future. *Current opinion in cell biology*, 15(5):614–620.

Wedlich-Soldner, R. and Li, R. (2003). Spontaneous cell polarization: undermining determinism. *Nature cell biology*, 5(4):267.

Wells, R. G. (2008). The role of matrix stiffness in regulating cell behavior. *Hepatology*, 47(4):1394–1400.

Wolfenson, H., Meacci, G., Liu, S., Stachowiak, M. R., Iskratsch, T., Ghassemi, S., Roca-Cusachs, P., O'Shaughnessy, B., Hone, J., and Sheetz, M. P. (2016). Tropomyosin controls sarcomere-like contractions for rigidity sensing and suppressing growth on soft matrices. *Nature cell biology*, 18(1):33.

Wu, T.-H., Li, C.-H., Tang, M.-J., Liang, J.-I., Chen, C.-H., and Yeh, M.-L. (2013). Migration speed and directionality switch of normal epithelial cells after tgf-β1-induced emt (temt) on micro-structured polydimethylsiloxane (pdms) substrates with variations in stiffness and topographic patterning. *Cell communication & adhesion*, 20(5):115–126.

Yanagishita, M. (1993). Function of proteoglycans in the extracellular matrix. *Pathology International*, 43(6):283–293.

Zaidel-Bar, R., Cohen, M., Addadi, L., and Geiger, B. (2004). Hierarchical assembly of cell–matrix adhesion complexes.

Zeng, X. and Li, S. (2011). Modelling and simulation of substrate elasticity sensing in stem cells. *Computer methods in biomechanics and biomedical engineering*, 14(05):447–458.

Zienkiewicz, O. C., Taylor, R. L., Nithiarasu, P., and Zhu, J. (1977). *The finite element method*, volume 3. McGraw-hill London.

Zimmermann, J., Enculescu, M., and Falcke, M. (2010). Leading-edge–gel coupling in lamellipodium motion. *Phys. Rev. E*, 82:051925.